Assessment on the Local Climate Effects of Solar Photovoltaic Parks

Maria Makaronidou

This dissertation is submitted for the degree of Doctor of Philosophy

June 2020

Lancaster Environment Centre

This dissertation is dedicated to my family and my friends who were always supporting me during those 12 academic years…

Look up to the stars and not down at your feet. Try to make sense of what you see and wonder about what makes the universe exist. Be curious.

-Stephen Hawking-

Declaration

This thesis has not been submitted in support of an application for another degree at this or any other university. It is the result of my own work and includes nothing that is the outcome of work done in collaboration except where specifically indicated. My supervision team, Dr Alona Armstrong (Lancaster Environment Centre), Prof Nicholas J. Ostle (Lancaster Environment Centre) and Dr Nicholas Kettridge (University of Birmingham).

Lancaster University, UK

Abstract

Transition to low-carbon energy sources is the primary driver of the wide deployment of ground-mounted solar photovoltaic (PV) technologies (solar parks). Despite of this notable land-use change impacts of solar parks on local climate and the associated ecosystem functions are poorly resolved. Field study conducted at a temperate UK grassland, showed cooler air and soil temperatures under panels during the growing season compared to the gap between the PV panel rows. Further, higher soil moisture under, during growing season compared to the gap and evidence for spatial variability on soil physical properties; likely the result of compaction and vegetation management during and after solar park construction. Microclimatic changes had no spatial effect on leaf area index nor net ecosystem exchange and water vapor fluxes. Acknowledging the effects of solar parks on soil temperatures HIS-PV (Heat-In a Solar PV park) model was built and sensitivity analyses reported that dense canopies and wet soils increased model errors during growing season whilst low dense canopies decreased model errors post-growing season. HIS-PV model was applied to simulate soil temperature, incoming short-wave (SW) and potential evaporation (PE) across different climatic zones. Annual incoming SW was strongly affected; control areas received 60% more solar radiation than under panels across all tested zones. Soil temperature and PE demonstrated the largest differences between under and control areas in arid environments, followed by evidence for lower amount of growing degree days under the panels at both the arid and the equatorial zones. Regardless of the wide solar parks' deployment and the undoubtable importance of terrestrial ecosystems, local climatic changes caused by solar parks and implications for ecosystem services provided by the hosting landscape are poorly resolved. This study provides the first synthesis of emerging understanding in this area. Research findings are urgently needed to enhance understanding and thus explore the potential for managing solar parks to provide multiple ecosystem services.

Acknowledgements

Thank you to my family and parents for the unlimited support and love through all those years. Special thanks to my colleagues and friends from Lancaster and the Lancaster Environment Centre. Special thanks to Dr Heather Stott, who helped me both as a friend and as a peer during my fieldwork and my data analysis. Further, many thanks to Dr Pedro Batista, Dr Jon Murray and Brittany Heap who helped me reviewing my drafts before my PhD submission. Massive thanks to my dearest friends Sasa Mavrommati (MA), Galateia Georgoudi (MSc), Dr Natalia Kyrtata and Dr Robert Holdbrook for their unconditional love and support through difficult personal and studying periods of my life. Last, I need to thank my incredibly helpful and supportive supervision team, Dr Alona Armstrong, Dr Nicholas Kettridge and Prof Nicholas J. Ostle. I am so grateful and lucky to have had you next to me through this academic journey, hoping that all supervisors are and will be standing by their students as these three did for me. Without you all, I would not be able to survive all these experiences and sudden changes of my personal and academic life and still make it to submit my PhD thesis on time.

Contents

List of Tables

List of Figures

List of Abbreviations and Acronyms

C_s volumetric heat capacity ($J \cdot m^{-3} \cdot K^{-3}$)

d zero plane displacement height (m)

E evaporation (W/m^2)

ET evapotranspiration (W/m^2)

H sensible heat flux (W/m^2)

k thermal conductivity ($W \cdot m^{-1} \cdot K^{-1}$)

k_v vapour transfer ($W \cdot m^{-1} \cdot K^{-1}$)

K_c incoming short-wave (SW) radiation; vegetation canopy (W/m^2)

$K_{c\,dif}$ incoming diffuse SW radiation; vegetation canopy (W/m^2)

$K_{c\,dir}$ incoming direct SW radiation; vegetation canopy (W/m^2)

K_f incoming SW radiation; park (W/m^2)

K_s incoming SW radiation; soil surface (W/m^2)

$L_{c\downarrow}$ incoming long-wave (LW) radiation; vegetation canopy (W/m^2)

$L_{f\downarrow}$ incoming LW radiation; park (W/m^2)

$L_{s\downarrow}$ incoming LW radiation; soil surface (W/m^2)

$L_{s\uparrow}$ outgoing LW radiation; soil surface (W/m^2)

LAI leaf area index (m^2/ m^2; unitless)

n	cloud cover
PV	photovoltaic
q	heat conduction (W/m^2)
Q_{Es}	latent heat flux for evaporation; soil surface (W/m^2)
Q_{Hs}	sensible heat flux; heat at the soil surface (W/m^2)
Q_s	energy balance at the soil surface; soil (W/m^2)
r_a	aerodynamic resistance (s/m^{-1})
r_{aT}	total aerodynamic resistance (s/m^{-1})
r_b	aerodynamic resistance between substrate and vegetation canopy (s/m^{-1})
r_s	surface resistance (s/m^{-1})
svf	sky view factor
T_a	absolute air temperature (Kelvin)
T_{ac}	air temperature; vegetation canopy (Kelvin)
u_r	wind speed at the data loggers' sensor height (m/s^{-1})
vdd_a	vapour density deficit of air (kg/m^3)
VWC	volumetric water content *(*m^3/ m^3)
z_0	surface roughness (m)
z_{0m}	roughness length of momentum transfer (m)

z_r reference height above the ground surface (m)

a albedo

ε^* effective emissivity of the sky

ε_s soil surface emissivity

ε_{leaf} emissivity of the leaf canopy

ε_0 clear sky emissivity

K von Karman constant equals to 0.41 m

λ constant dependant on the cloud type equal to 0.26

σ Stefan-Boltzmann constant equals to $5.670374419 \cdot 10^{-8}$ ($W \cdot m^{-2} \cdot K^{-4}$)

List of Appendices

Introduction

Since the industrial revolution, the developed world has depended on non-renewable energy to satisfy lifestyles, and commercial needs (Chu and Majumdar, 2012; Dincer, 2000; Gales et al., 2007). Energy demand has increased as a result of global population increase (higher than the expected average by 2%; Dincer (2000)), urbanization and modernization (Asif and Muneer, 2007; Bogardi et al., 2012). Meeting these energy requirements, prior to *The Convention on Climate Change* (or The Paris Agreement; UN (2015)), the world heavily relayed on exploiting and burning fossil hydrocarbon fuels (oil, gas and coal; Asif and Muneer (2007) and Voudouris (2013)), which contributed 80% to the global energy needs (IEA, 2018a). This has contributed to the increase in atmospheric carbon dioxide (CO_2) concentrations from 280 ppm pre-industrial, to 387 ppm in 2009 (Rockström et al., 2009) and to 415.26 ppm in 2019 (The Keeling curve; NOAA (2019)). This increase in CO_2 has generated significant changes to our climate with severe implications for ecosystems and humanity (Mendelsohn et al., 1994; Asif and Muneer, 2007; Pedraza, 2012; Chu and Majumdar, 2012).

According to the WHO (2014), within 2030-2050 climate change side-effects are expected to cause around 250,000 additional deaths, annually. Consequently, more

sustainable solutions in the energy sector are urgently needed (Asif and Muneer, 2007; Dincer, 2000). A transition to low-carbon energy resources, is believed to be the best solution to mitigate these energy-related environmental problems (Asif and Muneer, 2007; Dincer, 1999). Renewable energy is now the fastest growing energy sector in the world and is expected to surpass and ultimately replace conventional energy resources.

Renewable sources began gaining global attention as an important element of global power generation in early 2000s (Frontini et al., 2013). In 2017, renewables contributed 24% of power demand (IEA, 2018b), and has been projected to supply the world with 75-80% of electricity by 2050 (IPCC, 2018). Across the EU, deployment of renewable energy resources is increasing rapidly. For example, installation capacity has increased on average by 5.3% per annum, whilst energy consumption has increased by 6% per annum, over the period 2005–2016 (Eurostat data; Carrosio and Scotti (2019) and EEA (2018)). During 2017, 30.6% of the total electricity generation derived from renewables and in order to achieve the 2030 targets (40% consumption by renewables, 27% mitigation of GHGs, 27% improvement on energy efficiency), the rate of the annual energy consumption by renewables is required to increase by 6% every year (EEA, 2018; Tulus et al., 2019).

Comparing all renewable types based on environmental, economic, and safety criteria, solar energy appears the most promising (Bórawski et al., 2019). Further, solar energy was reported to be one of the most sustainable among the other energy sources (Kamat, 2007; Pogson et al., 2013) and a “common sense vision” (Ginley and Parilla, 2013). Solar energy is the fundamental basis of the Earth’s ecosystems’ survival, driving both climate and meteorological conditions (Ginley and Parilla, 2013). Judging by its abundance and its inexhaustibility across the Earth, at the moment solar energy generation leads the growth in renewables by 64%, throughout the projection period of 2050 (EIA, 2018). In

2017, 98 GW of solar power infrastructures was installed globally, equating a 31% increase when compared with the 2016 records of the Boomerang New Energy Finance (IEEFA, 2018). Across the EU, solar energy currently produces 4% of the electricity and is expected to provide 10% of total electricity by 2030 (Bórawski et al., 2019).

Solar energy is divided in two types of technologies which convert solar energy: concentrated solar power (CSP) and solar photovoltaic (PV). CSP is only viable in areas of direct solar irradiances of greater than 4 $kW \cdot h \cdot m^{-2} \cdot d^{-1}$, limiting its geographical spread to low latitude regions (Hernandez et al., 2015). In contrast, PV generates electricity under lower and diffuse solar radiation conditions and thus can be deployed in a range of climates (Pogson et al., 2013). Solar PV is a relatively mature energy source with development efforts significantly decreasing costs while increasing the PV technology efficiency (Sánchez-Lozano et al., 2013; Tulus et al., 2019). The compound annual growth rate in the EU was highest for solar PV systems (48%) during 2005-2016, compared with other types of renewables, including CSP (EEA, 2018).

Solar PV can be installed as building-mounted or ground-mounted systems. Ground-mounted solar PV parks, hereinafter referred to as solar parks, vary in size and design and are formed by a metal frame that is driven into the ground to hold the panels up at a fixed angle. They have been deployed in large areas of land across the world (Armstrong et al., 2016; Hassanpour Adeh et al., 2018; Ravi et al., 2014; Barron-Gafford et al., 2016). Within the UK approximately 59% of PV electricity, was generated by ground-mounted PV panels covering an area of ~85 km^2 (UK National Statistics, 2017), creating niches regarding potential environmental impacts deriving by this land-use change. Given the increasing land-use pressure for production including food, fibre and fuel, it is important to resolve the implications of the expansion of solar parks.

The physical presence of PV arrays will affect the photosynthetic active radiation (PAR), radiative flux balance and distribution of precipitation (Armstrong et al., 2016; Hassanpour Adeh et al., 2018). Solar PV panels also reduce the park's albedo; panels are darker and thus have a lower albedo (~0.1) compared with soil and/or vegetated surfaces (a typical temperate grassland's albedo is ~0.25; Barron-Gafford et al. (2016)). Observed changes in microclimate have as a result been substantial. For example, under PV panels summer and winter soil temperature decreased by 5.2 ºC and 1.7 ºC, respectively, while soil moisture was surprisingly high under due to rainfall falling along the PV panel supporting frame (Armstrong et al., 2016).

Changes in microclimate may have significant effects on ecosystem processes, including productivity, decomposition, vegetation morphology, carbon cycling, soil erosion and evapotranspiration rates (Dupraz et al., 2010; Marrou et al., 2013a; Marrou et al., 2013b; Armstrong et al., 2016; Armstrong et al., 2014a; Marrou et al., 2013c; Barron-Gafford et al., 2016; Hassanpour Adeh et al., 2018; Hernandez et al., 2015). Notably, microclimate impacts have been observed to influence solar park's ecology and the associated crop ecology. Variability in air and soil climates at the gap between solar PV panel' rows (e.g. diurnal air temperatures warmer at the gap during growing season and around 2.5 °C cooler during the winter) compared to the area under the PV panel, decreased vegetation growth (Armstrong et al., 2016).

Leaf area index (LAI) of lettuces have also been shown to increase under shade despite a decrease in the number of leaves (Marrou et al., 2013a). Overall, research has shown that changing the proportion of shade in an agrivoltaic system would require less management compared to a typical arable grassland (Marrou et al., 2013b). Thus, designing and planning of a solar park strongly affects all those parameters discussed.

Despite these wide-ranging and potential important perturbations, research examining the potential effects of solar parks on the local climate is limited. Moreover, understanding the changes may support enhance park design on land management to enable multiple-use including crop growth under agrivoltaic schemes firstly introduced by Goetzberger and Zastrow (1982)) under the panels and around panels, (Ravi et al., 2014), grazing (BRE, 2014) and habitat provision, including pollinators (Walston et al., 2018). Consequently, given the global deployment of solar parks, it is important to predict the microclimatic effects, and thus allow inference of potential implications for ecosystem processes, function and service delivery, across different climate zones.

Considering the cost of and time required for field instrumentation, a modelling approach to predict local climate impacts is appealing. Modelling approaches have been used to evaluate the optimal placement of solar PV units on rooftops (Calvert and Mabee, 2015; Sánchez-Lozano et al., 2013; Sánchez-Lozano et al., 2014; Uyan, 2013). However, to date, there is no modelling tool available to explore microclimatic behaviour in solar parks.

Recognising the rapidly accelerating land-use change for solar parks and the poorly resolved understanding of the effects on the hosting ecosystem, the overall aim of this PhD was to quantify the effects of solar parks on local climates and to enable these potential implications for ecosystem processes, function and service delivery to be inferred. Below provides a breakdown of the chapters of the thesis:

Chapter 1, the aim of this study was to characterise this spatio-temporal variability in the air and soil climate, LAI, greenhouse gaseous fluxes and soil physical properties within a solar park. We hypothesised that:

H1. Photosynthetic Active Radiation (PAR), soil and air temperature, under the PV panels will be lower compared to the gap during growing season but are expected to demonstrate similar spatial distribution/trend from under towards the gap, during non-growing season. Soil moisture is expected to be higher under the PV panels in comparison to the gap, as a result of precipitation runoff from PV panels side framing, reaching the surface under the PV panels.

H2. Soil bulk density will be higher under PV panels and organic matter lower under PV panels due to compaction, high soil heterogeneity across the park and water runoff as affected by the design of the solar PV panels.

H3. LAI spatial and seasonal variability will be explained by leaf condition and management of the solar park, notably sheep grazing in winter and mowing throughout the year.

H4. The area under the panels will act as a sink of carbon dioxide (CO_2) and demonstrate lower water vapor density in comparison to the gap which will act as a source of CO_2 and demonstrate higher ratios of water vapor density throughout the year due to shade from the PV panels.

Chapter 2, the aim of this study was to develop and evaluate a physically based, spatially explicit solar park soil temperature numerical model (HIS-PV, Heat In the Solar PV park). The following objectives were addressed, within an exemplar UK grassland solar park:

O1. Construct and parameterise a physically based numerical model to simulate grassland soil temperature.

O2. Evaluate the performance of the HIS-PV model for simulating spatio-temporal variation in soil temperatures.

O3. Determine the sensitivity of simulated soil temperatures at 10 cm depth to variations in key model parameters surface resistance (r_s), volumetric water content (VWC) and LAI under different meteorological conditions.

Chapter 3, the aim of this study was to assess the impacts of solar parks on crucial environmental drivers which among others regulate the microclimate and thus the annual Growing Degree Days (GDDs) at the host-environment across different climate zones. To address the magnitude of these effects, the following objectives were addressed:

O1. Assess the effect of solar parks in different climatic zones on soil temperature in 10 cm depth, Potential Evaporation (PE) in the summer and the annual incoming short-wave (SW) radiation at the soil surface.

O2. Quantify the variability in GDDs caused by the physical presence of a solar park of a land in different climatic zones.

Chapter 4, the aim of this study was to rapidly advance understanding of the climatic impacts of solar parks and postulate the implications for ecosystem function and consequently service provision. Moreover, to use the synthesis to identify key knowledge gaps to direct future research. To achieve this the following objectives were assessed:

O1. Synthesise current understanding of the local climate impacts of solar parks.

O2. Outline the potential implications of the altered climate on ecosystem processes and services.

O3. Identify critical research needs, optimizing solar parks hosting ecosystem sustainability.

1 Chapter 1: Impacts of a Solar Photovoltaic Park in a Grassland on Microclimate and Ecosystem Response

1.1 Abstract

Globally, there is an increase in the number and size of ground-mounted (land-based) solar photovoltaic (PV) installations. Despite this land-use change, the potential impacts of solar PV parks on ecosystem functions are poorly resolved. Understanding the impacts of solar PV parks on microclimate is crucial, as climate is a key driver of ecosystem processes, function and service provision. This study quantifies the microclimatic impacts, and ecosystem response in a grassland hosting a solar PV park, in Wiltshire, UK, during 2015-2016. The spatio-temporal effect was assessed during growing and non-growing season using five linear transects, each running perpendicular between two PV panel rows. Under the PV panels mean air and soil temperature during the growing season were cooler compared to the gap between the PV panel rows, by approximately 2 °C and 4 °C, respectively. Further, the soil moisture under the panels was higher during growing season compared to the gap. Under the PV panels, soil bulk density was higher, and the organic matter lower, likely the result of compaction and vegetation management during and after construction. However, the induced microclimate showed no spatial effect on leaf area index (LAI) nor on the net ecosystem exchange (NEE) and the water (H_2O)

vapor fluxes. The findings suggest that the host environment shows potential of recovery within five years post-construction and the grassland's adaptation under the induced microclimatic change. To optimize the characterization of a land hosting a solar park and promote ecosystem functions, long-term monitoring and modelling approaches to upscale the research characterising the effects under diverse conditions of air and soil climate, are strongly suggested.

Keywords: photovoltaics, solar park, grasslands, spatio-temporal variability, microclimate, leaf area index, carbon dioxide fluxes, water vapor fluxes, bulk density, organic matter

1.2 Introduction

Renewable energy production is increasing, with solar energy reported to be one of the most sustainable energy sources with resource potential across the world (Kamat, 2007; Pogson et al., 2013). Globally, photovoltaics (PV) solar power generation showed a historical increase of 40% from 2014 to 2017 (around 460 TWh), representing 2% of the total world energy electricity generation (IEA, 2018b). Until 2016, the UK ranked fourth in the global solar markets (RECP, 2017), increasing its power generation by 9%, from 2016 to 2017, (total of 10.4 GWh; UK Government (2018)). In 2017, solar PV contributed 12.75 GW to the UK national grid, with 0.5% of the total UK power generation deriving from 937,421 solar PV installations (UK National Statistics, 2017). Ground-mounted PV solar, hereinafter referred to as solar parks, accounted for 59% of PV energy generation (UK National Statistics, 2017).

Solar parks vary in size and design and are formed by a metal frame that is driven into the ground to hold the panels up at a fixed angle. They have been deployed in large areas across the world, in a range of ecosystems from desserts to grasslands (Armstrong et al.,

2016; Hassanpour Adeh et al., 2018; Ravi et al., 2014; Barron-Gafford et al., 2016). Within the UK solar parks, cover an area of ~ 100 km^2 (Capell, 2016). Hypothetically, the UK energy demand could be supplied by 2,700 km^2 (~1% of the country's area) of solar parks based on a total capacity of 410 GW (EcoExperts, 2018).

European solar parks are primarily deployed on converted arable lands and grasslands (EIAs; (BRE, 2013; Armstrong et al., 2016)). Converting arable lands and grasslands induces a modified microclimate and is expected to affect environmental processes including vegetation and soil carbon (C) stocks (Rounsevell and Reay, 2009; Ostle et al., 2009a). Grasslands ecosystems' importance on the Earth's energy balance is undoubtable, providing critically globally significant ecosystem services, such as food and water, supporting nutrient cycles and oxygen production, also grasslands are regulating local and regional climates (DeGroot et al., 2002; Novick et al., 2004). Grasslands can be an important ecosystem for biodiversity (Qi et al., 2018), creating habitats for a wide variety of flora and fauna (Cardoso et al., 2013). Grasslands are also a large and important soil C store (Thornley et al., 2006); within the UK, they store 240 ± 200 kg of C per hectare (ha) per year resulting in a total UK store of approximately 9.8 ± 2.4 billion tonnes of C (Ostle et al., 2009b).

Despite the influence of microclimate on ecosystem processes with implications for ecosystem services (Stenseth et al., 2002), the spatio-temporal effects of solar parks on a grassland's microclimate, are poorly understood. Recent research addressed the temporal magnitude of microclimate and its effect on greenhouse gaseous (GHG) fluxes and biodiversity in a typical solar park (Armstrong et al., 2016). The solar PV arrays, reduced the park's albedo; panels are darker and thus have a lower albedo (~0.1) compared with soil and/or vegetated surfaces (a typical temperate grassland has an albedo of ~0.25; (Barron-Gafford et al., 2016), and intercept of light and precipitation.

These changes alter regulators of microclimate on a spatio-temporal scale, such as evaporation, wind speed, soil moisture, soil temperature and air temperature (Armstrong et al., 2014a). PV panels have been observed to alter the microclimate beneath them, decreasing the summer soil temperature by 5.2 ºC while increasing winter soil temperature by 1.7 ºC under the PV arrays relative to control areas (Armstrong et al., 2016). Soil moisture was surprisingly high under panels due to rainfall falling along the PV panel supporting frame (Armstrong et al., 2016). Modifications of the park's albedo, air temperature and soil moisture contents, causes perturbation to all associated fluxes of the surface energy balance, such as soil-evaporation and vegetation-transpiration, (Oke, 1987; Armstrong et al., 2014b; Jackson, 1973). Effects on evapotranspiration (ET), and thus soil moisture will further impact vegetation growth (Marrou et al., 2013c).

Reduced incoming short-wave (SW) solar radiation under the PV panels, leads to reduced photosynthetic activity (Oke, 1987). However, microclimate change caused by solar PV panels shading in agricultural land had a significant effect on productivity, increasing the total yield of lettuces (Marrou et al., 2013a). On the other hand at a grassland site, microclimatic change reduced biomass production to 25% under the PV panels compared with control areas (Armstrong et al., 2016). Such effects on vegetation growth, imply impacts on leaf area index (LAI), which may depend on plant species (Marrou et al., 2013a). LAI directly quantifies canopy structure and can be used to predict primary productivity and plant growth (Waring and Running, 2007). In addition, LAI is a crucial input parameter in environmental modelling because it has an important influence on exchanges of energy, water (H_2O) vapor and CO_2 between plants and the atmosphere (Best et al., 2011; Adams and Keith, 2013; Lee and Park, 2007; Wang and Jarvis, 1990).

Together, microclimate and LAI changes regulate GHG fluxes, both through reduced solar radiation receipts under PV arrays but also through other microclimatic changes. As

a result, CO_2 exchange (NEE) and H_2O vapor concentrations will likely vary spatiotemporally within solar parks. Both H_2O vapor and NEE, are important greenhouse gaseous fluxes for temperate grasslands (Verma et al., 1989) for water availability and C release or sequestration.

The microclimatic variability, the subsequent impacts on vegetation and GHG fluxes along with the land use disturbance during and post-construction (i.e. the removal of vegetation and compaction caused by the machinery during construction (Saini, 1966)), are also expected to affect soil physical properties (Bardgett et al., 1999). Soil bulk density and organic matter are important physical properties which affect soil health and plant growth. Soil bulk density would be expected to increase, and the organic matter to decrease (Keller and Håkansson, 2010; Gao et al., 2012; DelVecchia et al., 2014). However, Armstrong et al. (2016) found no spatio-temporal effect of bulk density and organic matter in a solar park.

1.2.1 Research aim

Rapid global solar PV deployment along with the associated land-use change to grassland ecosystems, have the potential to affect ecosystem services. The ecological importance of grasslands and the need to transition to renewable energy, means that the effect of solar parks on the microclimatic spatial variability, needs to be resolved. Consequently, this study aims to characterise this spatio-temporal variability in the air and soil climate, LAI, GHG fluxes and soil physical properties within a solar park. We hypothesised that:

H1. Photosynthetic Active Radiation (PAR), soil and air temperature, under the PV panels will be lower compared to the gap during growing season but are expected to demonstrate similar spatial distribution/trend from under towards the gap, during non-growing season. Soil moisture is expected to be higher under the PV panels in comparison

to the gap, as a result of precipitation runoff from PV panels side framing, reaching the surface under the PV panels.

H2. Soil bulk density will be higher under PV panels and organic matter lower under PV panels due to compaction, high soil heterogeneity across the park and water runoff as affected by the design of the solar PV panels.

H3. LAI spatial and seasonal variability will be explained by leaf condition and management of the solar park, notably sheep grazing in winter and mowing throughout the year.

H4. The area under the panels will act as a sink of carbon dioxide (CO_2) and demonstrate lower water vapor density in comparison to the gap which will act as a source of CO_2 and demonstrate higher ratios of water vapor density throughout the year due to shade from the PV panels.

1.3 Materials and methods

1.3.1 Site

Data were collected from Westmill Solar Park, Wiltshire, UK (51° 37' 03" N 01° 38' 45" W, altitude 100-106 meters, Figure 1.1(a); (Westmill Solar Farm, 2011). The 5 MW capacity solar park was installed in 2011. The park had a parallelogrammical design, formed by 36 PV panel rows to the west and 33 rows to the east of a central north-south passageway. The park covers a total of 121,000 m² (Figure 1.1(b)). The area under the PV panels was 29,000 m², the gap area between panel rows was 58,000 m², and the area between the PV panels and boundary fence 34,000 m². The park was seeded after construction (in 2011-2012) with a species-rich meadow mix. The grassland was sheep grazed in the winter and strips parallel to the northern and the southern PV panel row

edges (straight line strip of 1.50 m width; Figure 1.1(c)) mowed twice annually to prevent PV panels' shading.

1.3.2 Experimental design

The study consisted of eight sampling periods between two to five days in duration, spread between March 2015 and March 2016. May, June, July and early September sampling periods were classified as growing season and October, December and March as non-growing season (Table 1.1). Microclimatic characteristics of each visit are available in Tables 1-4 in Appendix 1 - SI.1, p. 207.

Table 1.1: Field sampling days, timers and average temperatures (from the spatial explicit experiment). The daily air temperature means derived from the spatial explicit experiment. M stands for morning, A for afternoon and E for evening sets of measurements.

Visits	Dates	Time of Measurement	Air temperature (daily mean)
1.	30.03-31.03.2015	(Pilot and soil sampling)	5.1 °C
2.	13.05-14.05.2015	M, A and E	15.4 °C
3.	22.06-25.06.2015	M, A and E	21.2 °C
4.	14.07-18.07.2015	M and E	20.6 °C
5.	02.09-05.09.2015	M and E	14.2 °C
6.	28.09-01.10.2015	M, A and E	15.2 °C

7.	30.11-01.12.2015	M and A	11.8 °C
8.	04.03-06.03.2016	M and A	5.2 °C

Five linear transects, 11.25 m in length running perpendicular between two PV panel rows were randomly located within the solar park (Figure 1.1(b)). Fifteen sampling points were identified at equal distance (0.75 m intervals) along each transect (total sampling points n = 75). The initial 4.5 m length (six sampling points), of each transect was under the panels, hereinafter mentioned as 'under'. The section of the transect in the gap between the two panel rows, hereinafter mentioned as the gap, was 6.75 m in length (nine sampling points). The length connecting two sampling points at 4.5 m and at 5.25 m, were under the northern panel edge of the panel, hereinafter mentioned as northern panel edge, and the last transect point at 11.25 m distance, was the point close and/or under the southern panel edge of the next panel row (two transects had their last sampling point under this edge), hereinafter mentioned as southern panel edge. At each transect, air and soil microclimate, soil properties and LAI were measured at each sampling point. Gaseous fluxes were recorded at one point under, at sampling point 1.25 m, and in the gap, at sampling point 7.5 m.

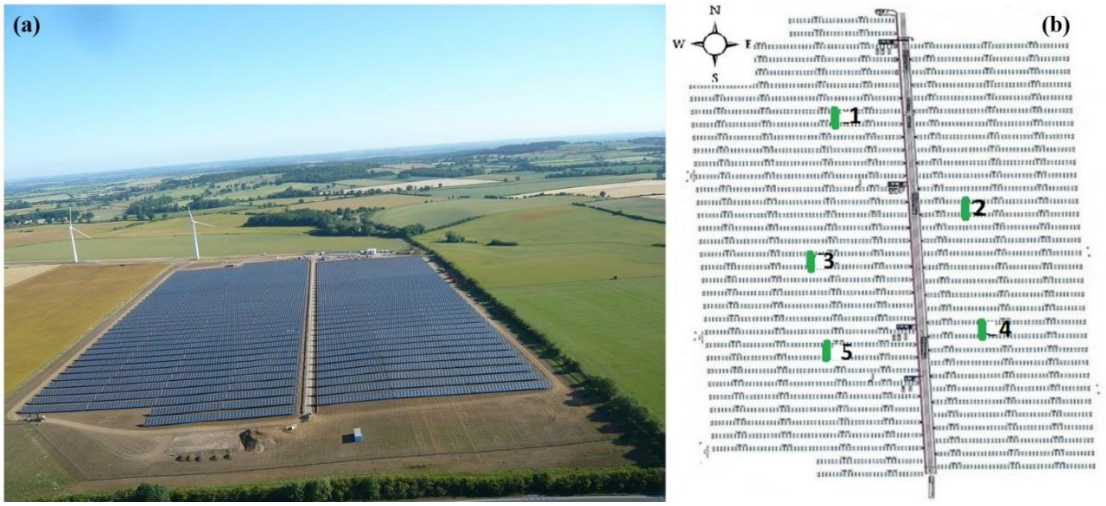

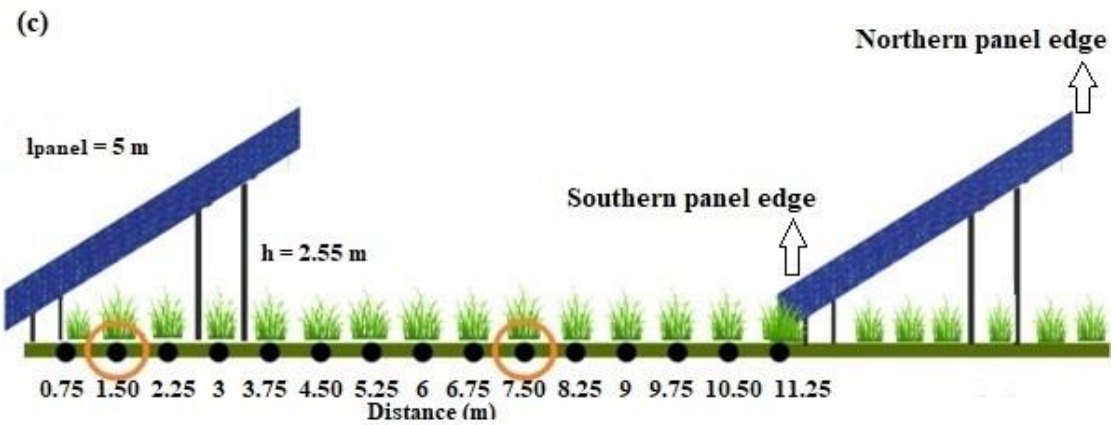

Figure 1.1: (a) Westmill Solar PV park panoramic photograph and (b) the construction map illustrating the placement of the five linear transects (green coloured lines). (c) Linear transect experimental design with a 0.75 m interval. The length under the panels was 4.5 m and the length at the gap between two panel rows was 7 m. Gaseous fluxes were measured from two plastic collars at 1.5 m sampling point under and at 7.5 m sampling point in the gap between two panel rows (orange circles). lpanel, is the length of the PV panel surface, h, the height of the northern edge of the panel.

1.3.2.1 Microclimatic spatial variability

For all 75 sampling points, soil moisture (volumetric water content; VWC), Photosynthetically Active Radiation (PAR), soil temperature and air temperature were measured during every sampling period two to three times per day (M for morning, A for afternoon and E for evening. VWC was measured using a theta probe (MM3 Theta Probe Soil Moisture Sensor; Delta-T Devices (UK-b)) in the top 6 cm of soil (m^3/m^3), PAR ($\mu mol\ m^{-2}\ s^{-1}$) was measured above the vegetation canopy using a SKR 110 Red/Far-Red pyranometer sensor with the SKR100 display meter (Skye Instruments, UK). Soil (°C; 10 cm depth) and air temperature (°C; above vegetation canopy) were measured using two Superfast Thermapens (Global FSE, UK). All measurements across the five transects

were conducted within 50 minutes. All the equipment was calibrated before and after each visit.

Precipitation and open water evaporation, at the soil surface were measured using 75 precipitation gauges and mini evaporation pans (surface areas = 56.7 cm^2). Pairs of jars were installed in the ground, at each sampling point of the transects on the 22nd of June. Nets were used to secure the top of the jars to prevent animals and insects entering. Sampling took place twice, summer (22nd of June-4th of September 2015) and autumn season (5th of September-1st of December 2015). Evaporation pans were initiated with a 60 mm depth of water and the rain gauges with 20 mm depth of lower density vegetable oil to prevent evaporation.

Evaporation was calculated using data from both jars in the following equation: *E = [w - ow] - injected water proportion*, where, evaporation *E*, measured in mm, *w* the amount of water collected in the water jar and *ow*, amount of water in the oil jar during data collection.

1.3.2.2 Soil properties spatial variability

Soil bulk density (g/cm^3) and organic matter (%) were determined from soil samples collected on the 31.03.2015. Soil samples were collected from each of the 75 sampling points using a bulk density steel core with a 7.5 cm diameter and 5.5 cm height (core volume = 242.86 cm^3). Soil analysis was performed in accordance with Emmett et al. (2008).

Bulk density was determined, by oven drying samples at 105 °C until constant weight. Immediately after, soil was sieved to separate stones; stone density was measured due to high intensity of stone particles. Soil and stone weight as well as stone volume (Lang and

Thorpe, 1989), were recorded and bulk density was calculated using the following equation:

$$\text{Bulk density}\left(\frac{\text{g of soil}}{\text{cm}^3\text{ core volume}}\right) = \frac{[\text{Dry weight core (105 °C)(g)} - \text{Stone weight (g)}]}{[\text{Core volume (cm}^3) - \text{stone volume (cm}^{-3})]} \quad (1),$$

Soil gravimetric water content (GWC) was calculated using the following equation:

$$\text{GWC}\left(\frac{\text{g of water}}{\text{g of soil}}\right) = \frac{[\text{Fresh Soil Weight (g)} - \text{Dry Soil Weight (g)}]}{\text{Dry Soil Weight (g)}} \quad (2),$$

Organic matter was determined by loss on ignition (LOI), 10 g of oven dried soil (at 105 °C) was put in a muffle furnace at 375 °C for 16 hours. To calculate the organic matter (OM %) of the soil samples the following equation was used:

$$\text{OM (\%)} = 100 * \frac{[\text{Prior Ignition weight (105 °C)(g)} - \text{Post Ignition weight (375 °C)(g)}]}{\text{Prior Ignition weight(105 °C)(g)}} \quad (3),$$

1.3.2.3 Leaf Area Index (LAI)

LAI was assessed by harvesting all above ground biomass from 40 cm² at each point on the transect in May, June, October and December. This represents the growing season (May and June) and the non-growing season (October and December). During July and early September (growing season) samples were collected from 1.5 m, 4.5 m, 7.5 m and 11.25 m along each transect, (two points from under and two from the gap). Samples were stored overnight in a cool room and then (12-24 hours after cut) were separated to dead (non-transpired dry and brown; NT) and alive (transpired wet and green leaves; T) vegetation, excluding the plant stems. Two methods were used to analyse the LAI, a conventional scanner and ImageJ software (Schneider et al., 2012) for May, June, July and early September samples and a LI-3100C Area Mater (LI-COR, 2017) for October and December samples. An investigation was performed to evaluate and compare the two methods ($R^2 = 0.8$).

1.3.2.4 Gaseous fluxes

NEE and H_2O vapor flux were measured using a portable static chamber system approach (Trucco et al., 2012; Armstrong et al., 2015; McEwing et al., 2015). CO_2 concentrations and absolute humidity (water vapor pressure in millibars (mb)) were measured from 10 collars, 30 cm diameter, installed along the five transects (Figure 1.1(c)), using an EGM-4 infrared gas analyser (IRGA, PP Systems (USA)), attached to a transparent chamber. Collars were carefully sealed in the soil to minimise root disturbance one month prior to the first measurement; 22nd of June 2015. Measurement across the site were performed over a period of approximately one hour and 30 minutes. Measurements were not performed during rain and during periods were the PAR < 5 μmol m^{-2} s^{-1} under and at the gap (Trucco et al., 2012).

NEE was calculated using the following equation (McEwing et al., 2015),

$$F_{CO_2} = \mathrm{S} \cdot \frac{\mathrm{V} \cdot \mathrm{M_{CO2}} \cdot 273.16}{\mathrm{A} \cdot \mathrm{V_m}\ (273.16+\mathrm{T})} \cdot\ 3600\ \cdot\ 1000 \quad (4),$$

where, F_{CO_2}, is the flux (mg m^2 hr^{-1}), S , the gradient of CO_2 concentration changes over a time interval (IRGA's 124 seconds), V, the volume of the chamber (0.019 m^3), M_{CO_2}, the molecular mass of CO_2 (44.095 g/moles), A, the area of the collar (bottom chamber; equal to 0.071 m^2), V_m, the universal gas constant (82.058) and T, is the air temperature in degrees Celsius (°C).

H_2O flux (mm H_2O hr^{-1}), was determined analogues to equation 4 as:

$$F_{\mathrm{water}} = \rho \cdot \frac{\mathrm{V} \cdot \mathrm{M_{water}} \cdot 273.16}{\mathrm{A} \cdot \mathrm{V_m}\ (273.16+\mathrm{T})} \cdot\ 3600\ \cdot\ 1000 \qquad (5),$$

As a form of quality control, for the fluxes included in the analysis, regression plots and their R-squared (R^2) values of concentration towards sampling time duration, were used.

During the summer R^2 values below 0.8 and during winter measurements (McEwing et al., 2015), R^2 values below 0.5 were rejected from the analysis (because out of the growing season C fluxes in grasslands ecosystems are relatively stable; Trucco et al. (2012)).

1.3.3 Data analysis

The statistical analysis was conducted using R programme language within the RStudio environment version 3.3.2 (RStudio, 2015). The packages used for statistical analysis and data representation were, gam (for model predictions prior analysis; (Hastie and Tibshirani, 1986)), scales (Hadley Wickham, 2017), ggplot2 (Hadley Wickham, Winston Chang, 2016) and dplyr (Hadley Wickham, Romain Francois, Lionel Henry, Kirill Müller, (R Core Team, 2017)). Results were reported as significant when p values ≤ 0.05. ANOVAs (analysis of variance) and a post-hoc Tukey HSD (Honest Significant Difference) test was applied to indicate means that differed significantly (Tukey, 1977). Tukey post-hoc is considered a thorough and strict method which considers all possible pairwise differences at the same time and is accepted widely in ecology (Day and Quinn, 1989).

For H1, to assess the probability of PV arrays physical presence creating temporally dynamic microclimatic niches, a three-way ANOVA was used with distance along the transect, hereinafter mentioned as distance (which could also be assessed as categorical as it is a count variable; specific distance along transects from one point to the other), time of day and season as the explanatory variables. For evaporation, the data were transformed by adding 100 to each measurement (to avoid having negative values in the dataset). For H2, soil bulk density and organic matter spatial variability post construction,

generalised additive models (GAMs), which capture non-linear patterns (Wood, 2006) were used with distance along the transect and stone density as explanatory variables.

To assess H3, to investigate the spatio-temporal variability in LAI, distance along the transect, growing season (in and out) and leaf condition (T and NT) were used as explanatory variables using a three-way ANOVA. LAI data were transformed by adding 1 unit to each measurement (for zero values in the dataset) and then log transformed, given the data distribution, to avoid violation of statistical assumptions. Finally, for H4, to assess the spatio-temporal variability of NEE and water vapor in the solar park, location and date, were used as explanatory variables using a four-way ANOVA, and the maximum negative value +1 was added to all fluxes (water vapor density and CO_2) to avoid having negative values in the dataset.

1.4 Results

1.4.1 H1. Microclimatic spatio-temporal variability

1.4.1.1 Air Temperature

During growing season, morning, afternoon and evening, air temperature under the PV panels was significantly cooler than the gap by 1.2-2.2 °C ($p < 0.001$; Figure 1.2). Overall, in the morning the mean air temperature along the transect was cooler (16.4 °C) compared to the afternoon and evening metrics which were similar throughout (20.1 °C and 20.2 °C, respectively), with $p < 0.001$ among the three times of day. The difference between the minimum air temperatures under and at the gap was similar (less than 1 °C; Table 1 in SI.1) with under warmer in the morning and the afternoon. The maximum air temperatures in the morning and in the evening, showed a 3.5-4 °C difference between under and gap (warmer throughout the day). The difference was at its peak during the afternoon, with the gap exceeding the under by 10 °C (Table 1 in SI.1).

During non-growing season, mean air temperature increased by 3 °C throughout the day ($p < 0.001$). The minimum and the maximum air temperatures between under and gap were similar (less than 0.5 °C difference; Table 1 in SI.1) with under slightly cooler and gap slightly warmer in the morning and afternoon, respectively. The overall trend along the transect was different to the growing season, with temperatures gradually cooling down, up until the northern panel edge and gradually warming up by ~3 °C along the gap, especially in the afternoon and evening periods (Figure 1.2).

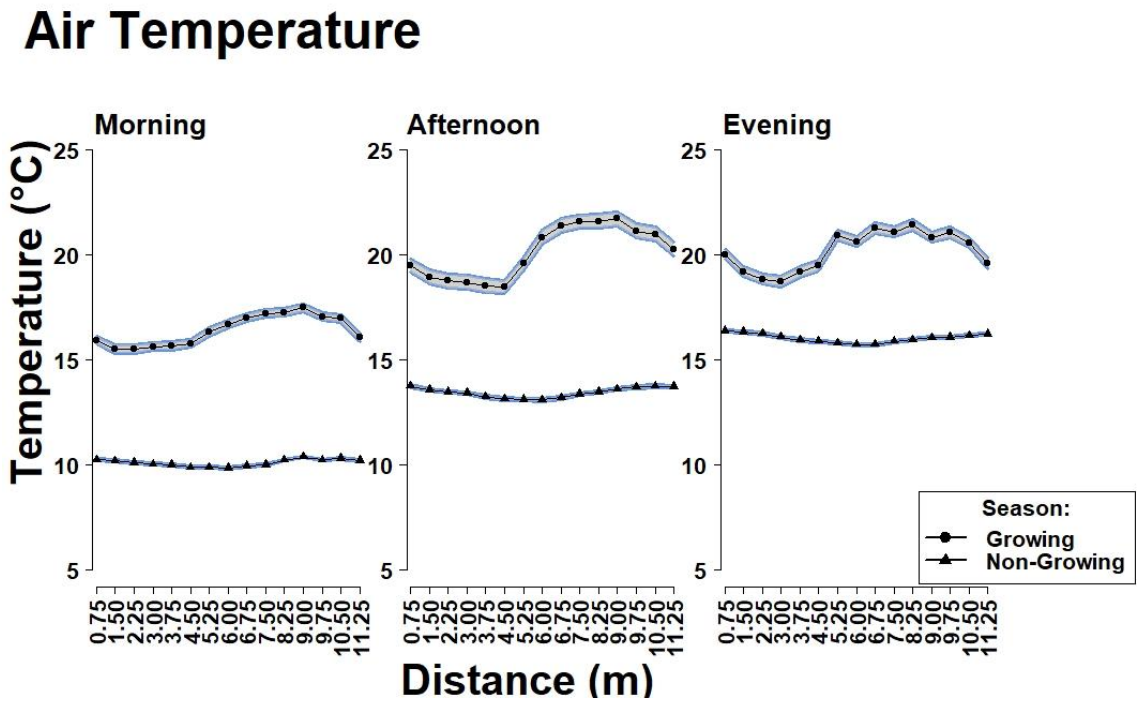

Figure 1.2: Air temperature metrics spatial distribution of the means, in three times of the day during growing and non-growing season along the five linear transects. Blue shaded area illustrating the standard error of the mean.

1.4.1.2 Soil Temperature

Growing and non-growing season soil temperatures along the transect demonstrated a similar pattern compared to air temperatures, but with the soil remaining cooler than the air and the transitions from under to the gap being sharper at each time period (Figure 1.2

and Figure 1.3). During the growing season, soil temperature under the PV panels was cooler throughout the day compared with the gap ($p < 0.001$). Further, soil temperatures demonstrated sudden increases at the northern panels' edges, which in the evening reached 5 °C ($p < 0.001$). The differences between the minimum temperatures under and the gap ranged from 1.3 °C in the morning to 2.4 °C in the evening, while the maximum temperatures ranged from 3.2 °C in the morning to 8.8 °C in the evening. In the afternoon the difference between the maximum soil temperatures were minor (0.3 °C; gap warmer) and between the minimum soil temperatures the difference was 2 °C (gap warmer; Table 2 in SI.1).

During the non-growing season, morning and afternoon soil temperature trends along the transects were more similar with slightly warmer soils in the afternoon (Figure 1.3). Soil temperatures along the transect were gradually increasing from morning to afternoon and afternoon to evening (15.2 °C, 16.4 °C and 17.3 °C respectively). Morning and afternoon mean under and at the gap were the same, 9.2 °C, with gap's minimum and maximum values warmer by 1 °C in the afternoon (Table 2 in SI.1). Soil temperature mean increased gradually at the northern panel edge, (breaking points at 3.75 m-5.25 m along the transect; alike the air temperature). Both soil temperature means under and at the gap in the evening were ~1 °C warner compared with the morning and afternoon temperatures ($p < 0.001$). There was a sudden increase of the minimum soil temperatures in the evening of 7 °C (was ~2.5 °C in the morning and the afternoon) while the maximum temperature was increasing by 1 °C from the morning to the evening (Table 2 in SI.1).

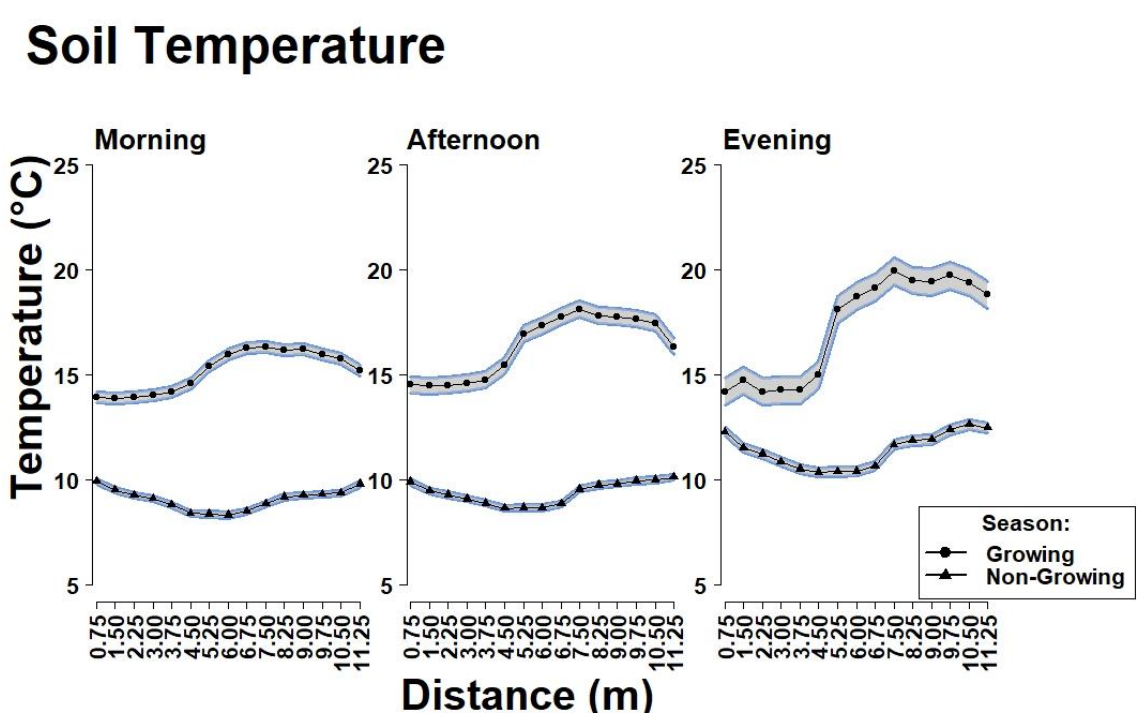

Figure 1.3: Soil temperature metrics spatial distribution of the means, in three times of the day during growing and non-growing season along the five linear transects. Blue shaded area illustrating the standard error of the mean.

1.4.1.3 Soil moisture

Soil moisture demonstrated the greatest small-scale variations of all the examined microclimatic variables (Figure 1.4). This was notable under the panels regardless of season or time of the day. Further, there were sharp and significant fluctuations under the panels from one point to another ($p < 0.001$), while at the gap the most significant change occurred at the last sampling point (southern panel edge). Despite these small-scale variations, during growing season, under was on average moister than the gap regardless time of day ($p < 0.001$). Further an abrupt transition between under and the gap was evident at sampling point 4.5 m (northern panel edge). During the non-growing season, the gap demonstrated a reversed trend with distance along the transect; the soil moisture decreased towards the southern panel edge. Overall, the section of the transect under the PV panels was drier compared to the gap ($p < 0.001$).

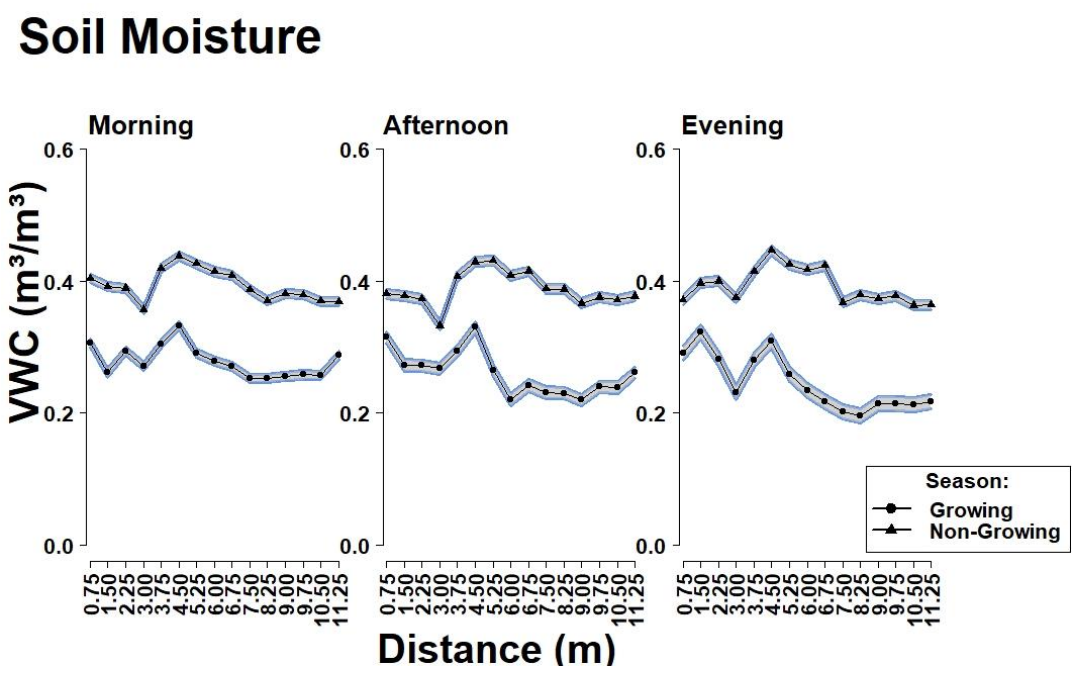

Figure 1.4: Soil moisture metrics spatial distribution of the means, in three times of the day during growing and non-growing season along the five linear transects. Blue shaded area illustrating the standard error of the mean.

1.4.1.4 PAR

PAR increased over a short distance at the northern panel edge and reduced over a short distance at the southern edge (Figure 1.5). Further, PAR, was constantly lower under the PV panels compared to the gap, regardless of time of day, during growing and non-growing season ($p < 0.001$). The maximum difference between under and gap, was in the afternoon of the growing season were the gap reached 975 μmol m^{-2} s^{-1} and under received just 218 μmol m^{-2} s^{-1} ($p < 0.001$; Table 3 in SI.1). PAR in the morning and evening of the growing season demonstrated similar magnitudes and were significantly different to the afternoon ($p < 0.001$). The standard error of the mean was higher in the afternoon during both seasons for both under and gap.

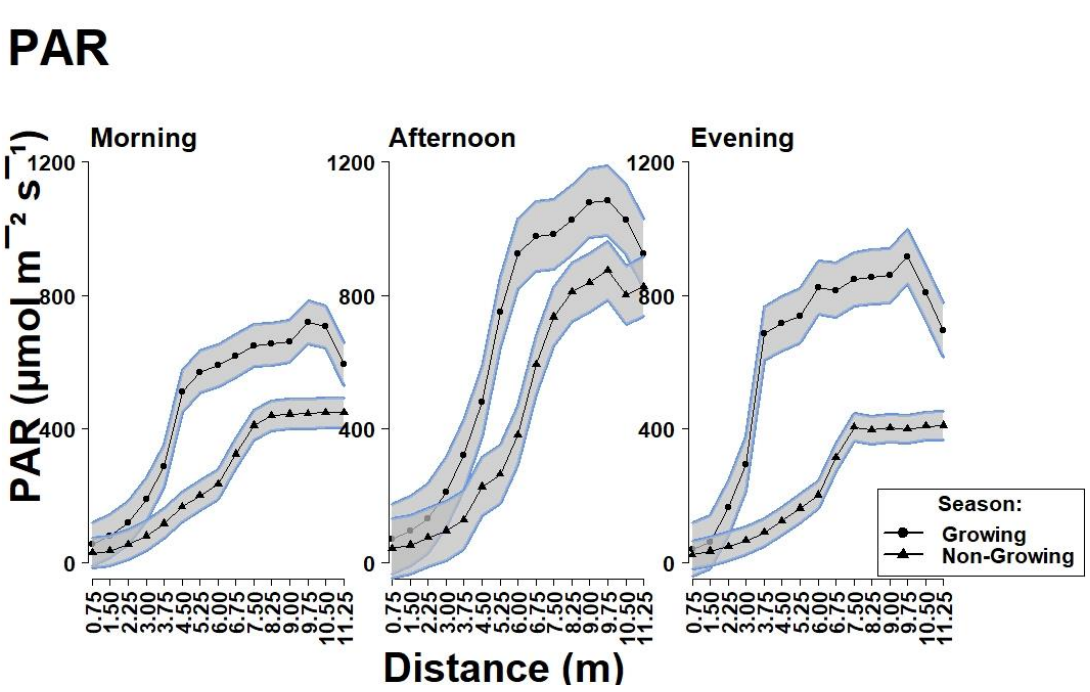

Figure 1.5: PAR metrics spatial distribution of the means, in three times of the day during growing and non-growing season along the five linear transects. Blue shaded area illustrating the standard error of the mean.

1.4.1.5 Precipitation and Evaporation from an open water system

Precipitation differed significantly between growing and non-growing season along the transect ($p < 0.001$). Further, the spatio-temporal interaction (season and distance) showed evidence of significance with $p < 0.05$. Over the entire sampling period, under and gap precipitation differed significantly, with precipitation under the panels being always lower ($p < 0.001$) with a different distribution at each period tested (Figure 1.6). In addition, smoother transitions from one sampling point to the next, were observed during the growing season compared to out of season (Figure 1.6), with maximum precipitation deriving from 9 m along the transect (statistically different to both under and gap sampling points along the transect; $p < 0.001$). At the northern panel edge, precipitation demonstrated a steep rise, from under to the gap, with this sudden increase being sharper during non-growing season. The Tukey pairwise analysis illustrated a

statistical significance of those sampling points at the northern panel edge compared with the other under and at the gap ($p < 0.05$).

Evaporation did not illustrate a statistically significant spatial and/or temporal variation. However, during the non-growing season, there were some sudden spikes especially at 2.25 m, 8.25 m and 11.25 m along the transect (Figure 1.6). On the other hand, during growing season, the amount of the evaporation under the panels was gradually increasing towards the gap.

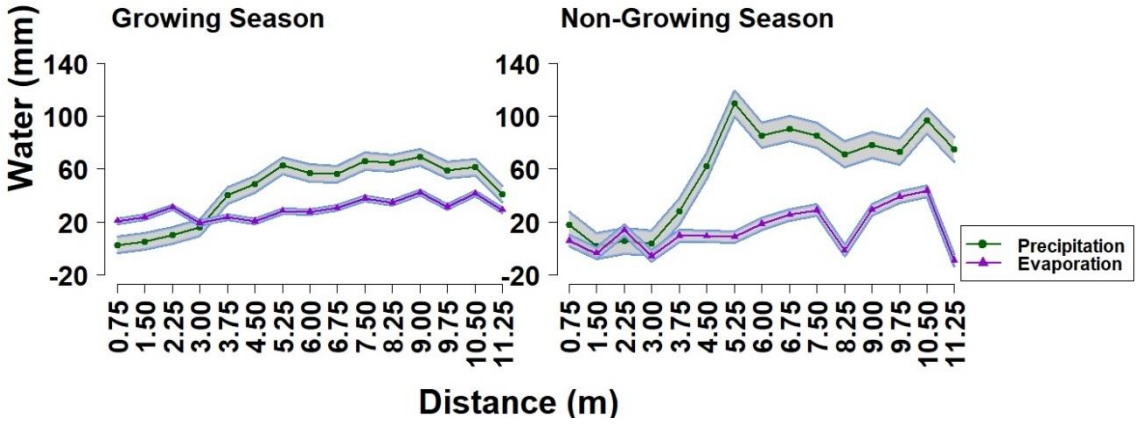

Figure 1.6: Precipitation and evaporation spatial distribution of the means during growing and non-growing season along the five linear transects. Shaded area illustrating the standard error of the mean.

1.4.2 H2. Soil properties spatial variability

Soil bulk density ($p < 0.001$ and $R^2 = 50\%$) and organic matter ($p < 0.05$ and $R^2 = 29.5\%$) varied significantly along the transect. Soil bulk density under was higher, compared with the gap (Figure 1.7a). Organic matter content increased slightly along the transect from the northern panel edge, with fluctuations in the gap ($p < 0.001$). Organic matter under, was lower compared with the gap ($p < 0.001$). Further, it was negatively correlated with the bulk density (Figure 1.7b). Stone density had also an impact on the bulk density and

on the organic matter variabilities along the transects ($p < 0.01$ and $p < 0.001$ respectively).

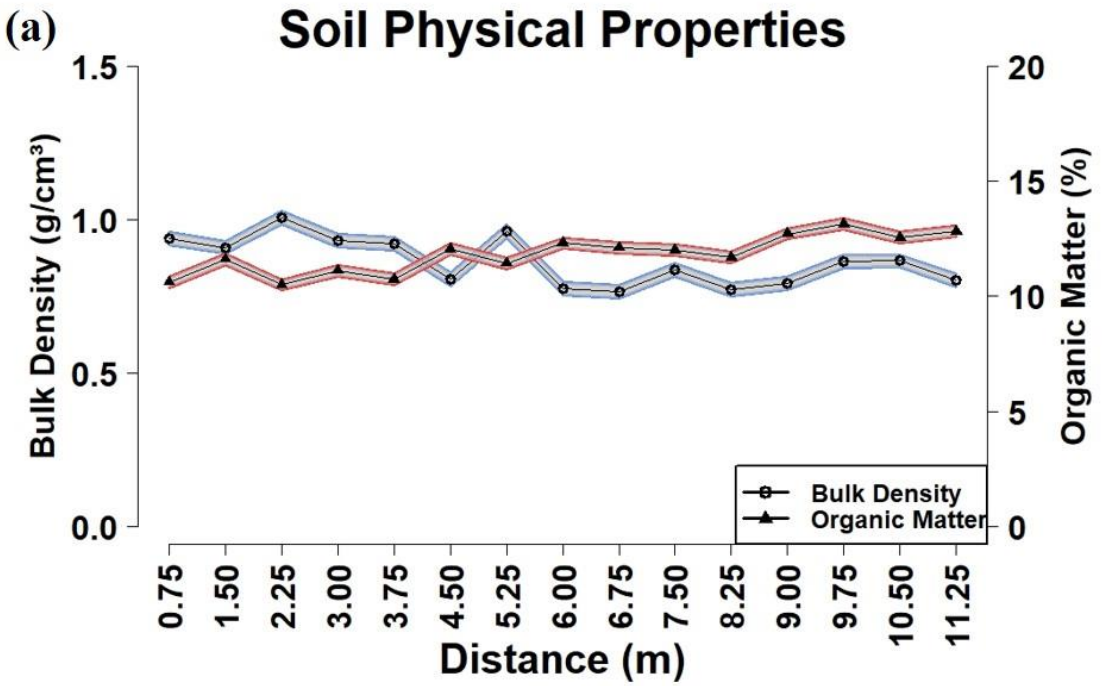

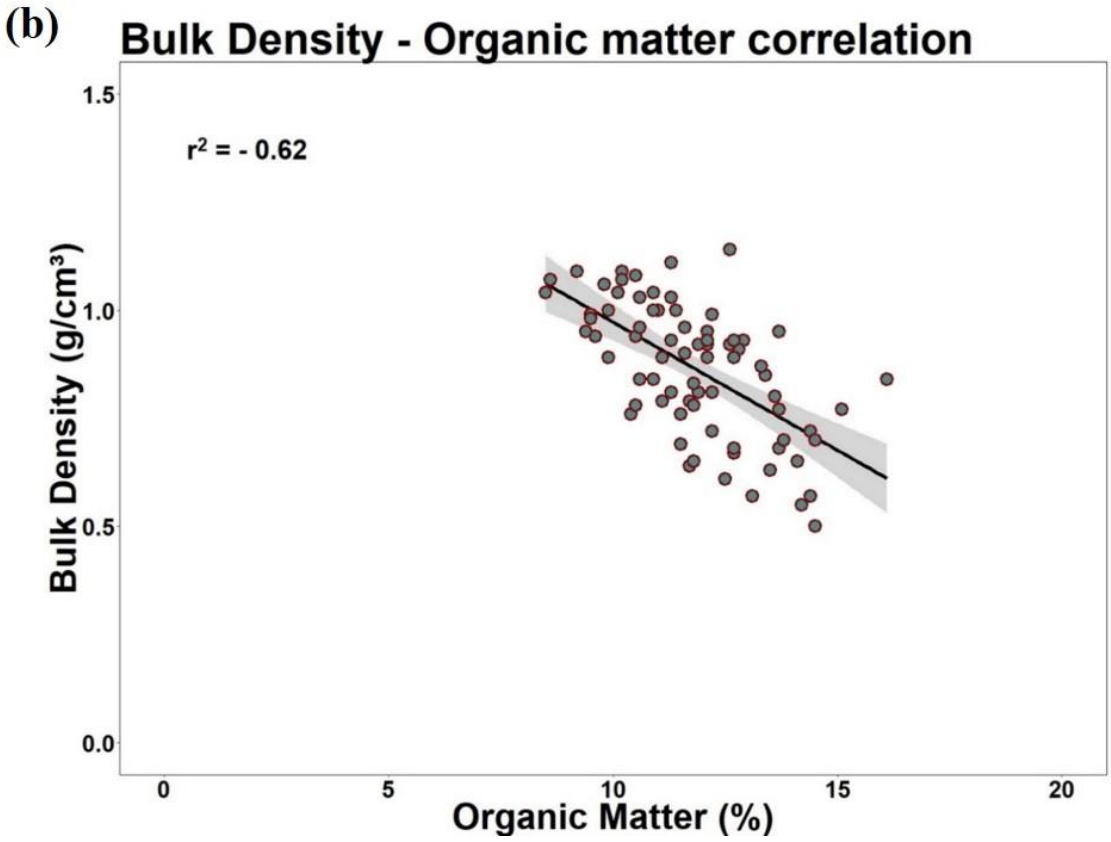

Figure 1.7: (a) Soil bulk density and soil organic matter with the error bars illustrating the standard deviation of each point along the transect. (b) The relationship between bulk density and organic matter, with the grey shaded area and smoothing line illustrating the 95% confidence intervals.

1.4.3 H3. LAI seasonal and spatial variability

LAI differed significantly with season, condition (T and NT) and their interaction ($p < 0.001$, Figure 1.8) and did not demonstrate a statistically significant variation with distance along the transect. There was more alive (T; green) than dead vegetation (NT; dry or decomposed) during the non-growing season ($p < 0.001$). Alive (T) vegetation was significantly different in growing season compared with the non-growing season and the pattern with distance along the transect was complex ($p < 0.001$ among sampling points on the transect).

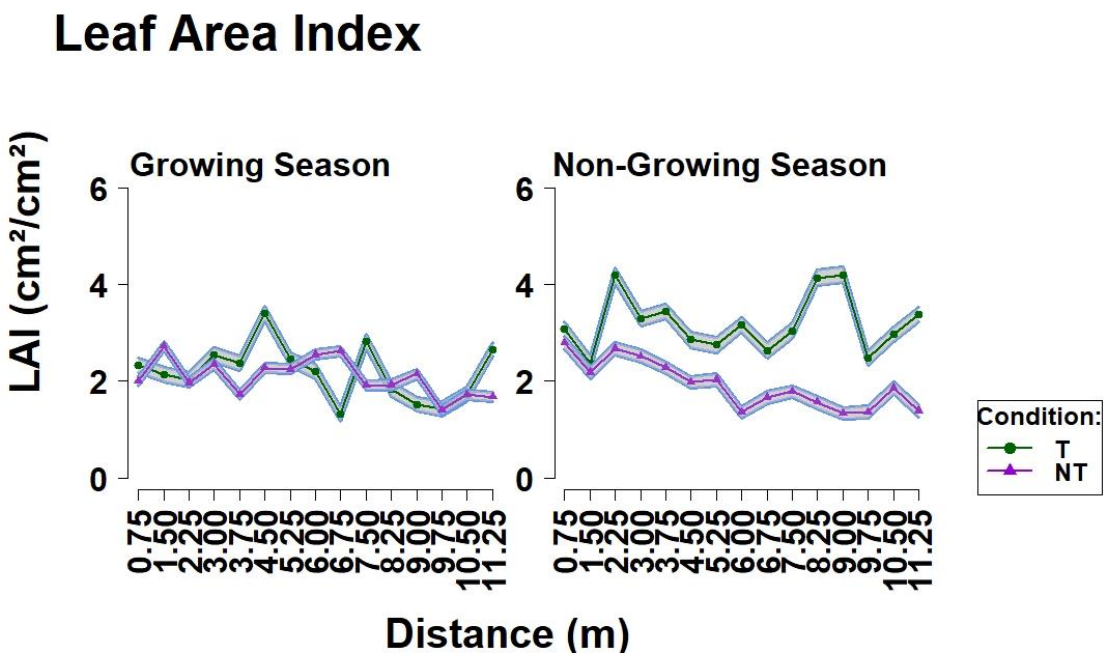

Figure 1.8: Leaf area metrics spatial distribution of the means of each condition (T ● and NT ▲), during growing and non-growing season along the five linear transects.

1.4.4 H4. NEE and Water vapor flux spatio-temporal variability

Overall, under and gap CO_2 and H_2O vapor fluxes differed significantly regardless of season ($p < 0.01$ for NEE and $p < 0.05$ for H_2O vapor). The area under the panels, was generally a sink for CO_2 in growing season (Figure 1.9 (a)). Further, the gap area appeared as a sink for CO_2 for all the dates apart from the 30th of November (non-growing season). Water vapor fluxes illustrated a statistical significance at the gap between the 1st of December and the 23rd of June ($p < 0.05$; Figure 1.9 (b)). The area under the panels was lower than the gap throughout apart from the 30th of November where the gap was lower than under.

(a)

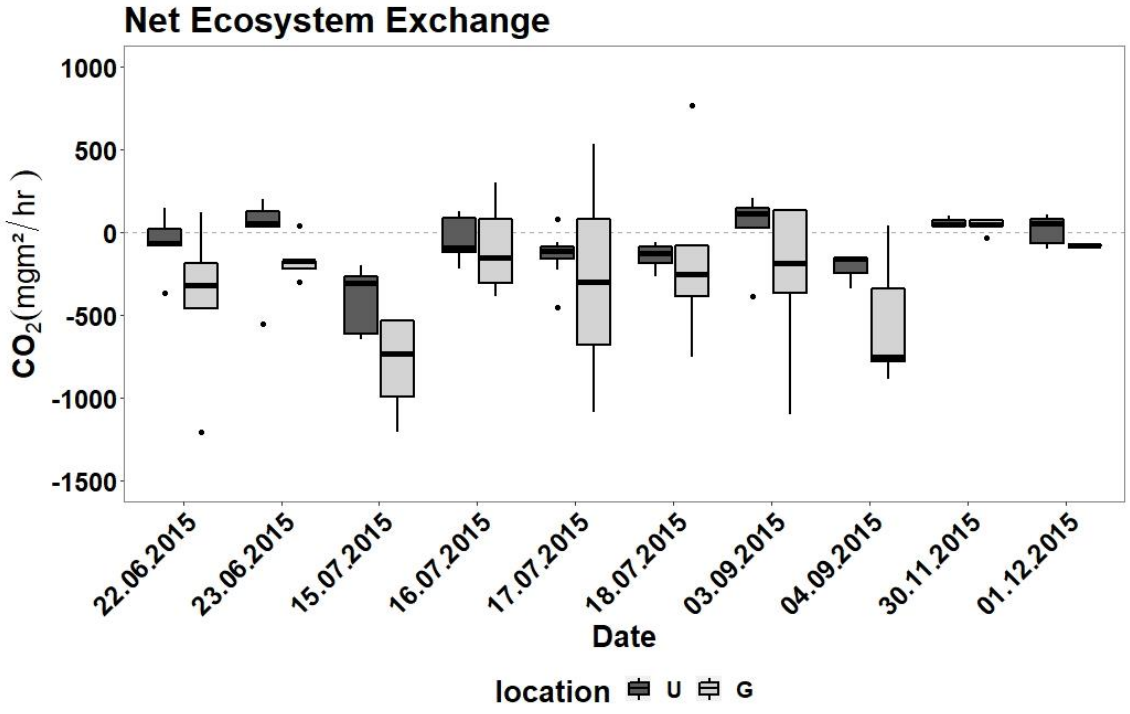

(b)

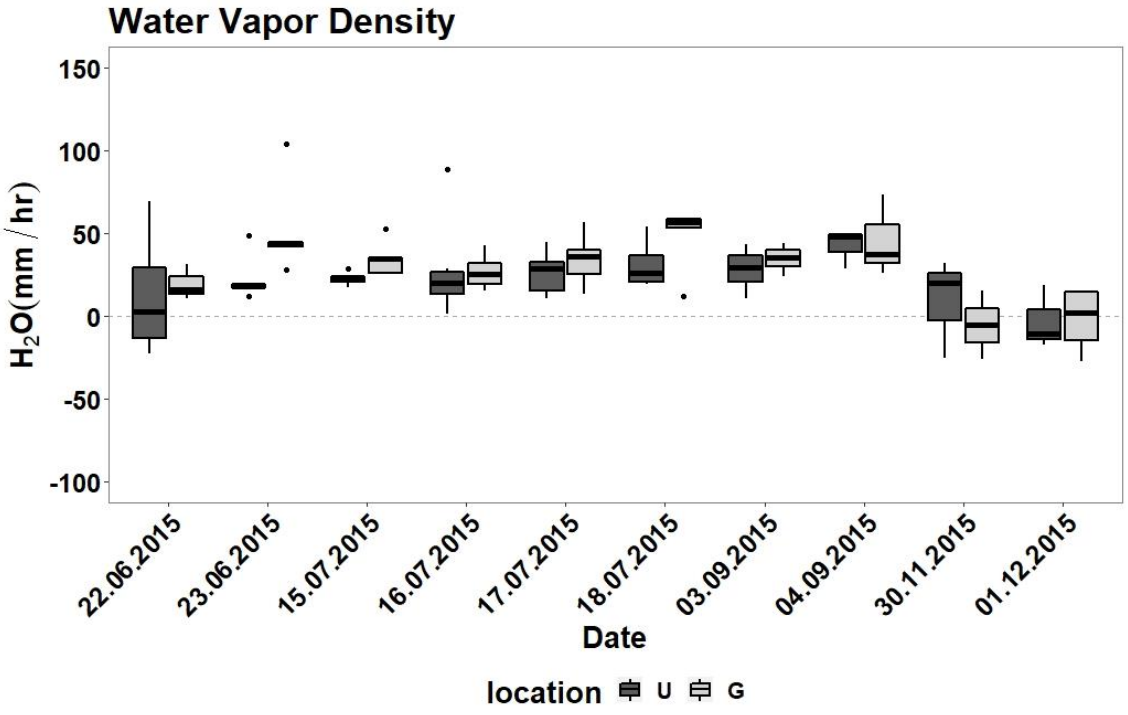

Figure 1.9: (a) CO_2 concentrations flux metrics represented as the NEE of two locations (under; U dark grey and gap; G light grey) and (b) H_2O in the solar PV park towards the date of the measurement. Box plots displaying minimum, first quartile (25th percentile), median, third quartile (75th percentile) and maximum CO_2 concentrations.

1.5 Discussion

There has been exponential growth in solar park deployment yet there is limited understanding of the impact of solar parks on the microclimate and implications for ecosystem processes. We found significant variation in microclimate and soil physical properties along the transects from the south edge of solar array rows to the south edge of adjacent rows. In contrast, LAI and GHG fluxes illustrated a seasonal effect (expected seasonal variation in LAI in a temperate climate) but no spatial effect (no difference through the solar park). Overall the PV panels' southern edge along with the northern

panel edge (Figure 1.1 (c)), were breakpoints of the sudden changes for most variables. Below we discuss the four hypotheses in turn.

1.5.1 H1. Presence of the solar parks creates temporally dynamic microclimatic niches

Soil and air temperature, soil moisture and PAR, are key ecosystem drivers, and were shown to vary spatially and temporally within the solar park (Clinton, 2003; Barnett and Facey, 2016; Davidoff and Selim, 1988; Armstrong et al., 2016; Federer, 1968; McEwing et al., 2015). All assessed microclimate variables followed a similar trend along the transects (lower under the PV panels and higher in the gaps) during growing and non-growing season, except for the VWC, which demonstrated a reversed relationship during growing season (see Figures under section 1.4.1). The spatial distribution of all aspects of microclimate during the non-growing season differed to those in the growing season likely due to the combination of PV panels and the daily and hourly variation of the azimuth and elevation.

For all tested aspects of microclimate, PV panels' edges, specifically the northern and the southern panel edges, were breakpoints. Air and soil temperature and PAR were lower under the PV panels, increased smoothly or sharply at sampling point 4.5 m (northern panel edge) and throughout the gap for all three times of the day. All variables decreased at the final couple of sampling points along the transect, close to the southern edge of the subsequent solar array apart from metrics during non-growing season. VWC was the only variable which demonstrated higher ratios during non-growing season and slightly increased soil moisture at the gap; along the final four sampling points towards the southern panel edge (Figure 1.4). This could be due to precipitation water runoff from the

PV panels which created water pools in front of the southern PV panels edge the cooler air temperature and the lower PAR under compared with the gap.

PAR is known to be positively correlated with rates of evaporation (Clinton, 2003), however, in this study, variations in PAR along the transect could not be strongly correlated with the evaporation as the spatial distribution of the later was quite stable (no spatiotemporal significance $p > 0.05$; Figure 1.6) with minor fluctuations along the transects. Whilst there were fluctuations in evaporation during the non-growing season, these could be explained by the occasional cover of the jars by the leaves in the middle of the transect (e.g. sampling point 8.25m); There were already interventions made from park's management, with grass occasionally being cut with machinery at the PV panels' southern and northern edges (park's management operating cuts at random periods per annum, when shading of panels from vegetation growth was a risk).

The fact that under the PV panels, both PAR and precipitation were lower compared to the gap, initially implied disturbance of the evaporation and therefore a direct effect on soil-plant interactions (Gupta et al., 2015). Evaporation under the panels during growing season, was approximately double the precipitation. This would imply drier soil under the panels, but soil moisture findings supported that the soil was wetter under and both air and soil temperatures cooler than the gap. It was assumed that there were limitations during the evaporation and precipitation (jars) experiment, because the area of the jars was small and thus easier to be covered by plants.

Assessing evaporation and precipitation from this solar park, the interest was placed on where were the patterns of variability across the site, and this small pan approach, whilst with limitations in its accuracy, provides reasonable precise measures that enable these patterns to be explored. Several studies using atmometers (small area of the belani plate) have been proven to assess evaporation with a good level of accuracy (Kettridge and

Baird, 2006; Alam and P. Trooien, 2001; Carder, 1960; Qian et al., 1996; Thom et al., 1981). Thus, even if it is recognised that the absolute values might not be so representable, in general is an approach widely used. Thus, it was anticipated that in this experiment, a small pan area provided reasonable precise measures that enable patterns to be explored.

Installing jars of wider area, would compromise the logic (spatiality) around the linear transect experimental design. The idea of implementing this type of spatial experiment was to grasp data from as many points as possible along a 11.25 m length (15 sample points on a 11.25 m transect) and thus get a point per point variability of the measured variables, which would be even more descriptive. Also, it has been proven that size of pans did not implement major differences into the actual result (Carder, 1960; Oke, 1987; McIlroy and Angus, 1964). In addition, having installed 150 jars in total on five transects across the solar park running the same experiment throughout, creates assumptions regarding the oasis effect (Agodzo et al., 1997; McIlroy and Angus, 1964; Li et al., 2013). Thus, the installation of bigger jars, would only increase any potential impacts.

PAR metrics demonstrated a significant gradient along the gap (wider margins of the standard error of the mean), regardless season (Figure 1.5), especially during the afternoon metrics (sun at a vertical position). This variability could be potentially explained by implications during measurements due to differences of time of day during measurement, as position of the sun in the sky changes. Further, as mentioned in Methods (and mainly at section 1.3.2.1), PAR was measured along five transects in a 121,000 m^2 area solar park at vegetation height, which as expected differed from one area to the other. In addition, the graphs illustrate mean PAR ratios taken by five transects of four campaign visits in the growing and four campaign visits out of growing season (Table 1.1). Naturally, PAR, that is known to be a sensitive parameter to measure as could be altered on the spot, by clouds or even by the time needed to get from one transect to the next

thus, was logically assumed to demonstrate these gradients especially at the gap (unsheltered area; Figure 1.5).

Air and soil temperature were significantly cooler under the PV panels compared to the gap, regardless of the time of the day and season. The changes between under and gap minimum and maximum values, were not of a magnitude known to impact plant processes, as location did not cause the temperature to cross the growing temperature thresholds of 5 °C to 25 °C, that define grassland growing season in temperate environments nor the frost level 0 °C during the non-growing season (Moot et al., 2000; Hassan et al., 2007), thus the impact on grass growth was assumed minor judging by the smalls differences between under and gap (Figure 1.2 and Figure 1.3). However, the temperature differences were of the magnitude known to impact ecosystem process rates.

The soil under the PV panels, was frequently wet due to water input from the edges of the PV panels' and supporting frame. Whilst evaporation rates were broadly similar to the gap, transpiration rates given the lower LAI, may have promoted higher soil moisture. In addition to lower PAR and air temperature, the higher VWC and evaporation rates under the panels during the growing season, could also have contributed to the lower air and soil temperature under PV panels, compared with the gap. Soil temperature is strongly correlated to soil moisture (Abu-Hamdeh, 2003; Davidoff and Selim, 1988; Alvenäs and Jansson, 1997; Davidson et al., 1998) as precipitation and evaporation (Figure 1.6) regulate soil temperature with feedbacks on soil moisture content.

The microclimatic niches were created on the grassland by the physical presence of the PV panels and were considered tenser but comparable to the observed effects of trees on grasslands (Morecroft et al., 1998; Yan et al., 2012). Tree canopies' size and shape vary with each species, and their artificial shade is directly correlated to the spatial microclimatic variability of the area at the sub-canopy as well as to temporal variability

such as season and time of day (agroforestry scheme). PV panels acting in a similar manner as tree canopies, create an artificial shade which had a spatio-temporal effect at the microclimate. Consequently, it should be possible to design solar parks to induce desirable microclimatic niches for ecosystem processes and mitigate crucial perturbations at the energy and water balance in a solar park ecosystem.

1.5.2 H2. Soil bulk density and organic matter vary spatially within solar parks

Soil bulk density and organic matter varied spatially through the solar park, confirming our hypothesis. Soil bulk density and organic matter was higher under and lower at the gap and the latter the opposite (Figure 1.7b). However, previous study performed in 2013 at the same site, showed no spatial effect of the PV arrays on the soil properties (Armstrong et al., 2016). Armstrong et al. (2016) took four samples under PV panels, four in the gaps and four in control areas rather than a transect approach as used here; different experimental design.

Microclimatic factors such as soil moisture, precipitation and evapotranspiration can affect, soil physical properties along with site management activities including the use of heavy machinery (Gong et al., 2003). Given Armstrong et al. (2016) did not find differences, it could be concluded that the differences arose because of the effect of different microclimate and implications for ecosystem processes. However, the choice of experimental design is crucial and the exact sampling locations could have caused the opposing results between the two studies. Alternatively, whilst compaction may have occurred during construction, vehicle use in on-going at the site, especially at the northern and southern panel edges during cutting and thus compaction could be being increased over time due.

Soil moisture content, affected by water runoff from the PV panels (discussed under section 1.5.1), may have had an effect on both organic matter and bulk density. Soil moisture depletion causes soil shrinkage creating cracks and fissures on the soil as observed at the site (Gavin and Agnew, 2000). The PV panels may have caused higher soil moisture under the panels but perhaps had a negative effect at the southern panel edge creating water pools. In addition, soil gravimetric content (data and analysis in SI.1 p.186) showed a strong correlation with bulk density (Figure 1 (b) in the SI.1) and a significant effect on both bulk density and the organic matter along the transect. Soil bulk density was increased with a similar manner to the GWC along the transect, reflected to the water run-off from the sides of the PV panels frame as well as the pools created at the front of the southern panel edge (Figure 1 (a) in the S.I.1).

These water pools might have a long-term effect on the soil porosity and the organic matter (Clinton, 2003; Gavin and Agnew, 2000), thus suggests further investigation. Finally, there was a negative correlation between bulk density and organic matter, as found in other studies (Keller and Håkansson, 2010; Gao et al., 2012; DelVecchia et al., 2014): as soil bulk density decreased, the organic matter increased. This pattern is attributable to compaction (Saini, 1966) and increased litter and soil decomposition caused by vegetation removal (Dagar and Tewari, 2017).

1.5.3 H3. LAI vary spatially and seasonally due to shading and grassland management

LAI, which is an indicator of vegetation productivity, was as high as in many other grasslands, with the mean ranging between 2-6 (Li et al., 2016). Overall, LAI did not vary through the solar park despite the known regulation of plant processes by climate and the observed differences in microclimate within the site. Specifically, the microclimatic

spatio-temporal variability and the evaporation, precipitation as well as soil and air climate in general, are known to directly affect vegetation and also indirectly due to effects on soil quality (bulk density and organic matter; (Gavin and Agnew, 2000; Liu and Luo, 2011; Davidoff and Selim, 1988; Song et al., 2013; Fowler and Brown, 1994).

As mentioned above, during the growing season the soil under the PV panels was wetter compared with the gap (Figure 1.6), providing more water for plant growth (Gavin and Agnew, 2000; Gupta et al., 2015). However, under was also cooler (low soil temperature) and PAR receipt also lower, which is generally associated with lower productivity in temperate environments (Hatfield and Prueger, 2015; Acevedo, 2002). Despite these in this temperate UK solar park, the LAI of NT (dead vegetation; dry or decomposed on the ground) was similar regardless season, and LAI of T vegetation was increased out of season.

Further with regards to PAR, research suggests that exposure to direct solar radiation can damage plants growth (Hatfield and Prueger, 2015) and diffuse light can sometimes be used more efficiently by plants; shade tolerant species (Li et al., 2014). In addition, depending on the season and the species, there is a specific amount of PAR that the species need to photosynthesize. The amount of daily PAR requirements for grassland species based on those found at Westmill solar park (Plant species survey; Table 5 in SI.1) is estimated around 200-230 μmol m^{-2} s^{-1} (quite same with the PAR findings under panels) and thus saturation will not have occurred under the PV panels (Unruh, 2015).

Lack of difference in LAI ratios for T and NT leaves during growing and out of growing season is also attributable to differences in vegetation species, with shade tolerant species dominating under the panels and shade intolerant species dominating in the gaps (e.g. *Trifolium repens*, sensitive to shade, *Plantago lanceolata* semi-tolerant). The plant species survey that was undertaken from May to September 2015 (Table 5 in SI.1) showed

the prevalence of *Poa annua* and *Festuca ovina* and *rubra* (both family *Poaceae*), growing under the panels. *Festuca rubra*, is also a species that has proven to grow well under trees (agroforestry). *Poa annua* is a known shade tolerant species (Vargas and Turgeon, 2003), while *Festuca ovina* is known for its moderate tolerance to shade but excellent tolerance in cold environments (Ogle et al., 2010).

A previous study has shown that for some crops shade conditions (and all the microclimatic turbulence this creates), could be ideal and increase crop yields of specific species (Marrou et al., 2013b; Marrou et al., 2013c). Also, Marrou et al. (2013a), measuring the leaf area index of lettuces under shade treatments, reported that it was increased despite the decrease in the number of leaves of each lettuce (Marrou et al., 2013a). This raises the question with regards to morphology and size of the leaves in this study. Whilst individual leaf dimensions were not assessed, the leaves of *Platango lanceolate* (broad leaves; appearing mostly at the gap), could vary more compared to *Festuca ovina* (clustered needle leaves; appearing under and at the gap) but further research is required. These difference in vegetation composition further explains why LAI did not vary reflected to spatial differences in soil and air temperature in the growing season was up to 3 °C, which is not assumed to strongly affect vegetation growth in a geospatially similar region (a Netherlands grassland; Song et al. (2013)).

Last, management of the solar park could have had an effect on the LAI. The park was grazed with sheep out of growing season and strips were cut at the southern and northern edges with machinery throughout the year. These solar park management actions occurred, when PV panels' shading was a risk and not following a specific schedule. Therefore, any assumptions were made carefully, because even though grazing is a typical management practice, lack of management and control of the grazing could alter

vegetation density (canopy; LAI) and microclimate drivers (Song et al., 2013; Klein et al., 2005).

Consequently, apart from high moisture content and precipitation and low air temperatures out of growing season, the high LAI ratios of T vegetation could be explained by the fact that sheep grazing periods were not enough. It was anticipated and would be interesting to investigate in the future, the potential of sheep showing preference on vegetation lying under the panels or at the vegetation species at the gap In addition, It is strongly suggested that in any multi-land use schemes, in this case a land hosting live-stock and a solar park, should follow a framework to manage this new type of ecosystem based on the subsequent species growing or been cultivated post-construction, in favour of food and energy supply from the same land unit (BRE, 2013; 2014).

1.5.4 H4. GHG fluxes will vary temporally and spatially within solar parks

GHG fluxes are influenced by microclimate, soil microbial communities and vegetation (Liu et al., 2015; Rochette et al., 1991). As microclimatic and soil physical properties varied spatio-temporally and LAI varied temporally, it is assumed that CO_2 ecosystem exchange and H_2O vapor would differ. Both under and gap were sinks of CO_2, which is the desirable result in order to achieve the reduction of CO_2 gases sourcing to the atmosphere (Frank, 2005; Forster and Ramaswamy, 2007; UN, 2015; Thomas et al., 2016). This finding contradicts the results from Armstrong et al. (2016), undertaken at the same site with a similar experimental design. Their study, conducted in 2013, identified the area under the PV panels as a source throughout the year except for January and the area at the gap as a sink throughout the entire growing season (May to August).

In our study both areas under and gap were mostly a sink of CO_2 during growing season. These differences could be attributable to differences in annual conditions, as it is established that C sequestration could differ from year to year (Conant Richard et al., 2017), thus the differences might also occurred due to this factor. Alternatively, it could be due to the choice of sampling days. Within this study, there was an obvious day-by-day variation which supports the need of a day-by-day monitoring of those GHGs. For example, in June the area under on the 23rd was acting as a source and a day earlier as a sink (Figure 1.9 (a)). Similar daily differences were reported in early September, were on the 3rd the area under was acting as a source but as a sink on the 4th.

Finally, the differences between fluxes in 2013 (Armstrong et al., 2016) and this study could be supported by the vegetation surveys of the two studies. The species differed, with fewer species found in this study, and there was more bare ground in 2013. Armstrong et al. (2016). Armstrong et al. (2016) research was conducted a year after the reseedings and as in any intervention, the system needs some time to adopt and recover (e.g. an agroforestry system needs up to five years to recover; (Morecroft et al., 1998; Yan et al., 2012)). It is known that in temperate grasslands the source of C after harvesting followed by a rapid LAI recovery, maintains C sinks during the summer (Novick et al., 2004). However, the reduction in species richness could be also explained by the sampling area size because the collar area was smaller compared to the plots (1 m x 1 m area) by Armstrong et al. (2016). However, the plant species survey for our study was carried out throughout growing season (May to September 2015), and the reported areas were the actual collars from which the gaseous fluxes sampling occurred.

The H_2O vapor under the panels was lower than in the gap during the growing season. Marrou et al. (2013b) also showed H_2O vapor decreased under more shade. During the

non-growing season, evapotranspiration was boarder line zero (the gap in November and under in December). Negative evapotranspiration values occur whenever rain exceed

s evapotranspiration and thus soil moisture is increased (Wilcox and Sly, 1976). It was assumed that the increased soil moisture at the gap in November, also explained the sourcing of CO_2, however it was not statistically supported.

1.5.5 Interactive effects related to the Water-Energy balance in a solar park

Given the variability and spatio-temporal differences between under and gap, and acknowledging that the observed climate aspects investigated for this study, (including air temperature, precipitation, soil moisture, evaporation), are related through the balance of incoming and outgoing energy combined with water at the surface, allowed us to also hypothesize critical interactive effects on energy and water balance in solar parks. It is assumed that in an already changed climate, seasonal and spatial differences in a solar park, especially of a large scale should be monitored, given their widespread deployment, as the effects on the local climate, are proportional to the potential effects on the global climate regulation. However, there are no studies (to our knowledge) investigating the potential impacts of an induced microclimate by solar parks at the water and energy balance, impacts which are acknowledged in this study.

In particular, due to solar PV panels' physical presence in the investigated UK temperate grassland and in particular the panels design, the observed water runoff creating water pools in front of the southern PV panels edge (oasis effect) and the water runoff from the panel sides reaching the soil under them, associated with the overall cooler air temperature and the lower PAR, under compared with the gap, resulted to lower

evaporation under for both growing and non-growing season. This observation implies direct effects on the water and energy balance under the panels.

In addition, vegetation cover is known for its ability to influence the exchange of energy and water vapor between the land surface and the atmosphere (Bonan, 2008). Results with regards to the LAI in this UK temperate grassland solar park, showed that the area under regardless of season, demonstrated constantly higher ratios compared to gap (for both green/transpired and decomposed/non-transpiring leaves, T and NT respectively), despite the lower PAR. Moreover, the water vapor results demonstrated fluxes close to zero in growing season and below zero out of growing season. However, similar results, with minor differences were observed at the gap. The soil surface at the gap, received higher ratios of PAR, the air temperature was warmer compared to under but water vapor fluxes and the NEE were similar throughout the season. Thus, it was anticipated that the plant cover (LAI) played a major role, regulating water and energy balance in this solar park.

Plant cover directly impacts the soil microclimate through modifications of near-ground solar radiation and soil temperature, and these interactive effects are relevant for key ecohydrological processes such as soil evaporation. Changes caused by vegetation cover in soil microclimate are season dependant (Villegas et al., 2010), ecosystem dependant (Armstrong et al., 2014a) and also are related to plants morphology and physiology. Vegetation strongly affects the amount of net solar radiation that is reflected by the soil surface, the partitioning of net radiation into sensible and latent heat fluxes, the rate of precipitation recycling and the partitioning of precipitation into soil moisture, evapotranspiration, and runoff (He et al., 2010).

All the above, implied effects on soil physical properties including soil bulk density and organic matter, but also imply further impacts on the water and energy balance in the investigated UK temperate grassland hosting a solar park. The negative correlation

between bulk density and organic matter as generally proven in several studies (Keller and Håkansson, 2010; Gao et al., 2012; DelVecchia et al., 2014): as soil bulk density decreased, the organic matter increased, was attributable to compaction (Saini, 1966) and increased litter and soil decomposition (Dagar and Tewari, 2017). As a matter of fact, the LAI of non-transpiring (decomposed) leaves, regardless of season, was higher under the panels compared to the gap, increasing litter decomposition and thus explaining the higher NEE ratios under than the gap (both locations mostly negative regardless season; sink of CO_2).

The percentage of organic matter under the panels was approximately 3% higher than the gap, which does not imply major differences between the two locations. However, it was anticipated that for the effects on soil physical properties, the observed microclimatic differences and the vegetation cover between under and gap, would also have a major effect on C cycling. Temperature, soil moisture and PAR are some of the key drivers of biosphere C cycling, with changes in temperature generally positively related to primary productivity and organic matter decomposition rates and the uptake and release of CO_2 and CH_4, always ecosystem and climate season dependant. Effects of solar park microclimate on C cycling have been assessed by Armstrong et al. (2016). Their study found no spatio-temporal differences related to soil physical properties. Although, in our study organic matter showed a positive relationship with air and soil temperature under and at the gap and thus an effect on the water-energy balance is anticipated.

Consequently, it should be possible to design solar parks to induce desirable microclimatic niches for ecosystem processes and mitigate crucial perturbations at the energy and water balance in a solar park's ecosystem. These feedbacks should be further investigated to quantify and establish the causes.

1.6 Conclusion

Energy is essential for domestic and commercial needs and the demand is projected to increase. The expansion of solar PV installations around the globe, represents a significant land-use change. Therefore, it is crucial to provide scientific information on potential ecosystem impacts in the host environments. The spatial and temporal variations of the microclimate are crucial for the general understanding of solar park ecosystem response (Liu and Luo, 2011). The quantified spatio-temporal variability in microclimatic aspects exhibited complex relationships with soil physical properties, LAI and GHG fluxes. These interactive effects observed in the induced microclimate caused by the physical presence of the solar park, suggest a variety of impacts on the water and energy balance in the park dependant to space and time. In an already changing climate, impacts as such highlight the need for urgent assessment, given the wide deployment of large-scale solar infrastructure across the globe. Better resolution of spatio-temporal microclimatic response in solar PV parks in different climatic zones and ecosystem types is required so that the full consequences of the growing land-use changes are understood. This will provide information for future solar PV park construction and management.

2 Chapter 2: Simulating the impact of a Solar Photovoltaic Park on a Grassland's Thermal Behaviour

2.1 Abstract

Ground-mounted solar photovoltaic (PV) panels are widely installed on grasslands. Grasslands are critical global ecosystems as they supply many ecosystems services, including carbon (C) storage. Soil temperature is the primary controller of many important ecological processes, including productivity and decomposition, the balance of which determines the carbon source-sink status. Despite this, the impact of solar PV panels on grassland soil temperatures is poorly resolved. In this study, a pseudo-three-dimensional (3D) physically based, spatial explicit numerical model was built, to simulate soil temperatures in a solar PV park in Wiltshire, UK. The HIS-PV (Heat In the Solar PV park) model simulated soil temperatures from standard meteorological data (SMD) and was evaluated against spatio-temporally explicit soil temperature measurements. Under a diverse range of meteorological conditions, the HIS-PV model provided a good representation of observed soil temperatures with root mean square errors (RMSE) of 1 °C - 1.5 °C. Sensitivity analysis assessing the potential effect of volumetric water content and surface resistance variations as well as the leaf area index (LAI) on soil temperatures was performed. Dense canopies and zero surface resistance increased model errors during

growing season and low dense canopies decreased model errors during post-growing season periods. Errors varied temporally, with extreme errors reaching 3 °C in some evenings of the tested periods. HIS-PV provides the foundation of a modelling tool to explore the impact of solar PV parks on soil temperatures and their associated ecosystem services across the world.

Keywords: ground-mounted solar park, photovoltaic, grasslands, numerical modelling, soil temperature, sensitivity analysis, surface resistance, volumetric water content, leaf area index

2.2 Introduction

Conventional energy resources lead to several environmental impacts such as greenhouse gases emissions, air and water pollution and are the dominant cause of climate change (Asif and Muneer, 2007; Evans et al., 2009). The need for an energy transition to renewable resources is urgent (UN, 2015) and solar energy is one of the most widely applicable renewable sources (Kamat, 2007; IEA/WEO, 2017; EIA, 2016). Globally, solar photovoltaic (PV) demand is expected to reach around 106 GW (from rooftop and ground-mounted), with ground-mounted reaching 33.1 GW only in China (currently world leader in solar energy capacity) by the end of 2018 (RECP, 2018). In the UK, ground-mounted solar PV installations (hereinafter referred to as solar parks) covered an area of 100 km^2 agricultural land in 2016 (Capell, 2016). Solar parks are primarily deployed on pasture or low grade arable land and subsequently managed as grasslands (BRE, 2013).

Solar parks have been found to alter the local climate, with significant effects on soil temperature and other microclimatic drivers such as solar radiation fluxes. The magnitude of change in soil temperature is particularly high, with differences of up to ~ 4 °C between

the areas under and at the gap of the solar PV panel rows (section 1.4.1.2 in chapter one of this thesis and Armstrong et al. (2016)), caused by perturbations to the surface energy balance. The PV panels reduces incoming direct short wave (SW) and outgoing long-wave (LW) radiation fluxes by the soil under them (Hassanpour Adeh et al., 2018; Marrou et al., 2013b; Yang et al., 2017; Hu et al., 2015). These spatial variations in radiative fluxes balance directly impact subsurface soil temperature, a crucial regulator of grassland productivity and decomposition processes with implication for carbon (C) sequestration (Liu and Luo, 2011; Teasdale and Mohler, 1993; Thornley et al., 2006). The perturbations to the surface energy balance (including net sensible and latent heat fluxes) will also affect evapotranspiration (ET).

Perturbation to the surface energy balance, caused by solar parks, affect ecosystem processes and properties, including photosynthesis, net ecosystem exchange (NEE), leaf area index (LAI) and plant diversity and productivity (Armstrong et al., 2016; Armstrong et al., 2014a; Barron-Gafford et al., 2016; Marrou et al., 2013b; Marrou et al., 2013a). For example, Armstrong et al. (2016), demonstrated that microclimate and vegetation management of a solar park induced changes on plant diversity and above ground biomass, with above ground biomass under the PV panels 25% of that in control areas. Further, photosynthesis and NEE varied and were correlated to microclimate, management and soil properties. Marrou et al. (2013a) investigated the consequences of solar parks on crop productivity, including lettuce species. They found that lettuce yield was maintained but the LAI per plant was increased under the PV panels while the number of leaves decreased. Following that, Marrou et al. (2013b), found that changes in soil temperatures had an effect on the leaf emission rate of cucumbers and lettuces, and suggested that the focus should be on the mitigation of light reduction as well as strategic plant selection to optimise the productivity of agrivoltaic schemes (mixed systems comprising food and energy production from the same land unit).

Considering the global importance of grasslands, and the wide spread of solar parks around the world, it is important to resolve the potential impacts on microclimate as this will regulate key processes and ecosystem service provision. Considering the cost of and time required for field instrumentation across a range of ecosystems and climates, a modelling approach to predict local climate impacts is appealing. A model that predicts soil temperature would be very valuable as this is the primary controller of grassland ecosystem function and carbon dynamics. In rural environments, modelling approaches were used to evaluate the optimal placement of solar PV units and there is understanding of the impacts of roof-mounted PV panels on urban temperatures (Calvert and Mabee, 2015; Sánchez-Lozano et al., 2013; Sánchez-Lozano et al., 2014; Uyan, 2013). However, to date, there is no modelling tool available to explore soil temperatures through solar parks.

2.2.1 Research aim

Given the wide spread deployment of solar parks and the poorly resolved impacts on local climatic conditions that regulate ecosystem functions, the aim of this study was to develop and evaluate a physically based, spatially explicit solar park soil temperature numerical model (HIS-PV, Heat In the Solar PV park). The following objectives were addressed, within an exemplar UK grassland solar park:

O1. Construct and parameterise a physically based numerical model to simulate grassland soil temperature.

O2. Evaluate the performance of the HIS-PV model for simulating spatiotemporal variation in soil temperatures.

O3. Determine the sensitivity of simulated soil temperatures at 10 cm depth to variations in key model parameters surface resistance r_s, volumetric water content (VWC) and LAI under different meteorological conditions.

2.3 Methods

2.3.1 HIS-PV model Description

HIS-PV is a pseudo-three-dimensional (3D) physically based, spatial explicit numerical model, based on the soil temperature models by Kettridge et al. (2008; 2013). The model was coded in Fortran compiled imperative programming language that is especially suited to numeric computation using NAG builder 6.1 environment (NAG, 2018). Our model was framed as a soil temperature model with an associated surface boundary layer (Figure 2.1) with a timestep established at 30 seconds for simulations conducted for five 10-day periods.

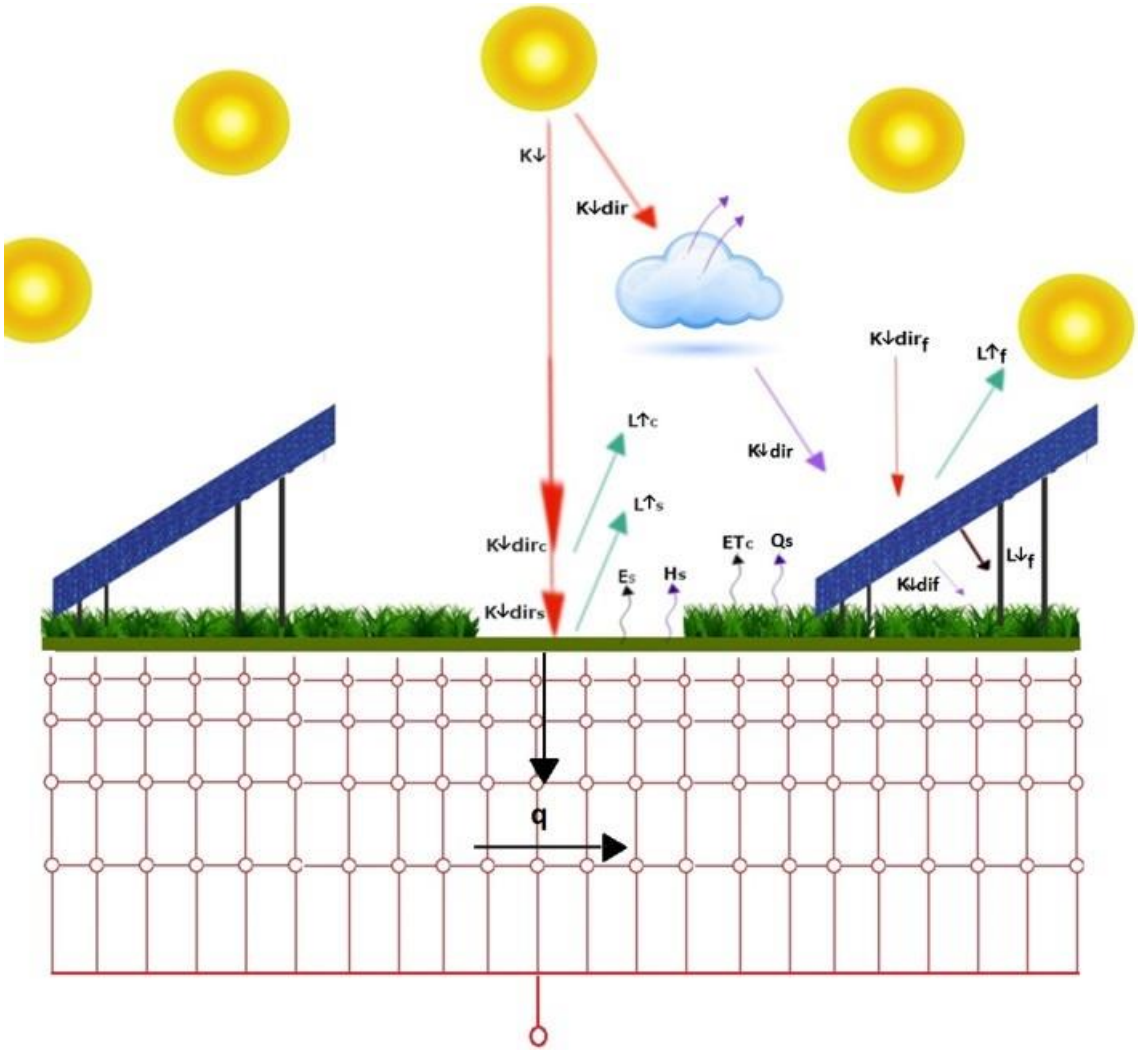

Figure 2.1: Virtual description of the model's incoming and outgoing radiation and energy balance components. K↓, the direct beam solar radiation, $K\downarrow_{dir}$, direct short-wave radiation, $K\downarrow_{dif}$, diffuse or scattered short-wave radiation, L↑, outgoing long-wave radiation, L↓ incoming long-wave radiation, E, evaporation, H, heat flux, Q_{Hs}, sensible heat flux and ET, for evapotranspiration. Subscripts for each energy layer were used with *s*, accounting for surface, *c*, for the canopy and *f*, for the PV panels. Subsurface for node depths also illustrated and *q*, to describe the conduction between the soil profile cells.

2.3.1.1 Soil subsurface model component

A 2D sub-model simulated the subsurface energy transfer and storage along a linear transect running perpendicularly top four PV panel rows of known dimensions (Figure 2.3b). The energy transfer simulated a 1 m deep profile composed of 19 vertical nodes. Node separation increased with depth ranging from 0.005 m at the soil surface to 0.1 m at a depth of 1 m. Horizontally, the transect was discretised into 100 nodes at an interval of 0.50 m. Subsurface energy transfer occurs through heat conduction, advection of vapour and advection of liquid. In the HIS-PV, energy transfer by conduction (q; W/m²), was simulated between adjacent nodes (vertically and horizontally), and was based on Fourier's Law:

$$q = -k\,\frac{dT}{dz} \quad (1),$$

where, T is the temperature gradient measured in (Kelvin), z, is the soil depth in (m) and k, is the thermal conductivity in ($W \cdot m^{-1} \cdot K^{-1}$).

Thermal conductivity is calculated by Farouki (1986):

$$k = (P-\theta)k_{\mathrm{a}} + (f_{\mathrm{o}}+\theta)k_{\mathrm{o}}^{\left(\frac{f_{\mathrm{o}}}{f_{\mathrm{o}}-\theta}\right)}k_{w}^{\left(\frac{\theta}{f_{\mathrm{o}}+\theta}\right)} \quad (2),$$

where, P, is the soil porosity, f_{o} is the volumetric fraction of organic matter (subscript o), θ, is the volumetric water content (VWC) and the subscripts α and w represent the air and the water, respectively.

Vapor transfer, was calculated in accordance with Krischer and Rohnalter (De Vries, 1963), where, k from equation (2), was assumed to be equal to the vapor transfer parameter k_v, measured in ($W \cdot m^{-1} \cdot K^{-1}$),

$$k_v = \frac{L_v \kappa P}{RT(A-p_{ws})}\frac{dp_{ws}}{dT} \quad (3),$$

where L_v, is the latent heat of vaporization of water ($J \cdot kg^{-1}$), R, the gas constant for water vapour ($J \cdot kg^{-1} \cdot K^{-1}$), κ, the diffusion coefficient of water vapor in the air (m^2/sec), A, the atmospheric pressure of the air in (Pa) and p_{ws} the saturated vapor pressure in (Pa).

Advection of liquid is assumed to be non-significant in accordance with Kettridge and Baird (2008). The implication of this simplification will be considered within the evaluation of the model performance (section 2.5.3).

Volumetric heat capacity C_s ($J \cdot m^{-3} \cdot K^{-3}$) of soil, was calculated by:

$$C_s = \theta_o C_w + f_o C_o + f_m C_m + f_a C_a \quad (4),$$

2.3.1.2 Boundary layers

The basal soil temperature was assumed constant and equal to the annual average of soil temperature of the solar PV park at a depth of 10 cm depth; equal to 10.4 °C (Oke, 1987; Florides and Kalogirou, 2007). Zero energy transfer was assumed at the sides and ends of the simulated transects as this would result in small errors at the ends of the transects. As such, analysis of the model considered only the nodes within the central solar PV panel rows at a distance greater than 35 m (out of 100 m transect length) from the boundary. The model was applied to simulate soil temperatures through the centre of solar PV arrays and thus transfer from the sides are considered negligible.

2.3.1.3 The three-layers design

The ground heat flux to the surface (top) of the soil profile (Q_s; W/m^2) was calculated from the surface energy balance of each surface node along the transect. HIS-PV model was designed in a manner where three energy exchanging layers were considered. These layers are the soil surface, the vegetation canopy and the solar PV panels. The model

simulated all primary fluxes acting on the soil surface (subscript *s*) considering the existence of these three layers. At the soil surface:

$$Q_s^* = (1 - a)K_s + L_s^* = Q_{Es} + Q_{Hs} + G_s \quad (5),$$

where, K_s^* (W/m²), is the net SW solar radiation, L_s^* (W/m²), is the net LW solar radiation.

2.3.1.3.1 Short-wave (SW) radiation (K_s^*)

Incoming SW radiation above the solar PV panels (subscript f), $K_f \downarrow$, derived from measured data (section 2.3.3.2), and was equal to:

$$K_f \downarrow = K_{f\,dif} \downarrow + K_{f\,dir} \downarrow \quad (6),$$

where, *dif*, the diffuse and *dir*, the direct radiation, respectively (Figure 2.1). The incoming SW radiation of the vegetation canopy layer below the solar PV panels (subscript *c*), is a function of $K_{f\,dif} \downarrow$ and $K_{f\,dir} \downarrow$ (W/m²). $K_{f\,dir} \downarrow$ was calculated for each position along the transect assuming a linear solar ray path between the position of the sun and the vegetation canopy surface. If this vector intercepts the PV panels (represented as defined planes in 3D space above the surface of the solar PV park; Figure 2.1), then the location was assumed to be in shade and $K_{c\ dir} \downarrow$ equals zero. If the ray does not intercept a panel then the location is in direct sunlight and thus $K_{c\ dir} \downarrow$ is equal to $K_{f\ dir} \downarrow$.

The diffuse SW radiation received at the vegetation canopy surface $K_{c\ dif} \downarrow$ was assumed equal to:

$$K_{c\,dif} \downarrow = V \times K_{f\,dif} \downarrow \quad (7),$$

where V , is the sky view factor, defined as the fraction of vectors between the canopy surface and equally position points across a hemispherical sky that do no intercept the defined panels (Essery et al. (2008), for further details).

The incoming SW solar radiation at the surface layer, was calculated considering Beer's Law where:

$$K_s \downarrow = K_c \downarrow \exp(-\kappa\, LAI) \qquad (8),$$

where κ, is the light extinction coefficient and LAI, is the leaf area index. The outgoing SW radiation from the soil surface is equal to:

$$K_s \uparrow = aK_c \downarrow \quad (9),$$

where α, is the albedo (unitless).

2.3.1.3.2 Long-wave (LW) radiation

Total incoming LW solar radiation above the PV panels, (W/m²), was calculated in accordance with the Stefan-Boltzmann equation (Brock and Arnold, 2000):

$$L_f \downarrow = \varepsilon^* \varepsilon_s\, \sigma T_\alpha^4 \qquad (10),$$

where, σ, the Stefan-Boltzmann constant (= 5.670374419 x 10^{-8} W · m^{-2} · K^{-4}), T_a, was the absolute air temperature (Kelvin) and, ε_s is the surface emissivity and ε^*, is the effective emissivity of the sky, calculated by Arnold et al. (1996):

$$\varepsilon^* = (1 + \lambda n)\varepsilon_0 \qquad (11),$$

where ε_0 is the clear sky emissivity (= 8.733 x 10 $T_\alpha^{0.788}$). The cloud cover, n (unitless), is calculated for the incoming K_s^* solar radiation, and λ, is a constant dependant on the

cloud type which was equal to 0.26 following Braithwaite and Olesen (1990) and according to Brock and Arnold (2000), representing the average of all cloud types.

Incoming LW solar radiation on the surface, $L_s\downarrow$, was calculated from Stephan-Boltzmann's Law and Beer's Law:

$$L_s\downarrow = \varepsilon_s \mathrm{V} \exp(-\kappa\, LAI)\; L_f\downarrow \qquad (12),$$

where, ε_s, is the surface emissivity, LAI the leaf area index and the view factor V, equal to the SW radiation.

Outgoing LW from the soil surface $L_s\uparrow$, was calculated from Stefan-Boltzmann Law and Beer's Law:

$$L_s\uparrow = \varepsilon_s{}^{*} V \sigma T_s^4 \exp\left(-\kappa_{diffuse} LAI\right) \qquad (13),$$

Solar PV panels vegetation and the soil surface were assumed to be similar in temperature and therefore the LW radiation fluxes between these components are for simplicity excluded from model simulations.

2.3.1.3.3 Turbulent fluxes

The latent heat flux for evaporation is Q_{Es} (W/m²), and was calculated in accordance with the Penman-Monteith equation (Oke, 1987):

$$Q_{Es} = \frac{L_v s(T_s - T_a) + L_v v dd_a}{r_a + r_s} \qquad (14),$$

where, T_a (Kelvin) is the air temperature, s, is the slope of the saturation vapour versus temperature curve (kg/m³ · K), vdd_a, is the vapour density deficit of air (kg/m³), r_a, is the aerodynamic resistance (m/sec) and r_s, is the surface resistance (m/sec).

The sensible heat flux Q_{Hs} (W/m²) at the surface, was calculated using Newton's Law of cooling:

$$Q_{Hs} = \frac{C_a(T_s - T_a)}{r_a} \qquad (15),$$

where, C_a, is the heat capacity of air.

For the HIS-PV model, the r_{aT} is the sum of two resistances, the one above, and the one under the PV panels' layer (Kettridge et al., 2013). The total aerodynamic resistance r_{aT}, (m/sec) according to Kettridge and Baird (2008), is equal to:

$$r_{aT} = \frac{\ln\left(\frac{z_r - d}{z_{0m}}\right)^2}{k^2 u_r} \qquad (16),$$

where, z_r, is the reference height above the ground surface (m), d, is the displacement height (m), z_{0m}, is the roughness length of momentum transfer (m), k is the von Karman constant (m) and u_r is the wind speed at the data loggers' sensor height (m/sec).

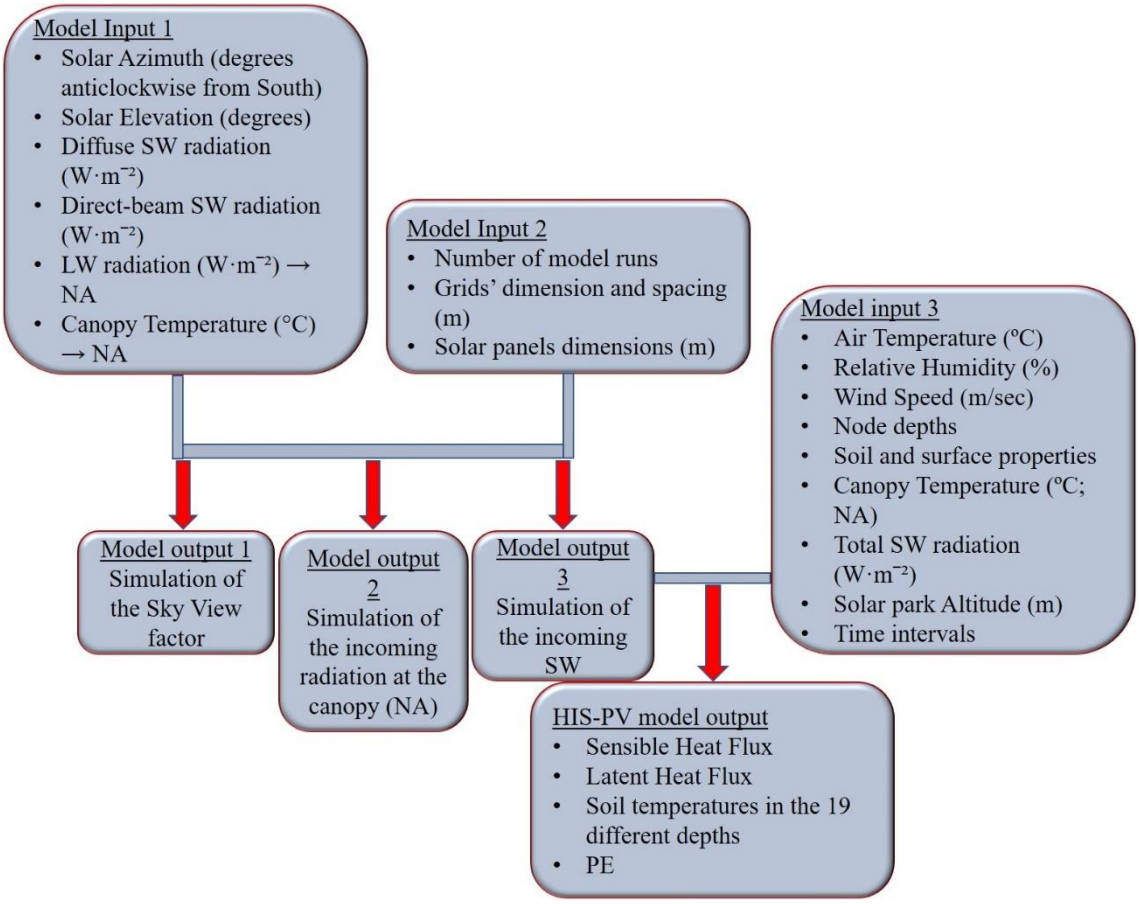

Figure 2.2: HIS-PV model input and output illustration comprising the Price and the HIP models by Kettridge and Baird (2008) and by Kettridge et al. (2013), which built was thoroughly described in chapter two of this thesis.

2.3.2 HIS-PV model Parameterization

2.3.2.1 Site and data collection

The study was undertaken at Westmill Solar Park, Wiltshire, UK (51° 37' 03" N 01° 38' 45" W, altitude 100-106 meters; Figure 2.3a Westmill Solar Farm (2011)). The 5 MW capacity solar park was installed in 2011 on a low-grade arable land. The park had a parallelogrammical design, formed by 36 PV panel rows to the west and 33 rows to the east of a central north-south passageway. The area under the PV panels was 29,000 m², the gap area between panel rows was 58,000 m², and the area between the PV panels and

boundary fence 34,000 m². The grassland was sheep grazed in the winter and a 1.5 m strip mowed at the northern and the southern edges of each panel row twice annually to prevent shading of the panels.

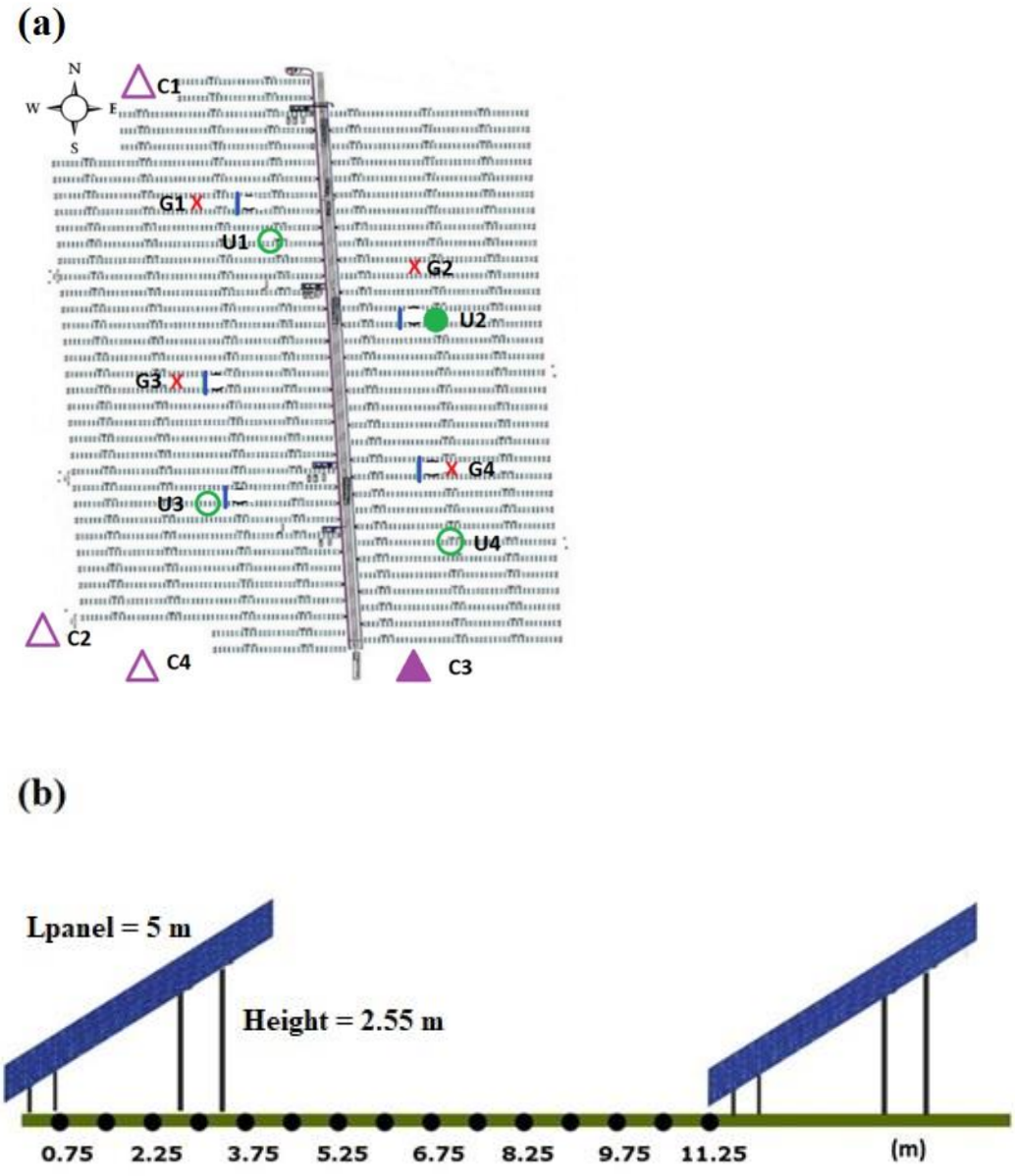

Figure 2.3: (a) The construction map showing the location of the 12 micro-meteorological stations. The stations at the gap were marked with X for the gap (G), Δ for the control (C) and O represents the plots under (U) the panels. Symbols ▲ and ● represent the stations with a total and diffuse sunshine data logger installed. The entrance was located at the northern border of the park. Temperature strings

were also installed within stations U2, G4 and C3 plots. Blue thick lines showing the location of the five linear transects. (b) The linear transect experimental design.

2.3.3 High frequency logged measurements

2.3.3.1 Initial conditions for soil temperature

In order to assess the temporal and spatial explicit performance of the model, standard meteorological data (SMD) as well as soil properties and LAI, were measured for one year, (March 2015 to March 2016), in Westmill solar park (Figure 2.3b). Initial conditions were set using the soil temperature datasets obtained at stations U2 (U for under the panels) and C3 (C for control areas away from the panels; Figure 2.3b). Soil temperatures at six depths (surface, 0.03 m, 0.07 m, 0.15 m, 0.3 m and 0.5 m) through the soil profile were interpolated from soil temperature strings, from stations G4 (G for gap between PV panel rows), U2 and C3 (Figure 2.3a).

2.3.3.2 Standard Meteorological data (SMD)

SMD were collected from four randomly selected plots under the PV panels (hereinafter referred to as under), four plots between panel rows (hereinafter referred to as gap) and four control plots (Figure 2.3a). At each plot soil temperature (°C; 10 cm below the surface), volumetric water content (VWC in m^3/m^3; 10 cm below the surface), relative humidity (RH%; 0.5 m above the surface), wind speed (m/sec; 1.5 m height) and air temperature (°C; 0.5 m above the surface), were measured. Furthermore, total and diffuse photosynthetic active radiation (PAR, in $\mu mol \cdot m^{-2} \cdot s^{-1}$; 1.3 m above the surface) were recorded from one plot under (U2; Figure 2.3b) and one plot at the control (C3), with a sunshine sensor (BF3 sunshine sensor; Delta-T Devices (UK-a)) installed parallel to the soil surface at 1.3 m height. Conversion to W/m^2, was performed by equations provided

in the User Manual for Sunshine Sensor type BF3; Appendix A: Conversion to Appropriate Units, Delta-T Devices (UK-a).

2.3.4 Spatially explicit instantaneous transect measurements

To assess the spatial variability of soil temperature and parameterize input model components, five linear transects of 11.25 m length with 15 equally distributed points at an interval of 0.75 m (total sampling points n = 75) running perpendicular between two PV panel rows were established (Figure 2.3b). The spatial location of these transects was randomly selected within the solar park. At each of the transects soil and air temperature, PAR, soil moisture, soil properties (bulk density and organic matter) and LAI were measured along the transect. Measurements were taken during eight sampling periods between two to five days in duration, spread between March 2015 and March 2016 (for further details regarding the field campaigns see Table 1.1in chapter one of this thesis).

2.3.4.1 Handheld microclimate metrics

Soil moisture (VWC in m^3/m^3, 6 cm below surface) was measured using a theta probe (MM3 Theta Probe Soil Moisture Sensor, (Delta-T Devices, UK-b). PAR (in μmol m^{-2} s^{-1}; above vegetation canopy) was measured using a SKR 110 Red/Far-Red pyranometer sensor with the SKR100 display meter (Skye Instruments, UK). Soil and air temperature (°C; 10 cm below the surface and above the vegetation canopy, respectively) were measured using two Superfast Thermapen (Global FSE, UK). Soil and air temperature, PAR and VWC, were measured during every sampling period, from all 75 sampling points two to three times per day (in the morning (M), afternoon (A) and evening (E); Table 1.1 in chapter one of this thesis).

2.3.4.2 Soil physical properties

Soil bulk density and organic matter were determined from soil samples collected at the start of the field season (30th and 31st of March 2015). Soil samples were collected from each of the 75 sampling points using a bulk density steel core of 7.5 cm diameter and 5.5 cm height (core volume = 242.86 cm³). Bulk density was determined, by drying samples, at 105 °C until constant weight. Stones were excluded from bulk density measurements given the high stone content of the soil cores. Stones were separated by sieving and stone volume determined through the Archimedes' principal (Lang and Thorpe, 1989) and the soil densities derived by Emmett et al. (2008). Organic matter was determined by loss on ignition (LOI) method, using a muffle with 10 g of oven dried soil (at 105 °C) at 375 °C for 16 hours (Emmett et al., 2008).

2.3.4.3 Soil surface properties

Soil properties (soil water, organic and mineral content) were assumed spatially and temporally constant during model simulations. Thus, for the initialization of the HIS-PV model, volumetric water content was set at 0.35 m^3/m^3, the organic content at 0.05 g/m^3 and mineral content at 0.45 g/m^3. The parameterization for soil surface properties including displacement height (d (m)), albedo (α), surface roughness (z_0 (m)), emissivity (ε), surface resistance (r_s (s/m)) for wet, moist and dry soils were parameterized based on existing literature (Table 2.1).

Table 2.1: Soil surface properties values used in the initial parameterization derived from existing literature.

Variable	Mean	St. Dev.	Publication
d (m)	0.015	0.020	Jin and Liang (2006); Zeng and Dickinson (1998); Zeng and Wang (2007); Best et al. (2011); van de Griend and Owe (1994); Gavin and Agnew (2000)
α	0.20	0.05	Mahfouf and Noilhan (1991); Kala et al. (2014); Allen et al. (1998)
z_0 (m)	0.021	0.022	Mahfouf and Noilhan (1991); Jin and Liang (2006); Zeng and Dickinson (1998); Businger et al. (1971); Deardorff (1974)
ε	0.95	0.01	Mahfouf and Noilhan (1991); Jin and Liang (2006)
r_s (s/m) for wet soils	0	0	Mahfouf and Noilhan (1991); Allen et al. (1998); Camillo and Gurney (1986); Gavin and Agnew (2000)

r_s (s/m) for moist soils	61.5	12.2	Allen et al. (1998); van de Griend and Owe (1994)
r_s (s/m) for dry soils	500	71	Shuttleworth and Wallace (1985); Camillo and Gurney (1986)

2.3.4.4 Leaf Area Index - LAI

LAI was measured by harvesting all above ground biomass from a 40 cm² area at each point on the transect in May, June, October and December, representing the LAI during the start (May and June) and the end of growing season (October and December). During July and early September samples were collected from 1.5 m, 4.5 m, 7.5 m and 11.25 m distances on each transect, (Figure 2.3b representing the LAI at the peak of growing season. Samples were separated into NT (non-transpiring; dead) and T (transpiring; alive) vegetation, excluding plant stems. Two different methods were used to quantify the LAI. A conventional scanner and ImageJ software (Schneider et al., 2012) was used for May, June, July and early September and the LI-3100C Area Mater (LI-COR, 2017) for October and December. A post-hoc investigation was performed to evaluate and compare the two methods ($R^2 = 0.8$).

2.3.4.5 Sky view factor

Solar PV panels within a 100 m x 100 m area were simulated using their real dimensions in the solar park. To evaluate the sky view factor for HIS-PV, photographs were taken

with a Nikon FC-E8 Fisheye Converter adjusted on a Nikon D60 camera and then analysed according to Frazer et al., (1999), using the Gap Light Analyser (GLA) software.

2.3.5 HIS-PV model Evaluation

The annual SMD records were examined and five periods with different meteorological conditions selected for model evaluation (Table 2.2). To examine the general performance of the HIS-PV model, two models with different parameterization were compared. One model was parameterized with SMD from the control plots (HIS-PV control) and one parametrised with SMD from the under and gap plots (HIS-PV u&g), (Table 2.3). The purpose of this was firstly to capture the potential of using the model to simulate effects in areas where there was no solar park SMD (i.e. where only the equivalent of control data is available) of any location across the world (e.g. control datasets). Secondly to demonstrate the model's response to biases in the input data (Best, 1998) by using under and gap SMD to simulate each location respectively. However, overall the differences between the two models were less than 1 °C (~0.9 °C under and ~0.3 °C at the gap) by average and because there are no SMD broadly available from under and gap between the panels, only the HIS-PV control model was assessed and reported in this study (see SI.2 for results using the under and gap SM data).

Table 2.2: The five ten-day periods tested with the HIS-PV and their general microclimatic characteristics. Where, HT for the hottest, H for hot, C for cold, D for dry, W for wet, M moderate. Abbreviation s, for the periods in which spatial field metrics were also used in the analysis. DOY, stands for day of the year according to the Julian calendar for the period March 2015 to March 2016.

Period	DOY	Mean Air temperature (°C)	Mean Wind Speed (m/sec)	Mean RH (%)	Net Precipitation (mm)	Net SW radiation (W/m^2)
HTs	173-183	17.9	1.2	73.3	2.8	232
HD	211-221	16.1	1.1	74.2	0	212
CD	102-112	10.5	2	76.2	0	203
CW	355-365	5.9	2.1	92.2	81.6	28.5
MCs	268-278	10.6	0.7	85	1.6	134.4

The surface properties were parameterized using the mean of the values found in the literature (

). The mean of T vegetation in the solar park within the entire sampling period (March 2015-March 2016) was used for LAI. The VWC was parameterized differently depending on the datasets of the instantaneous measurements during each period, while mineral and organic content were kept constant (0.05 m^3/m^3 and 0.45 m^3/m^3, respectively) throughout as they were not expected to change drastically within a year. Initial soil temperature from

under (station U2; Figure 2.3(a) was used to start the simulation from under and the gap soil temperature (station G4; Figure 2.3(a) to start the simulation showing the soil temperature at the gap. In Table 2.3 the HIS-PV u&g model parameterization is reported as well.

Table 2.3: HIS-PV models' parameterization of SMD data, the initial soil temperature and the volumetric water content based on the logged measurements. Surface resistance parameterization based on precipitation data (wet or dry soils) and LAI parametrization based on instantaneous measurements.

Model	**SMD**	**Initial Soil Temperature**	**VWC**	**r_s**	**LAI**	
					Under	Gap
HIS- PV control	control	u&g	0.35	500	2.33	2.33
HIS- PV u&g	u&g	u&g	0.20	500	3.50	2.99
HIS- PV u&g	u&g	u&g	0.28	600	4.30	3.30
HIS- PV u&g	u&g	u&g	0.34	600	1.10	1.10
HIS- PV u&g	u&g	u&g	0.36	0	1	2

HIS-PV u&g	u&g	u&g	0.38	500	4.15	5.16

2.3.6 Sensitivity analysis

To evaluate the sensitivity of the model variations in LAI (tested values 0, 5 and 10), r_s (tested values 0 s/m, 300 s/m and 500 s/m) and VWC (0.15 m^3/m^3, 0.3 m^3/m^3, 0.5 m^3/m^3), the HIS-PV control model was used. To quantify the impact of uncertainty in the inputted parameters given by the perturbations at the surface and their effects on soil temperature at 10 cm depth, the HIS-PV control was tested during the HTs and MCs periods (hottest and moderate cold periods, respectively). At each model run, one of the soil surface parameters (LAI, r_s and VWC) was changed whilst the others were held constant. The results of the sensitivity analyses were reported separately for each tested model input component compared with the instantaneous data.

2.3.7 Data analysis

Statistical analysis was conducted using R programme language within the RStudio environment version 3.3.2 (RStudio, 2015; R Core Team, 2017). To evaluate the performance of HIS-PV control as well as the sensitivity of the model to the variability of LAI, r_s and VWC, we compared the spatial distribution of the model with the mean of the *logged* and the *instantaneous*, at a soil temperature depth of 10 cm. The RMSE (root mean square error) used widely in environmental sciences on assessing predictive accuracy between measured and simulated data (Li, 2017; Li and Heap, 2011; Sándor et al., 2017; Phogat et al., 2016), was calculated and used as an indicator of the differences between measured and simulations. The lower the RMSE the better the model simulation. The packages that were used were scales (Hadley Wickham, 2017), ggplot2 (Hadley

Wickham, Winston Chang, 2016) and dplyr (Hadley Wickham, Romain Francois, Lionel Henry, Kirill Müller, (R Core Team, 2017)).

2.4 Results

2.4.1 O1. HIS-PV model evaluation

2.4.1.1 Sky View Factor

The model provided a reasonable representation of the sky view factor (RMSE = 10.57%), although slightly overestimated along the transect, apart from sampling point at 3.75 m (northern PV panel edge; described extensively at chapter one of this thesis; Figure 2.4). At the last sampling point along the transect, the simulated sky view factor demonstrated a sharper decrease than for the measured (sampling point at the southern PV panel edge; also described extensively in chapter one of this thesis).

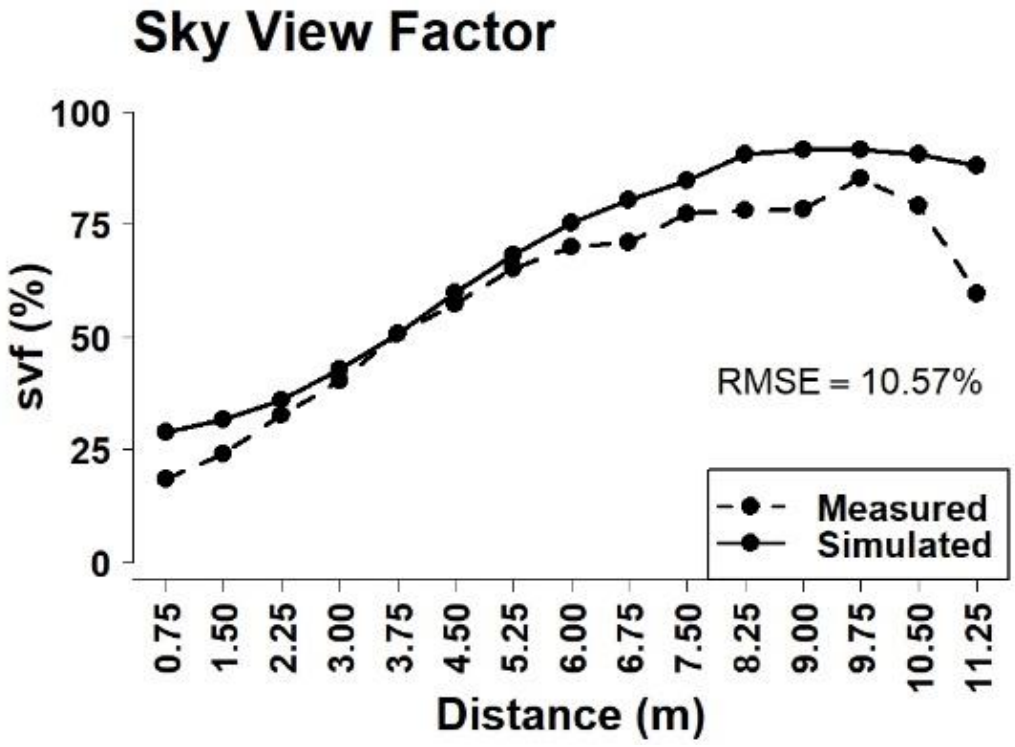

Figure 2.4: Sky view factor evaluation based on the relationship between measured (fisheye camera) and simulated along the linear transect.

2.4.1.2 HIS-PV model evaluation with logged data

HIS-PV predicted soil temperature well when compared with the logged data; overall the RMS errors did not exceed 1.23 °C under (MCs) and 1.06 °C in the gap (HTs; and Figure 2.5). For all the tested periods the simulated temperatures under the panels were warmer than measured, apart from period HD (Figure 1 in the SI.2). The gap simulations were cooler apart from MCs and CW periods (daytime), both under and gap simulations performed similarly, with RMS errors ~0.30 °C (Figure 2.5 and Figure 3 in SI.2).

Table 2.4: RMS errors between HIS-PV control and logged data of soil temperature at 10 cm depth

Period	HIS-PV control RMSE (°C)	
	Under	Gap
HTs	0.65	1.06
HD	0.52	0.95
CD	1.18	0.99
CW	0.26	0.30
MCs	1.23	0.98

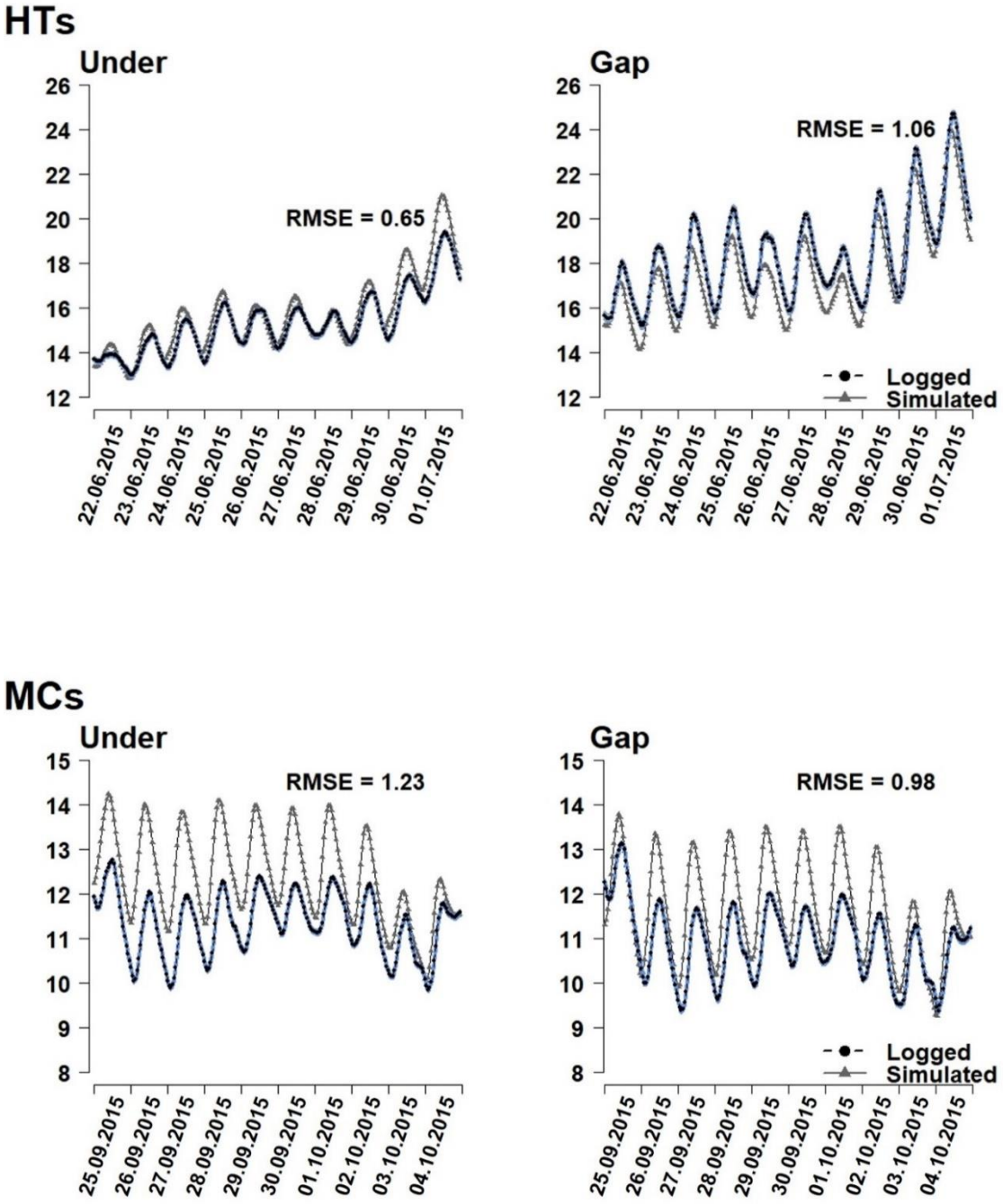

Figure 2.5: Comparison between simulated and logged soil temperature metrics during HTs the hottest and dry period and MCs the moderate cold period.

2.4.2 O2. HIS-PV control model evaluation with instantaneous data

The simulated data generally represented the instantaneous data taken along the transect in all periods. The model evaluation with the logged data demonstrated similar results

with the instantaneous where simulations under were warmer and at the gap cooler in the HTs period and both under and gap warmer in the MCs period. During the hottest (HTs) period, the simulated soil temperature along the transect was cooler than the instantaneous measurements at all three tested times of the day (TOD; Figure 2.6). For example, the RMS error in the morning was around 0.85 °C and increased in the afternoon (almost by 1 °C) reaching a 2.30 °C RMS error at the evening of the 25.06.2015; simulated soil temperature was cooling down with the passing of the day. During a moderate cold (MCs) period, the simulated soil temperature demonstrated similar distribution along the transect as the instantaneous measurements, however it was overpredicting (warmer) with the errors ranging between 1 °C-1.65 °C. The simulation cooled down along 3 m-6.75 m overlapping or being in the standard error margins area the instantaneous during all tested days (Figure 2.6).

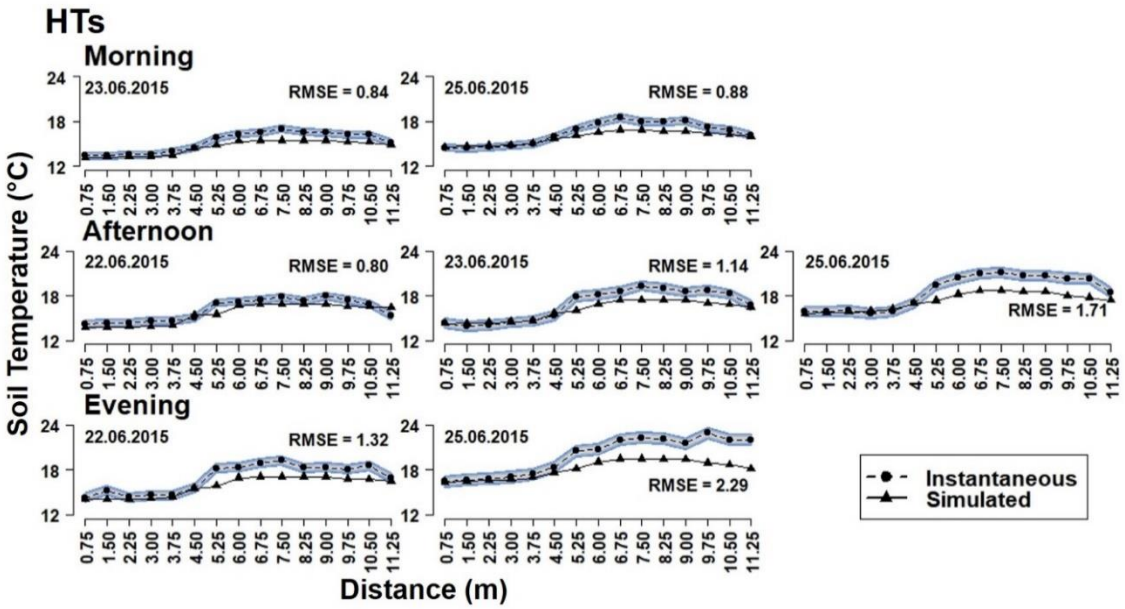

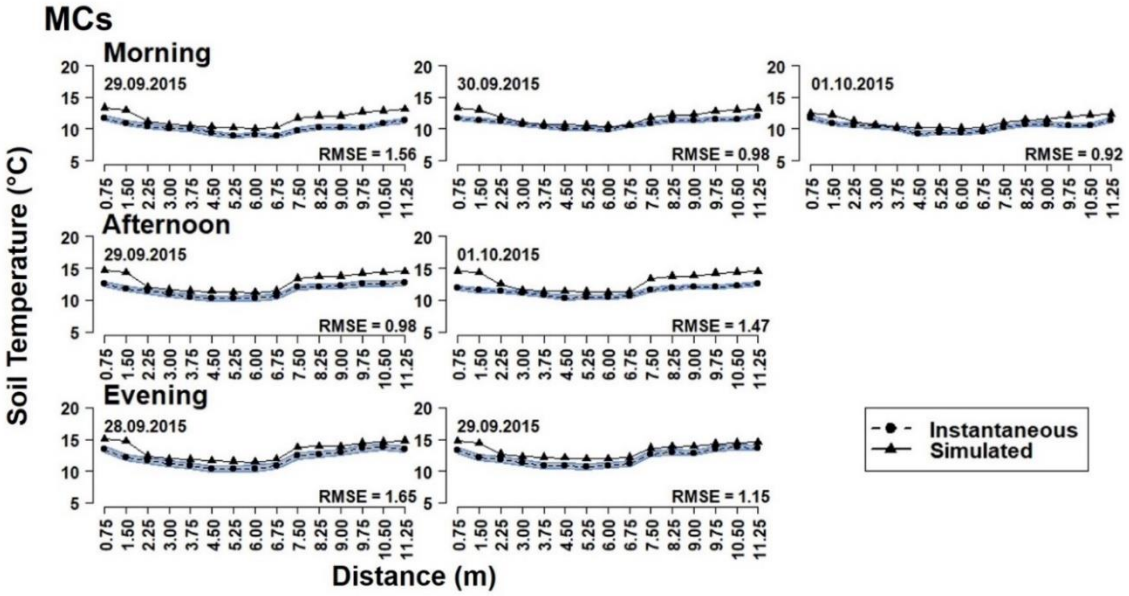

Figure 2.6: Period HTs and MCs, moderate cold, during morning, afternoon and evening illustrating the distribution of the means of the instantaneous (shaded blue area illustrating the standard error of the mean) and the simulations of HIS-PV model along the transect. RMSE indicating the error between the instantaneous and the simulation.

2.4.3 O3. Sensitivity analysis

The sensitivity analysis was performed assessing soil temperature simulations (10 cm depth) during periods HTs and MCs (hottest and moderate cold periods, respectively), during which instantaneous metrics were available (Figure 2.6 and Figure 2.7). The results of the sensitivity analyses were reported separately for each tested model component and the magnitude of change was reported comparing the values of RMS errors between simulated and measured (Table 2.5).

2.4.3.1 Sensitivity analysis during the hottest and driest period (HTs)

During the hottest (HTs) period assessed, the different parameterization of LAI surface properties' component, notably impacted soil temperature (Table 2.5). The simulations of soil temperature with denser canopies (LAI = 5 and LAI = 10) were cooler than when the actual LAI was used (LAI = 2.33), especially after ~ 4.5 m (gap area). The RMS errors increased gradually from morning to the afternoon and from the afternoon to the evening by approximately 1 °C-1.5 °C (Figure 2.7). With LAI=0, the simulations of soil temperature were similar to the instantaneous measurement, with an RMSE around 1.5 °C in the morning which increased by 1 °C in the afternoon and then dropped to ~1.5 °C in the evening. Further, the simulated soil temperature (setting LAI = 0) was constantly warmer than the instantaneous metrics along the transect (Figure 2.7).

The surface resistance had also an impact on soil temperature simulations when set to zero (wet soils; Table 2.5). The RMS errors where mostly driven by differences in the simulated and instantaneous soil temperatures in the gap.; the soil temperature predictions along the transect under the panels were similar to the instantaneous measurements (Figure 2.7). The simulation set to zero (wet soils) underestimated the instantaneous the most, compared with the rest of the different surface resistance parameterizations, especially at the gap (Figure 2.7). The RMS errors gradually increased from morning towards the evening by 0.5 °C. When parameterized as drier or dry soils (r_s = 300 s/m and 600 s/m, respectively), the soil temperature simulations where similarly distributed along the transect, underpredicting and the RMS errors compared with the instantaneous ranged from 1 °C-2.6 °C.

The impact of volumetric water content (VWC) component on the simulated soil temperature was smaller compared to the effect of the LAI and surface resistance (Figure 2.7). The simulated soil temperatures under the panels were similar to the instantaneous

measurements with the RMS errors driven by the changes at the gap (as for the surface resistance). The magnitude of the change on the soil temperature simulations, regardless of VWC parameterization, was ~1 °C in the morning, ~1.5 °C in the afternoon and between 2 °C and 2.5 °C in the evening. The RMS errors were increasing by approximately 0.5 °C-1 °C from the morning towards the evening.

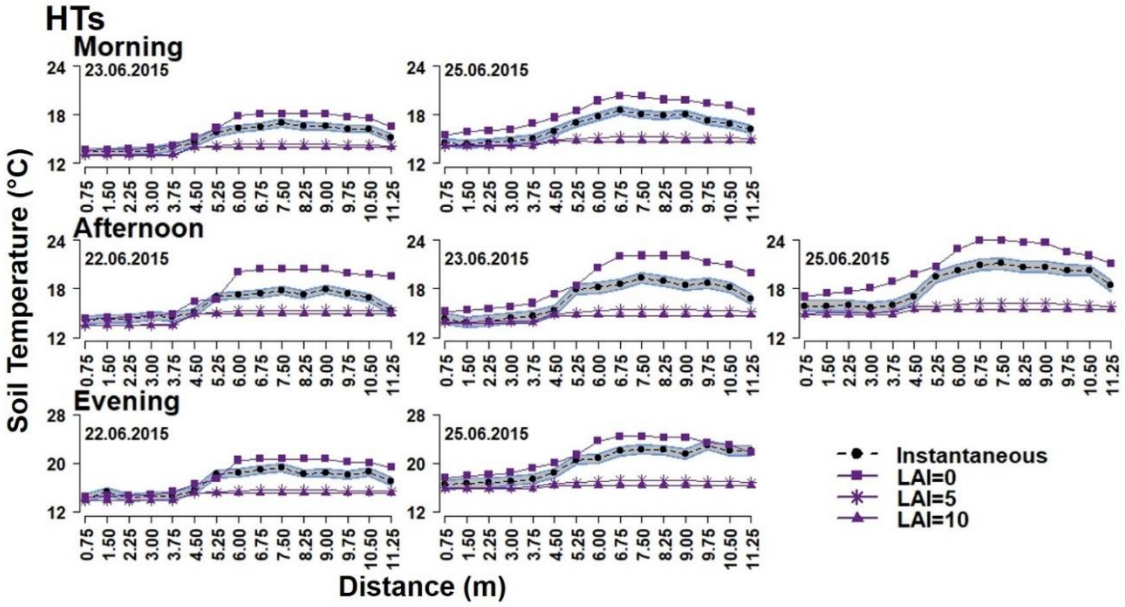

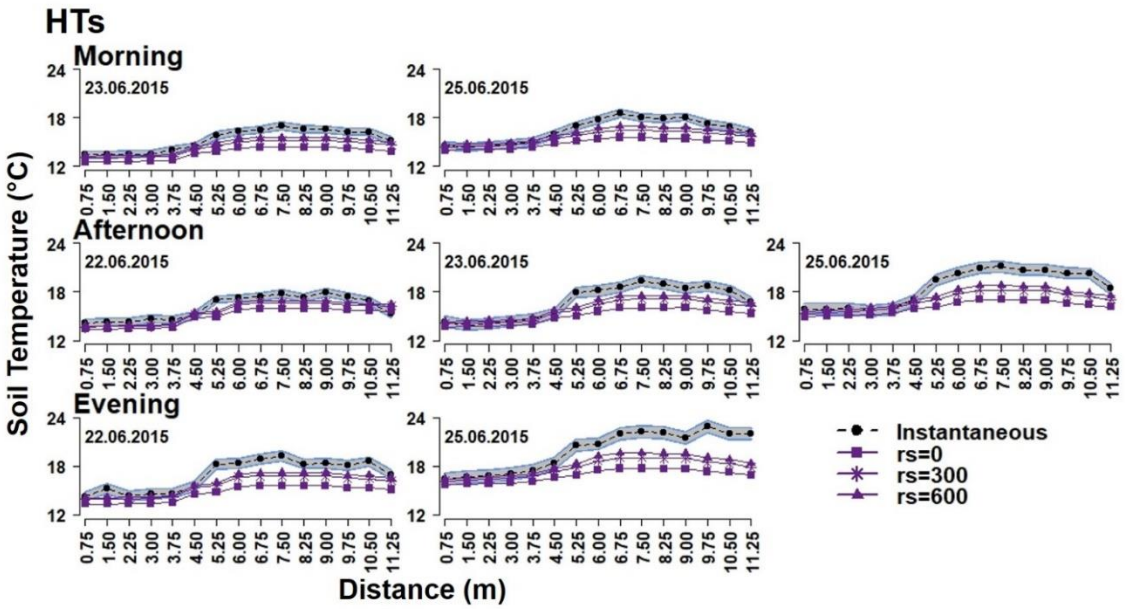

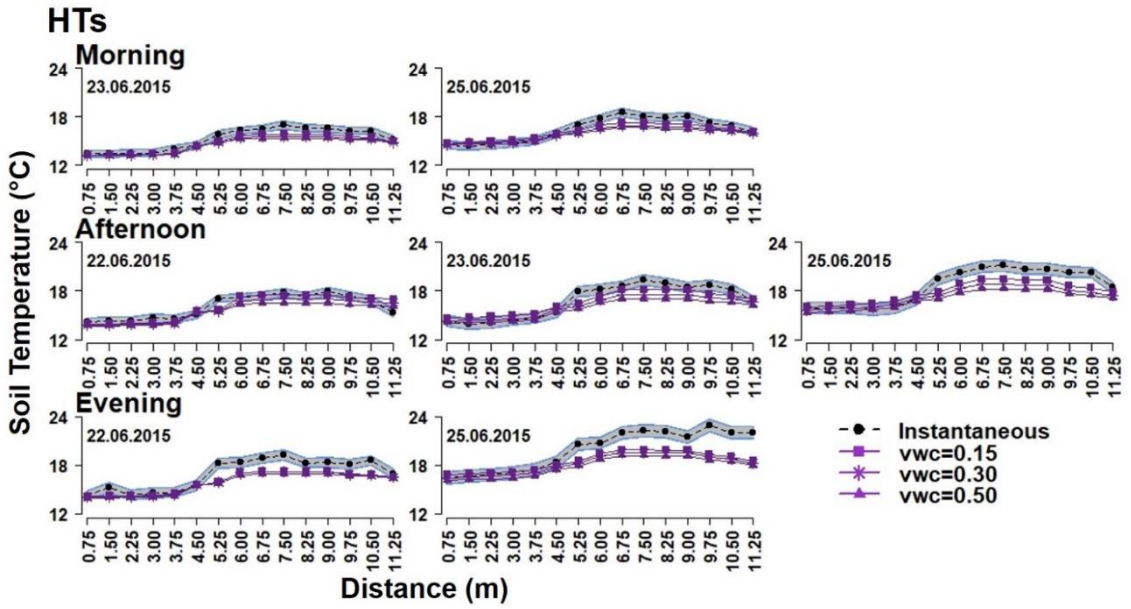

Figure 2.7: Period HTs, sensitivity analysis of the LAI model component, the surface resistance component and the volumetric water content component. Comparison with the mean of the instantaneous metrics along the transect during three times of the day (morning, afternoon and evening). Shaded area illustrating the standard error of the mean of the instantaneous metrics.

2.4.3.2 Sensitivity analysis during a moderate cold period (MCs)

The simulated soil temperatures when LAI was set to zero, demonstrated the greatest RMS errors, along the transects, with increases of ~2.5 °C from the morning to the afternoon and then decreases of ~1 °C towards the evening (Table 2.5). The simulated soil temperatures were warmer under the PV panels, cooler under the northern panel edge and warmer in the gap (Figure 2.8) during all times of day. The trends as well as the RMS errors were similar for both dense canopies (LAI = 5 and LAI = 10), during all three times a day (Table 2.5). Further the trends of soil temperatures with denser canopies remained constant along the transect (Figure 2.8).

The surface resistance parameter variation had a limited effect on the soil temperature simulations; RMS errors were ~1 °C-1.5 °C regardless of time of day (Table 2.5). All three tested values slightly overpredicted the instantaneous measurements and when parameterized for wet soils (0 s/m), the simulated soil temperatures were closer to instantaneous measurements (Figure 2.8).

Variation in volumetric water content had limited effect on the soil temperature simulation (Figure 2.8). The RMS errors in the morning, afternoon and evening metrics were 1.2 °C-1.5 °C regardless of parameterization and the simulated soil temperatures of the wetter soils (VWC = 0.50 m^3/m^3) were closer to the instantaneous distribution along the transect.

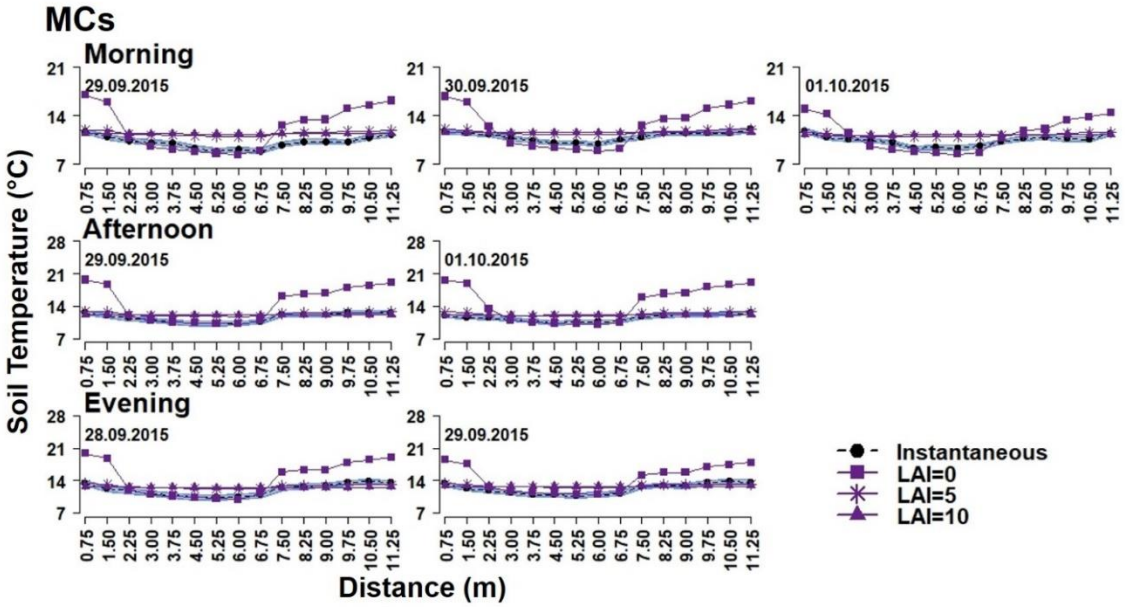

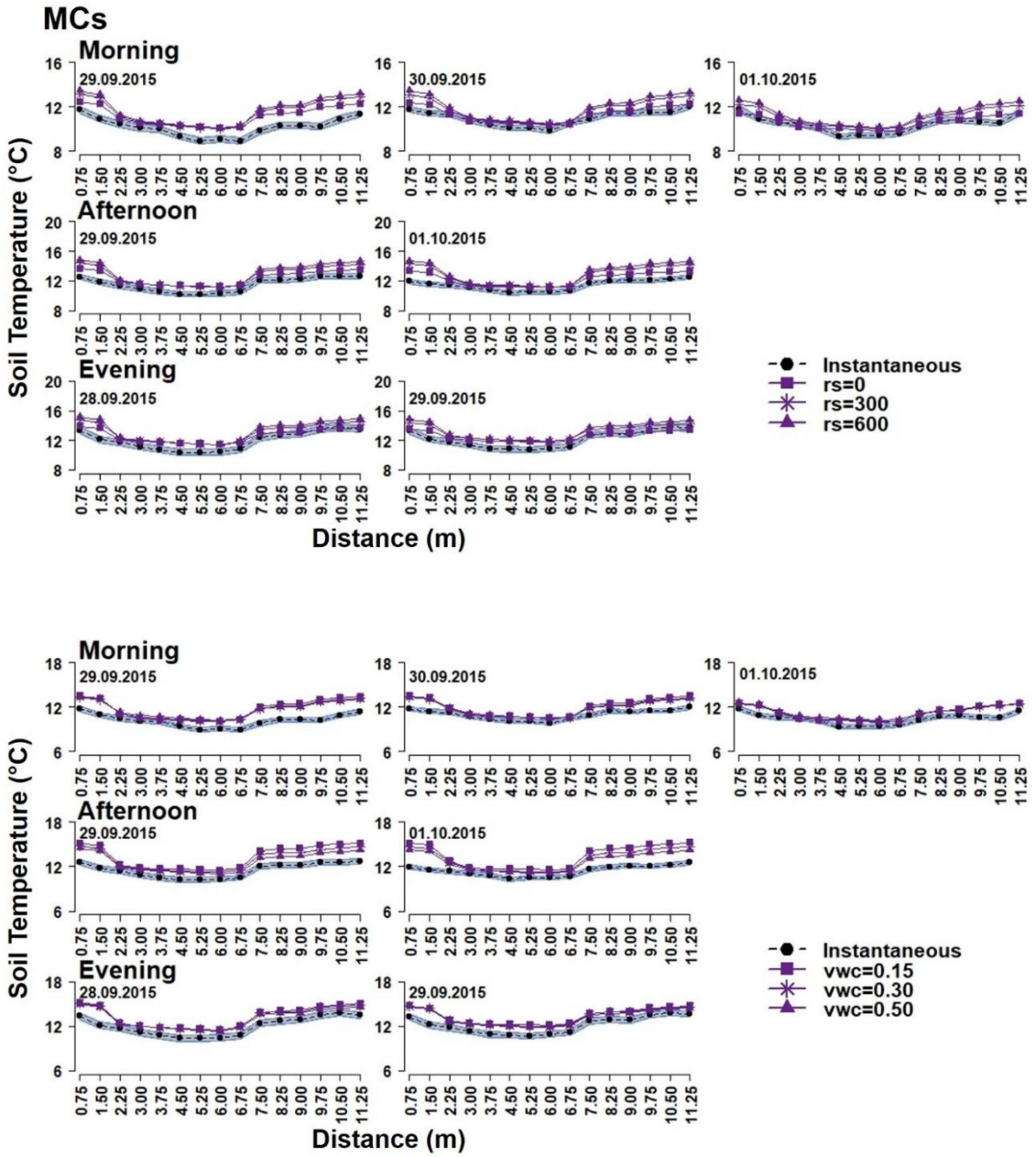

Figure 2.8: Period MCs, sensitivity analysis of the LAI model component, the surface resistance component and the volumetric water content component. Comparison with the mean of the instantaneous metrics along the transect during three times of the day (morning, afternoon and evening). Shaded area illustrating the standard error of the mean of the instantaneous metrics.

Table 2.5: Sensitivity analysis RMSE report for periods HTs and MCs using the C. HIS-PV model (LAI = 2.33, rs = 500, VWC = 0.35)

Period HTs	**23.06.2015**	**25.06.2015**	**22.06.2015**	**23.06.2015**	**25.06.2015**	**22.06.2015**	**25.06.2015**	**Mean**
TOD	**M**	**M**	**A**	**A**	**A**	**E**	**E**	**(Daily)**
LAI=0	1.10	1.82	2.24	2.42	2.47	1.55	1.75	1.91
LAI=5	1.59	1.91	1.61	2.41	3.29	2.31	3.82	2.42
LAI=10	1.86	2.29	1.93	2.88	3.87	2.67	4.38	2.84
r_s=0	0.99	1.81	1.33	2.10	2.85	2.47	3.55	2.16
r_s=300	1.04	1.10	0.89	1.34	1.99	1.54	2.60	1.50
r_s=600	0.77	0.81	0.77	1.07	1.61	1.25	2.18	1.21
VWC=0.15	0.59	0.63	0.66	0.78	1.22	1.21	2	1.01

VWC=0.30	0.80	0.84	0.75	1.05	1.61	1.29	2.22	1.22
VWC=0.50	0.92	0.98	0.95	1.36	1.98	1.42	2.51	1.44
Initial model parameterization	0.84	0.88	0.80	1.17	1.71	1.32	2.29	

Period MCs	29.09.2015	30.09.2015	01.10.2015	29.09.2015	01.10.2015	28.09.2015	29.09.2015	Mean
TOD	M	M	M	A	A	E	E	(Daily)
LAI = 0	3.15	2.70	1.94	4.16	4.71	3.57	2.82	3.29
LAI = 5	1.39	0.76	0.98	0.97	0.95	1.12	1.08	1.03
LAI = 10	1.47	0.86	1.10	1.08	0.95	1.31	1.22	1.14

$r_s = 0$	1.07	0.39	0.39	0.91	0.88	0.78	0.69	0.73
$r_s = 300$	1.42	0.82	0.76	1.31	1.47	1.11	1	1.13
$r_s = 600$	1.61	1.04	0.98	1.53	0.72	1.32	1.21	1.20
VWC = 0.15	1.72	1.15	0.91	1.96	2.18	1.40	1.28	1.51
VWC = 0.30	1.57	1	0.90	1.56	1.75	1.29	1.18	1.32
VWC = 0.50	1.55	0.96	0.99	1.26	1.44	1.15	1.06	1.20
Initial model parameterization	1.56	0.98	0.92	1.47	1.65	1.26	1.50	

2.5 Discussion

The HIS-PV model is the first to simulate variation in soil temperature within solar parks, predicting spatial variation at the 10 cm scale and temporal variation at 60-minutes intervals. Both spatial and temporal variations in soil temperature predictions were well aligned with measured soil temperatures collected in a solar PV grassland in the UK. Moreover, the model was evaluated during five time periods with a diverse range of meteorological condition. The majority of the RMS errors between simulated and logged (temporally dynamic) were lower than 1 °C and between simulated and instantaneous (spatially distributed) were ~1 °C-1.5 °C. In addition, the sensitivity of the model to LAI, surface resistance and VWC using instantaneous measurements during warm and cold periods (HTs and MCs) demonstrated that the model was most sensitive to LAI and relatively not sensitive to surface resistance and VWC.

Given this high sensitivity of the LAI, an opportunity for re-evaluating this component to a key driver of the HIS-PV simulations, arises. Limitations from inputting the LAI as a fixed parameter and not as a value of multiple ranges, for example adding different nodes of LAI ranging from 0-6 for a grassland with a 0.5 interval (i.e. 0,0.5,1,1.5 up to 6), could be also assumed. Regardless, the HIS-PV model at this stage, has the potential to provide useful simulations under a range of diverse weather characteristics in a temperate UK grassland solar park. Therefore, it is anticipated that across a range of climates and meteorological conditions, will be further in place to provide useful insight to ecosystem response to this growing land-use change.

2.5.1 Sky View Factor model component

The HIS-PV model successfully simulated the sky view factor on a linear transect running perpendicular between two PV panel rows. The RMS error was ~10.6% (Figure 2.4) and the overall spatial distribution along the transect was satisfactory for model evaluation. It was assumed that the error of overestimation was evident due to field of view implications. Photographs were taken at day-time of a cloudy day and GLA software, was reported to estimate diffuse light very well (Hardy et al., 2004). Thus, the error was assumed to be driven by the type of fish-eye lenses used which is generally shown that even from perfectly equiangular projections and restrictions in field of view, affect the results of sky view factor (Blennow, 1995). In particular, methods (computing or on printed photographs) used on images produced by the same camera (older version) and lens (same length and specifics) that were used to take the photographs in this study, also overestimated the sky view factor (Blennow, 1995).

2.5.2 Model sensitivities during warm periods

Warm periods HD (hot and dry; Figure 1 in the SI.2) and HTs (Figure 2.5) differences between measured and simulated soil temperatures under and at the gap were of the same magnitude ~0.4 °C (Table 2.4). Further, the simulated trends represented the measured (logged and instantaneous) well during the two warm periods. The analysis of HIS-PV model sensitivity on LAI variation showed a major effect on the simulated soil temperatures during the HTs period. Our findings were in agreement with a simulation study by Kang et al. (2000). In their study, it was demonstrated that risen air temperatures and variation of the LAI has shown to affect the spatial variability of the soil temperature at 10 cm depth, with the errors increasing from 1.55 °C-4.71 °C analogue to increasing densities of LAI from 0-10.

During the HTs period, in the afternoon (12 pm) there were constant overpredictions of ~0.5 °C which increased to ~2 °C during the last two days of the period under the panels and constant underpredictions of the same range at the gap, apart from the last two days were measured and simulated overlapped (Figure 2.5). This warming up (under) and cooling down (gap) respectively, during the last two days, could be related to the increased proportion of direct SW radiation (~900 W/m²; data not presented) and the risen temperature which in the afternoon of the 30th of June reached ~35 °C (data not presented; (Lenderink et al., 2007). During HD period where under and gap simulated soil temperatures were underpredicting, assumingly the high SW radiation which reached a maximum of ~820 W/m² on the 2nd of August (simulated and logged overlapping; see Figure 1 in the SI.2) might have had an effect on the simulated soil temperatures.

In addition, it is assumed that the initial model parameterization might have caused a conflict and affected the simulated soil temperatures during the two warm periods. More specifically, the HIS-PV control model parameterization (same for all periods assessed), had components such as VWC and r_s set as if the soil was quite wet (0.35 m³/m³) and at the same time, quite dry (r_s = 500 s/m; Table 2.3). Therefore, potentially, if r_s was parameterized around 300 s/m, the simulated soil temperature would be closer to the logged during both periods. In fact, the sensitivity studies on r_s during HTs period showed that when soils are parameterized as semi-dry and dry (300 s/m and 600 s/m, respectively) the RMS errors between simulated and instantaneous were lower and the trends were in close agreement to the instantaneous (overlapping under and slight underpredicting at the gap; Figure 2.7).

2.5.3 Model sensitivities during cold periods

The simulated soil temperature during the assessed cold periods (MCs, CD and CW; Table 2.4), represented the measured (logged and instantaneous data) slightly better than the simulations in the warm periods (Table 2.4) during the model evaluation and the sensitivity analysis. When the LAI was set zero (during MCs period), the simulated soil temperature demonstrated the highest RMS errors among all comparisons in this study especially when compared with the instantaneous data taken in the afternoon (reached 4.71 °C on the 1st of October). Zero LAI would cause changes at the surface energy balance, as the incoming SW and precipitation interception at the soil surface and the subsequent processes including evaporation, would change (Reichstein et al., 2003). Land without vegetation (e.g. winter period, out of growing season), is expected to show increased soil evaporation and increase the proportion of incoming SW receipt at the soil surface compared to a land unit with vegetation (vegetation canopy absorbs a proportion of the incoming radiation). Thus, increased soil evaporation and incoming SW proportion on a bare soil would result in warmer soils at root zone depth (10 cm – 30 cm; (Gupta et al., 1981; Gupta et al., 2015)).

CW was a period with air temperature minimum reaching around -3 °C and total precipitation around 82 mm. The initial parameterization of the model (surface resistance r_s = 500 s/m; almost dry soil) and VWC (0.35 m^3/m^3), did not have an effect or created conflicts which would impact the simulated soil temperatures, as it was assumed during the two warm periods. This was mainly assumed since CW was the only one among the five period where simulated represented the logged best (RMS errors less than 0.3 °C; see Figure 3 in SI.2). Initially, the high amount of precipitation was assumed to have an impact on the simulations, because the model does not account

for the impact of energy transfer by liquid advection, (i.e. of water moving through the soil and transporting energy with it). We would expect this to be more impactful during or after periods of rainfall but the simulations during CW period proved that there was no impact even during a ten-day period of high precipitation ratios.

2.6 Future Model development

HIS-PV model predicts the effect of solar parks on soil temperatures, using SMD and surface properties aspects including LAI. Judging from the results of the sensitivity analysis assessing simulated soil temperatures driven by different parameterizations of LAI, surface resistance and VWC components, there are a few suggestions to further improve HIS-PV. The LAI should be a dynamic component in the model as it had a major effect on the simulated soil temperatures under a diverse range of weather characteristics. However, the range of the LAI, should perhaps be less fixed and have several LAI's tested and correlated with the other outputs of the model including soil temperature and solar radiation, along the transect design. Further, applying HIS-PV model in different climate zones, soil moisture should be also considered as a main model component, as temperature is not the only driver of leaf phenology and canopy; LAI (Arora and Boer, 2005).

In addition, the model was tested with SMD simulating conditions in a UK temperate grassland. For future model development and application of the HIS-PV model in different ecosystems it is important to further discern the variation in both soil moisture and LAI. Solar parks have been shown to have soil moisture and biomass variability under and at the gap between PV panels (Armstrong et al., 2016). Thus, modelling solar parks productivity predictions could be also considered to improve the simulations. The accuracy of the HIS-PV model would increase developing an incorporation with a

vegetation or a crop model (Sinclair and Seligman, 2000; Dinesh and Pearce, 2016; Arora and Boer, 2005; Dupraz et al., 2010). Assessment on evapotranspiration, monitoring the diurnal and nocturnal fluctuations, could further improve the simulations (Nemitz et al., 2009; Kettridge and Baird, 2006) and predict the effects on productivity in solar parks.

Regarding the PV panels physical presence, it is important to address the significant roughness that the panels induce where installed. Potential impacts on terms of evapotranspiration is a logical assumption since just vegetation management alone may not be useful. Apart from roughness, it would be very interesting to have solar panels dimensions component as a key driver of the simulations, which would upscale HIS-PV at a stage where it could be a useful tool for all construction companies prior-planning and designing of a solar park.

2.7 Conclusion

Given the global deployment of solar parks, establishing the effects on the microclimate of any given area, is crucial. This research demonstrates the capability of the HIS-PV model to predict fine temporal and spatial scale simulations of soil temperature, with confidence, in a solar PV grassland, and on lands where solar parks may be constructed under a range of weather conditions. HIS-PV requires standard meteorological data, that are readily available in many locations and some surface property data, namely VWC, soil mineral and organic content, LAI, albedo, displacement height, roughness, emissivity, surface and aerodynamic resistance. However, the results of this study, when initially parameterizing the model components, demonstrated that only LAI crucially affected simulated soil temperatures under a diverse range of weather characteristics; and is strongly suggested that it should be a dynamic model component. The model was

tested with standard meteorological data simulating conditions in a UK temperate grassland; however, the model should be assessed in other climate zones as well. In addition, the proposals for future model development could establish HIS-PV model as a widely applicable tool with the potential of creating frameworks of an effective vegetation management to promote agrivoltaic schemes, as well as any other multiple-use land and thus, optimize ecosystem services from the same land unit.

3 Chapter 3: Simulating the Impacts of Solar Photovoltaic Parks on Soil Temperature, Potential Evaporation and Incoming Short-Wave Radiation in different Climate Zones

3.1 Abstract

The need to transition to low-carbon energy sources is the primary driver of the large-scale deployment of ground-mounted solar photovoltaic (PV) technologies (solar parks). However, the impact of solar parks on microclimates across different climate zones is unresolved. The aim of this study was to assess the impact of solar parks on root zone soil temperature (10cm depth), potential evaporation (PE), incoming short-wave radiation (SW) and growing degree days (GDDs) across the Equatorial, Arid, temperate, boreal and polar climate zones. HIS-PV model was applied to simulate soil temperature, SW and PE in 25 hypothetical solar parks across five different climatic zones. Typical Meteorological Year (TMY) data from NREL USA, were used to simulate each solar park and its microclimatic conditions assessing the potential impact on GDDs in three treatments: under, between (gap) and away (control) from the PV panels. Annual incoming SW was strongly affected by solar park installation; control

received 60% more solar radiation than under and 8% more than the gap across all tested zones ($p < 0.001$). The summer daily mean soil temperature among treatments within the same zone showed significant differences with control being constantly cooler than under across equatorial, arid and temperate zones ($p < 0.001$). In the Arid zone soil temperature under was 3.1 °C cooler than control, when in the equatorial and temperate zones was 1.1 °C cooler. PE under, was strongly affected in the Arid (46% less and the Equatorial ((35% less)) zone, relative to the control; ($p < 0.001$). GDDs under were lower than control, especially in the arid and the equatorial zones. The overall differences among treatments were low (3-4%) apart from arid where control had 13% more GDDs compared with under. Our findings regarding the reduced amount of GDDs under the panels, especially at the arid, where most of solar parks are globally installed, deemed crucial, however were not statistically significant ($p > 0.05$) thus further assessment is required to establish the causes.

Keywords: soil temperature, potential evaporation, short-wave radiation, photovoltaics, solar parks, climatic zones, growing degree days

3.2 Introduction

Global efforts to mitigate climate change is forcing an energy transition from conventional to renewable resources (UN, 2015; IPCC, 2018) with solar energy having a progressively prominent role (IEEFA, 2018). Solar power-based generation in operation is increasing globally (IEEFA, 2018). In particular, ground-mounted photovoltaic (PV) technology is rising exponentially, increasing its capacity (RECP, 2018) across the world including Asia, America, Europe; a diverse range of climatic zones. The growth in solar PV installations (hereinafter referred to as solar parks),

causes an extensive land use change, since ground-mounted solar parks are primarily deployed on land.

This rapid deployment, especially in highly populated countries, has coincided with global rise of population, resulting in increased land-use competition for food, fibre and fuel. At the same time there is an increased pressure globally to follow sustainable practices and protect the environment. Solar parks require more space than other energy resources. To mitigate land-use pressures, new strategies that take advantage of the space under and around the PV panel rows need to be developed. For example, these strategies (multiple-lands use) involve food production under PV panels (agrivoltaic schemes firstly introduced by Goetzberger and Zastrow (1982)), the co-production of biofuel from agave plants grown around the panels (Ravi et al., 2014), the introduction of new habitats to promote, for example, pollinators (Walston et al., 2018), and small live-stock for grazing (BRE, 2014). Given that solar parks offer such potential regarding space, unlike other land use changes from other energy sources, multiple-use lands are appealing.

Despite the notable land use change from solar parks installations and the potential for multiple-use lands, the effects of the physical presence of solar parks on local climate is poorly resolved. Soil temperature, evaporation and incoming SW radiation are key environmental drivers which among others (including vegetation), regulate the microclimate. Research has highlighted the magnitude of the induced-microclimate caused by the PV arrays and its effect on ecosystem function and vegetation growth only in temperate and temperate-Mediterranean environments (Table 3.1).

In a UK grassland, the daily mean soil temperature under was 5.2 °C cooler and the above-ground biomass was four times higher compared with areas away from the solar

PV panels (Armstrong et al., 2016). Further, vapor pressure deficit was lower under the PV panels during the day and higher during the night compared with areas away (Armstrong et al., 2016). In addition, daily mean soil temperature on lettuce and cucumber cropland, located at Montpellier of France, was decreased under and implied changes on leaf apparition rate of juvenile leaves compared with areas exposed at full sunlight (Marrou et al., 2013b).

The effect of shade cover (i.e. PV panels) on soil temperature, incoming SW radiation and potential evaporation (PE) is in part determined by the existing vegetation communities (Teasdale and Mohler, 1993). According to Armstrong et al. (2016) the areas under PV panels (hereinafter referred to as under) were less productive and less diverse compared to areas away. However, in a previous study with a different spatial explicit design (chapter one of this thesis), evapotranspiration (ET) metrics were quite similar comparing under and the gap between two panel rows (hereinafter referred to as gap) and the leaf area index (LAI) was unaffected spatiotemporally during growing season. Further, differences were noticed with regards to the Net Ecosystem Exchange (NEE) where under and the gap demonstrated reversed pattern regarding sourcing and sinking of CO_2 during growing season.

Differences between the results of these studies are recognised and suggest that the effects of solar parks appear to be more complicated and the assessments were conducted only on temperate environments. In addition, all of the microclimatic effects described above are regulated through vegetation, as the microclimate determines physical, chemical and biological processes that control soil formation and plant distribution (Liu and Luo, 2011). Thus, any microclimatic changes at the surface energy balance are crucial because they will modify processes including ET which will then

alter the vegetation cover (Jackson, 1973). The effects on vegetation are difficult to summarise but Growing Degree Days (GDD) is a simple means and a fine scale quantifying approach, which allows prediction on the phenological transitions of living organisms (animals, plants etc.(Bonhomme, 2000; Hassan et al., 2007; McMaster and Wilhelm, 1997; Swan et al., 1987)).

Each living organism has a specific number of GDD (threshold) which must be accumulated to trigger phenological changes and this is expected to change with the presence of a solar park construction. The spatiotemporal microclimatic niches in a solar park, will have a strong effect on the GDD under and potentially within the gap. In a solar park in the UK (temperate zone), the total GDD were significantly lower under compared with areas away (control) from the PV panels by ± 36 °C daily (Armstrong et al., 2016). Need to consider here that the length of growing season varies at each climate zone and the up-to-date research findings have only assessed temperate environments.

Table 3.1: Published research up to date regarding solar parks impacts on the local climate

Publication	Country	Geospatial Characteristics	Climate Zone	Measurements	Findings
Dupraz et al. (2010)	Montpellier, France	43.15°N, 3.87°E, Elevation: 57 m	Temperate, Mediterranean	PAR, under two different shades associated with crop production (LAI as an indicator)	Predicted a 35-73% increase of global land productivity for the two different densities.
Marrou et al. (2013a)	Montpellier, France	43.15°N, 3.87°E, Elevation: 57 m	Temperate, Mediterranean	PAR, air and crop temperature (four varieties of	Total relative lettuce yield at harvest equal or

		lettuces), under and away from PV panels, Relative humidity (RH), total aerial dry matter, leaf length, width and number.	higher than the available solar radiation. Some lettuce varieties showed shade tolerance. Leaf thickness decreased, LAI increased, but length and width were unaffected under shade in growing season.

Marrou et al. (2013b)	Montpellier, France	43.15°N, 3.87°E, Elevation: 57 m	Temperate, Mediterranean	Air and soil temperature, RH, wind speed and PAR, crop temperature (lettuce, cucumber and durum wheat) and number of leaves, under and away from the panels.	Air temperature and RH similar under and away the PV panels. Soil temperature decreased significantly under. Diurnally, crop temperature and PAR ratio increased under the PV panels. Overall crop

					temperature under was unaffected.
Marrou et al. (2013c)	Montpellier, France	43.15°N, 3.87°E, Elevation: 57 m	Temperate, Mediterranean	Air and soil temperature, RH, wind speed and PAR, precipitation associated with ET variability, stomatal conductance and biomass production of four varieties of lettuce and cucumbers,	Shaded irrigated crops under PV panels saved 14-29% water; shade proportion dependant. Increased ratios of vegetation cover and stomatal conductance and soil evaporation more sensitive to

		under and away from PV panels.	plant transpiration under PV. Irrigation allowed evaporation and biomass production being close to their potential.
Armstrong et al. (2016)	Oxfordshire, UK	51.37°N 01.38°W, Temperate Elevation:103 m	Under, gap between PV panels and away, air and soil temperature, soil moisture, RH, wind speed and	Summer soil temperature under was 5.2 °C cooler than gap and away from the panels. In winter, the gap was

		gust, PAR and precipitation associated with site management and carbon cycling.	1.7 °C warmer compared to under and away. Above ground biomass and species diversity reduced under. Photosynthesis and Net ecosystem exchange reduced under panels during winter and spring.

Barron-Gafford et al. (2016)	Arizona, USA	32.09°N, 110.81°W, Elevation: 888 m	Temperate, Steppe	Air temperature 2.5 m above soil surface comparison among a semiarid desert, a parking lot, and a solar PV site.	PV heat island effect caused due to nocturnal air temperature above PV panels being 3-4°C warmer than wildlands.
Hassanpour Adeh et al. (2018)	Oregon, USA	44.34°N, 123.17°W, Elevation: 72 m	Temperate, Oceanic	Air temperature (different heights), RH, wind speed and direction, away and at the gap between PV	Under the PV panels 90% from May to August more biomass and 328% more efficient compared

	panels. Soil moisture, biomass from under, at the penumbra and away PV panels associated with microclimate	with away and area in the penumbra. Mean air temperature variability observed mostly close to the surface

Given the construction of solar parks across a diverse range of climatic zones and the focus of land-use impacts within studies mainly within temperate environments, a continental scale modelling approach to predict the scale and diversity of microclimate impacts is strongly suggested. HIS-PV model (built and evaluated in chapter two of this thesis), is a physically based, spatial explicit numerical model (based on the soil temperature models built by Kettridge and Baird (2008) and Kettridge et al., (2013). The model simulates soil temperatures through the soil profile, PE and incoming SW radiation across the solar park. Photosynthetic active radiation (PAR) is highly correlated with SW and determines the energy available for photosynthesis. Temperature regulates metabolic rates and therefore strongly impacts all productivity and decomposition processes. Last, water availability controls productivity and decomposition. PE can give an indication regarding the impacts of solar parks on the water availability for the subsequent processes, including plant growth.

It is important to secure and promote ecosystem functions at the hosting environment in order to achieve the optimum efficiency from both land (food) and PV panels (energy) at the same land unit. The wide deployment of solar parks across different climate zones and the introduction of new strategies such as multiple-use lands, will continue without fully understanding the impacts of solar parks at the local climate.

3.2.1 Research aim

The aim of this study was to assess the impacts of solar parks on crucial environmental drivers which among others regulate the microclimate and thus the annual GDDs at the host-environment across different climate zones. To address the magnitude of these effects, the following objectives were addressed:

O1. Assess the effect of solar parks in different climatic zones on soil temperature in 10 cm depth, PE in the summer and the annual incoming SW radiation at the soil surface.

O2. Quantify the variability in GDDs caused by the physical presence of a solar park of a land in different climatic zones.

3.3 Methods

3.3.1 Sites and data selection

To assess the effect of hypothetical solar parks installed across different climate zones, five locations at each climate zone (n = 25; Figure 3.1 and Table 3.2) were selected in the USA based on the Köppen Climate Classification (KCC; (Kottek et al., 2006). USA provides the option of using a great and widely accessible database of typical meteorological year data (TMY) from hundreds of stations and sensors installed across all states at any given time and for free (NREL, 2005). Further, the USA is a climatically diverse country (covering all five KCC climate zones) which spreads across a 9,834 million km^2 area with a full range of weather phenomena strongly affected by the Atlantic and the Pacific stream. The annual average of precipitation in the USA is ranging from around 1618 mm in Hawaii to 218 mm in Nevada and the annual average of air temperature is ranging from 21.5 °C in Florida to -3 °C in Alaska.

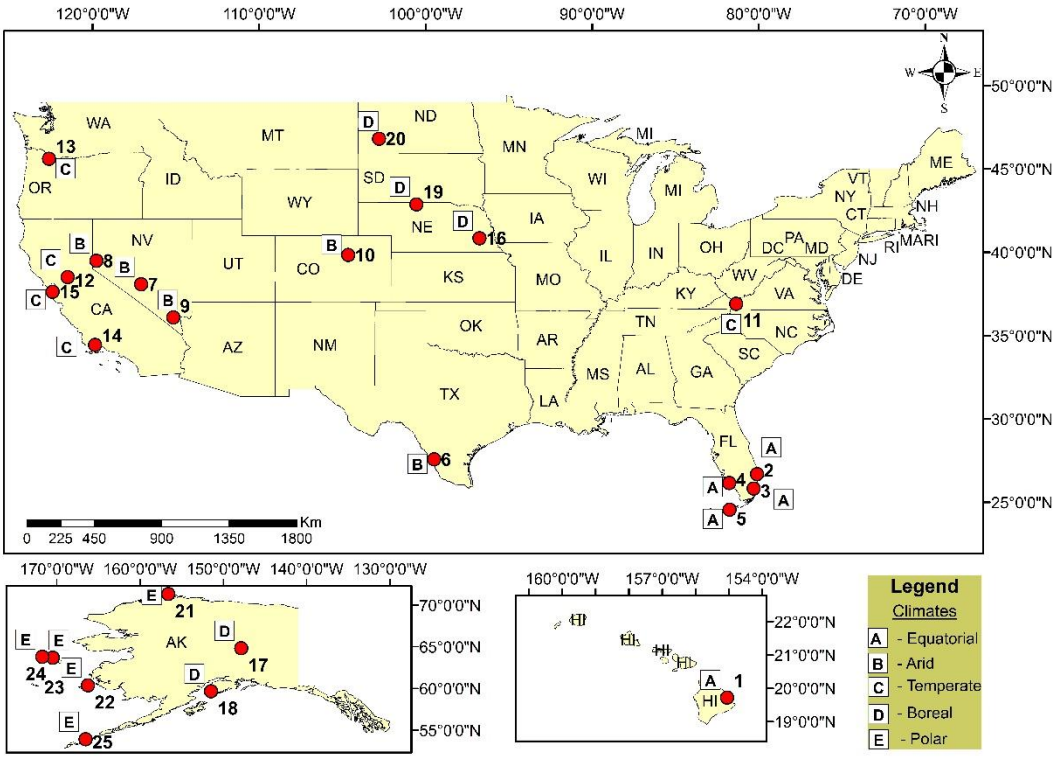

Figure 3.1: Location of the 25 meteorological stations assessed. Longitude, latitude and the climate zone classification based on Köppen created in ArcMap Environment version 10.1 of the ArcGIS (ESRI, 2011) by the author.

Simultaneously is one of the top five leading solar PV markets-countries (China, Japan, Germany, USA, Italy), ranking forth for 2016 and 2017 regarding its solar PV installations capacity (WEC, 2016; REN21, 2017; RECP, 2018). Thus, the impact on microclimate caused by the land-use changes (establishment of solar parks), at a country of a geospatial and marketing footprint such as the USA, will further have a major effect on the global climate compared with a country of smaller size and of a smaller solar PV market. In addition, the wide and free accessibility to online TMY datasets (NREL, 2005), offers an opportunity to undergo a study for further application of the HIS-PV model across different climatic zones.

TMY data are widely used in environmental, climate modelling and in generally in solar energy systems studies (Hall et al., 1978), to describe the solar climate of a region. Measurements are made at hourly intervals over a few years to build up a non-biased picture of the local climate (Cebecauer and Suri, 2015). The TMY data used for the input in the HIS-PV model were, air temperature (sensor at 2 m above surface measured in °C), relative humidity (sensor at 2 m above surface measure in %), wind speed (sensor at 90 m and measured in m/sec) and diffuse, direct and total SW radiation (several feet above ground level measured in $W \cdot m^{-2}$).

Table 3.2: Sites geospatial and climatological information

No	KCC	Climatic description	Location	Altitude (m)	Daily air temperature (°C)			Growing Season (total DOY)
					min	max	mean	
1	Af	Equatorial, fully humid	Hilo, Hawaii	9	13.9	31.1	23.1	365
2	Af	Equatorial, fully humid	West Palm Beach, Florida	6	-1.1	33.9	23.6	365
3	Am	Equatorial, monsoonal	Miami, Florida	11	5	35.6	24.5	365
4	Aw	Equatorial, winter dry	Naples, Florida	3	3	33.9	22.9	365
5	Aw	Equatorial, winter dry	Key West, Florida	1	9.4	33.3	25.6	365
1	BSh	Arid, Steppe, hot arid	Laredo, Texas	142	22.4	41	22.4	290

2	BSk	Arid, Steppe, cold arid	Reno, Nevada	1342	11.1	37.8	19	140
3	BSk	Arid, Steppe, cold arid	Denver Int Airport, Colorado	1650	16.2	40	10.9	177
4	BWh	Arid, Desert, hot arid	Las Vegas, Nevada	648	3.3	44.4	19.8	299
5	BWk	Arid, Desert, cold arid	Goldfield, Nevada (Tonopah Airport Met Station)	1655	-11.1	37.8	11.2	188
1	Cfb	Warm Temperate, fully humid, warm summer	Wytheville, Virginia	780	-19	32.6	11.9	204
2	CSa	Warm Temperate, Steppe, hot summer	Sacramento, California	5	-2	40	15.55	310

3	CSb	Warm Temperate, Steppe, warm summer	Portland, Oregon	6	-4.4	37.8	12.2	241
4	CSb	Warm Temperate, Steppe, warm summer	San Francisco, California	2	2.2	32.8	13.8	365
5	CSb	Warm Temperate, Steppe, warm summer	Santa Barbara, California	3	0	32.2	14.7	365
1	Dfa	Snow, fully humid, hot summer	Lincoln, Nebraska	357	23.3	38.9	11.2	189
2	Dfc	Snow, fully humid, cool summer	Fairbanks, Alaska	133	-38.3	-30	-1.4	94
3	DSc	Snow, Steppe, cool summer	Homer, Alaska	27	-20.6	23.9	3.8	148

4	DWa	Snow, Dessert, hot summer	Valentine, Nebraska	789	-25	41.7	9.7	157
5	DWb	Snow, Desert, warm summer	Dickinson, North Dakota	788	-33.9	39.4	5.3	104
1	ET	Polar	Barrow, Rogers Airport, Alaska	10	16.1	-41.7	-11.8	NA
2	ET	Polar	Dutch Harbor, Alaska	4	-15.6	22.2	4.7	NA
3	ET	Polar	Gambell, Alaska	8	-27	16.6	-2	NA
4	ET	Polar	Mekoryuk, Alaska	15	-29.4	21	0.9	NA
5	ET	Polar	Savoonga, Alaska	17	-29.4	10.2	-3.3	NA

3.3.2 Model Description

HIS-PV is a pseudo-three-dimensional (3D) physically based, spatial explicit numerical model, based on the soil temperature models by Kettridge and Baird (2008) and by Kettridge et al. (2013). The model was coded in Fortran compiled imperative programming language that is especially suited to numeric computation, using NAG builder 6.2 environment (NAG, 2018). A 2D sub-model simulated the subsurface energy transfer and storage along a linear transect running perpendicular to three PV panel rows of known dimensions in a 100 m x 100 m simulated solar park. The energy transfer simulated a 1 m deep profile composed of 19 vertical nodes. Node separation increased with depth ranging from 0.005 m at the soil surface to 0.1 m at a depth of 1 m. A synopsis of HIS-PV model parameterization and thorough description regarding the built of the model can be found in chapter two of this thesis (section 2.3.1).

For this study, HIS-PV was framed as a soil temperature model with an associated surface boundary layer with a timestep established at 30 seconds for 8754 hours in total (annual period of 365 days; starting time interval at 06:00 on the 1st of January and finishing time interval at 22:00 on the 31st of December). HIS-PV model was further edited to simulate the potential evapotranspiration (PET):

$$E = \frac{L_v s(T_s - T_a) + L_v v d d_a}{r_a} \qquad (1),$$

where, T_s, is the surface temperature, T_a, is the air temperature (both in Kelvin), s, is the slope of the saturation vapour versus temperature curve ($kg \cdot m^{-3} \cdot K^{-1}$) and vdd_a, is the vapour density deficit of air ($kg \cdot m^{-3}$). L, was calculated from Stefan-Boltzmann Law and Beer's Law (see section 2.3.1 for full model description).

3.3.3 Model Parameterization

3.3.3.1 Soil and surface properties input data

Initial conditions (input soil temperatures in different depths), were calculated for each of the 25 locations, using a model calculator for soil temperatures in depth; heat transfer from one cell to the next one based on Fourier's law (Sobota, 2014). This calculator is a numerical solution to the second law of heat conduction created by Dr Andrew Baird (University of Sheffield). It calculates the temperature in a given cell at time from the temperature at the previous time step plus the subsequent change in the cell temperature during the time step. The temperature that was set as the surface boundary condition of this model was air temperature from the TMY datasets (detailed description under section 3.3.1). The addition of energy to the cell is the balance between energy entering the cell and the energy leaving the cell; calculated using Fourier's law. The soil and surface properties for each climate zone were parameterized based on an extensive literature review and the mean of each variable was used in the simulations (Table 3.3).

Table 3.3: Literature review for soil and surface properties parameterization input across all five climate zones

Variable	Equatorial	Arid	Temperate	Boreal	Polar	Publication
d (m)-displacement height	0.34	0	0.20	0.08	0.10	Jin and Liang (2006); Zeng and Dickinson (1998); Zeng and Wang (2007); Best et al. (2011); van de Griend and Owe (1994); Gavin and Agnew (2000); Gallagher et al. (2002); Xuan et al. (2017); Cao et al. (2012)
α (unitless)-albedo	0.15	0.15	0.15	0.44	0.65	Mahfouf and Noilhan (1991); Kala et al. (2014); Allen et al. (1998); Barron et al. (1980)
z_0 (m)-surface roughness	0.06	0.09	0.12	0.90	0.02	Mahfouf and Noilhan (1991); Jin and Liang (2006); Zeng and Dickinson (1998); Businger et al. (1971); Deardorff (1974); Hales et al. (2004); Claassen and

						Riggs (1993); Gallagher et al. (2002); Hoffmann and Jackson (2000)
ε (W/m²)-emissivity	0.98	0.90	0.96	0.97	0.97	Mahfouf and Noilhan (1991); Jin and Liang (2006); Snyder et al. (1998); Tian et al. (2014)
r_s (s/m)-surface resistance	50	600	500	70	20	Mahfouf and Noilhan (1991); Allen et al. (1998); Camillo and Gurney (1986); Gavin and Agnew (2000) Allen et al. (1998); van de Griend and Owe (1994) Shuttleworth and Wallace (1985); Camillo and Gurney (1986)
r_a (s/m)-aerodynamic resistance	128	128	128	128	128	Shuttleworth and Wallace (1985)

LAI-Leaf Area Index	1.1	0.3	2.5	3	2.5	Masson et al. (2003); Champeaux et al. (2006); Mahfouf et al. (1995); Hoffmann and Jackson (2000); HU et al. (2008)
Volumetric Water Content	0.15	0.05	0.35	0.25	0.25	James et al. (2003); Kemp et al. (1997); Stursova and Sinsabaugh (2008); Jacome et al. (2013); Granberg et al. (1999); Paruelo et al. (1988); Farley et al. (2004); HU et al. (2008)
Organic content	0.40	0.06	0.05	0.50	0.01	Schlesinger (1984); FAO (1996); Stursova and Sinsabaugh (2008); Jones (1973); Jenny et al. (1948); Chen et al. (2012); Hewins et al. (2018) Paruelo et al. (1988); Farley et al. (2004)
Mineral content	0.25	0.05	0.50	0.20	0.40	Chen et al. (2012); Preston et al. (2017); Paruelo et al. (1988); Pérez (1996)

3.3.4 Experimental design

Soil temperature and PE in the equatorial, arid and temperate zones (hereinafter referred to as warm zones) and incoming SW radiation (across all five climate zones) were simulated for a year (365 days) in a 100 x 100 m solar park with three PV panels' rows (Figure 3.2). The boreal and polar zones where not assessed, because the foundation of HIS-PV model does not consider ice and frost dynamics (snow cover and soil frost). Further, in this study we focused assessing the differences of soil temperatures, PE and the GDDs among the three treatments across the zones where the solar PV parks are predominantly installed.

The area without PV panels had a 15 m length (control), the areas under spread along 5 m and the gap along 10 m. Two linear transects were selected to assess the objectives of this study (Figure 3.2). The mean of ten data-points under the second panel row and ten data-points at the gap between the second and the third panel row along the first linear transect, were used to represent treatments: under and gap, respectively. The control metrics derived by the mean of ten data-points on the second linear transect south and away from the solar PV panels. The selection of the two transects was opportunistic as both transects were selected in a distance of at least 5 m away from the northern and southern sides of the simulated solar park.

Soil temperature at the surface (to calculate the growing degree days, described next), soil temperature in 10 cm depth (root zone depth), PE and incoming SW radiation, were assessed under PV panels (hereinafter referred to as under and U), at the gap between the PV panels (hereinafter referred to as gap and G) and from a control area away from the PV panels (hereinafter referred to as control and C). Root zone is on average in

between 5 cm to 30 cm depth, remote sensing, Met Office and several companies measuring the microclimatology of an area with data loggers use the 10 cm depth (also for soil moisture metrics) as it is a sensible depth not far from surface and not too close at the water table (MetOffice, 2018).

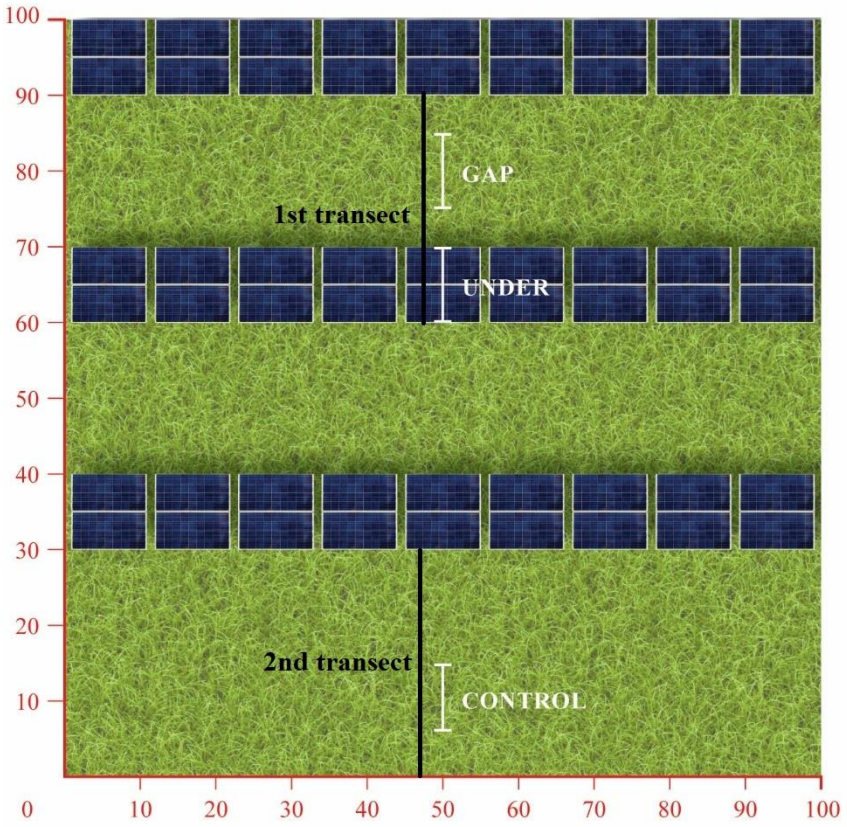

Figure 3.2: The simulated solar park of a 100 m x 100 m area illustrating the linear transects under, at the gap between the PV panels and the linear transect in the control area, away from PV panels (white colour lines).

3.3.5 Data analysis

O1. To assess the effect of solar parks on soil temperature at 10 cm depth and PE at the surface, we calculated the absolute differences in the daily means between control and under and control and gap during the northern hemisphere's summer (DOY 152-244).

To assess the effect of solar parks on the incoming SW radiation, we calculated the absolute differences in the daily means between control and under and control and gap for a year. Differences between gap and under were assumed low compared with the influence of the PV panels between under and an area without panels (control), and were therefore, not assessed. The simulation at the control treatments was used to subtract the ones from under and the gap respectively. The daily mean soil temperature, incoming SW and PE were tested against treatment and climate zone factors in a simple two-way ANOVA. A Tukey pairwise post-hoc test was performed to address any potential significance among their interactions.

O2. The simulated surface temperature dataset was used to derive GDD of each treatment in each of the five locations within each climate zone. Firstly, we quantified the length of growing season across the equatorial, arid and temperate zones (at each of the five met-stations per zone), counting from the last frost week of spring until the first frost week of autumn within the year (threshold of 0 °C for daily minimum air temperature; (Kunkel et al., 2004; NOAA, 2016)). Secondly, to calculate the GDDs during the growing season at each location, the following equation was used:

$$GDD = [\frac{(T_{surf.max} + T_{surf.min})}{2}] - T_{base} \qquad (2),$$

where, $T_{surf.max}$, the daily maximum surface temperature, $T_{surf.min}$, the daily minimum surface temperature and T_{base}, set equal to a minimum of 5 °C (Hassan et al., 2007). The GDDs of each treatment at each location were averaged to get the mean GDDs of each treatment at each zone. Last, the percentage difference between the GDDs under and the GDDs at the control as well as the between the gap and the control were calculated (equation 2). GDDs was tested with treatment and climate zone to

determine the potential effects, using a simple two-way ANOVA and a Tukey pairwise post-hoc test to address any potential significance among the factors' interactions.

The statistical analysis was carried out using R programme language within the RStudio environment version 3.3.5. (R Core Team, 2017) and p values ≤ 0.05 deemed significant. The packages that were used were scales (Hadley Wickham, 2017), ggplot2 (Hadley Wickham, Winston Chang, 2016) data.table (Matt Dowle, 2018) and dplyr (Hadley Wickham, Romain Francois, Lionel Henry, Kirill Müller, (R Core Team, 2017)).

3.4 Results

3.4.1 O1. Soil temperature, PE and incoming SW variability with and without solar panels

3.4.1.1 Simulated soil temperature in 10 cm depth

Soil temperature under was significantly lower compared with control treatments in the three assessed warm zones (arid, equatorial and the temperate zones) with $p < 0.001$ (Figure 3.3). There was no evidence for significant differences between gap and control treatments (negligible 0 to 0.1 °C difference). The mean soil temperature at the control was always warmer than under across the warm zones (Table 2 in the SI.1). The differences between the minimum and the maximum soil temperatures were larger across the arid zone (under 11.9 °C, gap 15.3 °C and control 15.1 °C). In the arid zone, the difference between the mean soil temperature under and control was the largest, 3.6 °C, while in the equatorial and the temperate the difference was 1.3 °C and 1.4 °C respectively (Table 3 in the SI.1).

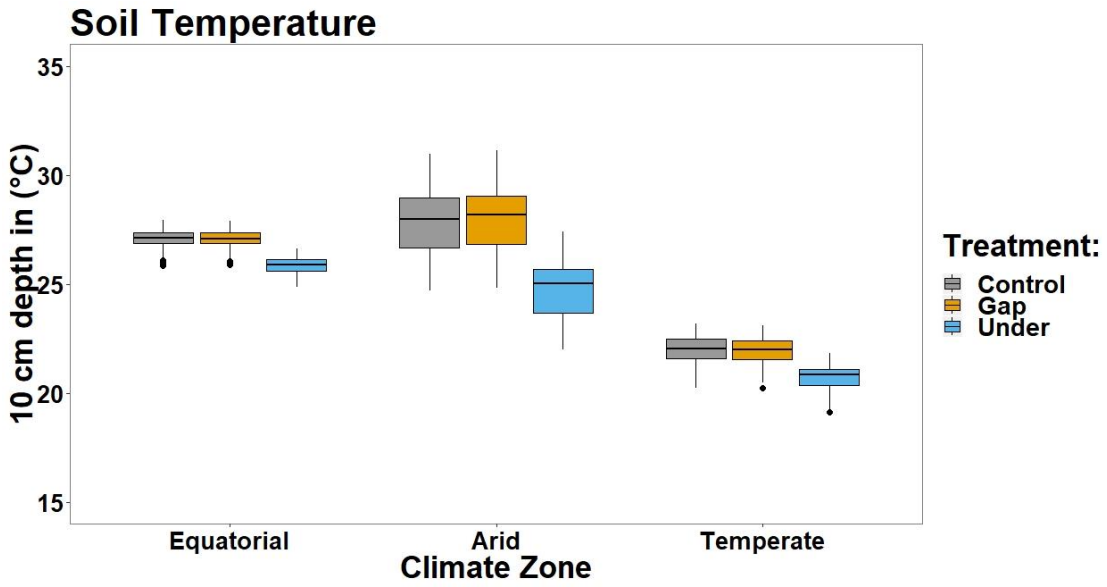

Figure 3.3: Illustration of the simulated summer soil temperature under, at the gap and at the control across equatorial, arid and temperate zones.

3.4.1.2 Simulated potential evaporation (PE) at the surface

The PE ratios under, were significantly lower compared with the control treatments within equatorial ($p = 0.001$) and the Arid ($p < 0.001$) zones in the summer (Figure 3.4). In the temperate zone, there were non-significant differences between control-under and control-gap treatments (Table 4 in the SI.3). Among the warm periods, the mean potential evaporation in the arid, demonstrated the largest difference between control and under, with the control showing 46% higher PE than under (Table 5 in the SI.3). Overall, the differences between control and under potential evaporation was decreasing by ~10 % from one zone to the other; increasing elevation.

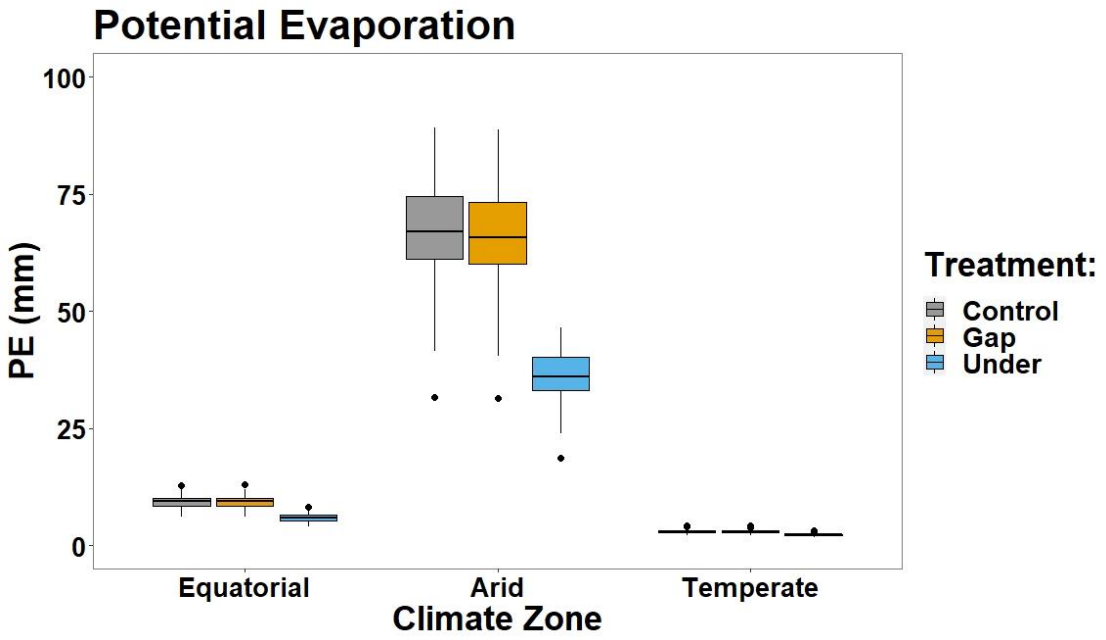

Figure 3.4: Illustration of the simulated summer potential evaporation (PE) under, at the gap and at the control across equatorial, arid and temperate zones.

3.4.1.3 Short wave (SW)

The annual incoming SW radiation under panels across all climate zones, was 50% to 60% less than control treatments ($p < 0.001$). Further the gap received by average 8% less SW, compared to the control, with exceptional statistical significance between gap and control at the equatorial zone ($p < 0.05$; Tables 6 and 7 in the SI.3). Regardless of climate zone, the solar parks annual effect on the incoming SW radiation was similar among the treatments, with the control receiving more SW than the gap and the gap more SW than under (Figure 3.5).

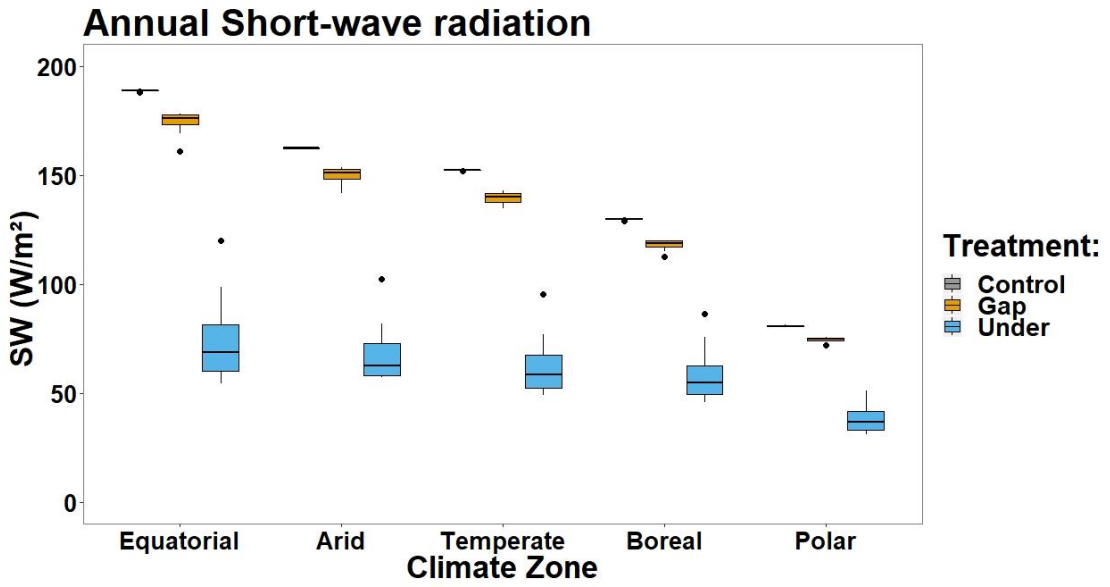

Figure 3.5: The amount of the total annual incoming SW radiation at each treatment across all five climate zones.

3.4.2 O2. GDD variability among Under, Gap and Control treatments

The difference of the total amount of GDDs at the gap compared with the control treatments, was less than 1%, while under and control comparison showed differences of higher magnitude at the equatorial and arid zones (Figure 3.6). However, these were not supported statistically ($p > 0.05$). In the arid zone, control counted 13% more GDDs compared with under. At the temperate there were not drastic differences among treatments, with the control counting 3% more GDDs than under. At the equatorial zone, control counted 4% more GDDs than under. The outliers at the equatorial zone derived by the met-station at Hilo, Hawaii, which demonstrated the lowest total of GDDs at the gap and under compared with the other met-stations assessed within the zone (Table 3.4).

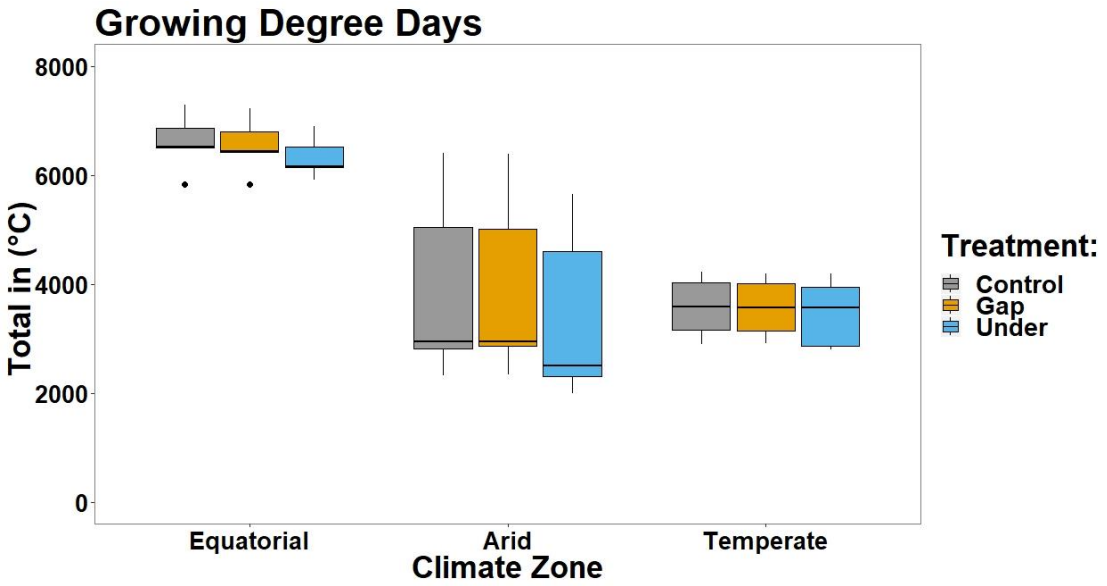

Figure 3.6: The total amount of the GDDs at each of the treatments across the three climate zones assessed.

Table 3.4: The total amount and daily mean of GDDs (derived from the division of the sum with the length of days of growing season) at each met station during growing season across the equatorial, the arid and the temperate zone.

No	KCC	Climatic description	Location	Growing Season		GDD – Under °C		GDD – Gap °C		GDD – Control °C	
				Dates	DOY	Total	Daily	Total	Daily	Total	Daily
1	Af	Equatorial, fully humid	Hilo, Hawaii	Entire year	365	5903	16.17	5834	16	5822	15.95
2	Af	Equatorial, fully humid	West Palm Beach, Florida	Entire year	365	6138	16.80	6421	17.60	6497	17.80
3	Am	Equatorial, monsoonal	Miami, Florida	Entire year	365	6514	17.85	6803	18.60	6859	18.80

4	Aw	Equatorial, winter dry	Naples, Florida	Entire year	365	6155	16.90	6436	17.65	6512	17.85
5	Aw	Equatorial, winter dry	Key West, Florida	Entire year	365	6886	18.90	7215	19.80	7284	19.95
6	BSh	Arid, Steppe, hot arid	Laredo, Texas	27/02-13/12	290	5649	19.50	6391	22.00	6409	22.10
7	BSk	Arid, Steppe, cold arid	Reno, Nevada	22/05-8/10	140	1993	14.25	2336	16.70	2317	16.55
8	BSk	Arid, Steppe, cold arid	Denver Int Airport, Colorado	23/04-5/10	177	2504	14.15	2951	16.70	2951	16.70

9	BWh	Arid, Desert, hot arid	Las Vegas, Nevada	16/02-12/12	298	4600	15.40		5010	16.80	5045	16.90
10	BWk	Arid, Desert, cold arid	Goldfield, Nevada	12/04-16/10	188	2306	12.30		2858	15.20	2805	14.90
11	Cfb	Warm Temperate, fully humid, warm summer	Wytheville, Virginia	19/04-8/11	204	2860	14.00		3138	15.40	3157	15.50
12	CSa	Warm Temperate, Steppe, hot summer	Sacramento, California	5/02-11/12	310	3948	12.75		4016	12.95	4028	13.00

13	CSb	Warm Temperate, Steppe, warm summer	Portland, Oregon	15/03-10/11	241	2798	11.60		2903	12.05	2902	12.00
14	CSb	Warm Temperate, Steppe, warm summer	San Francisco, California	Entire year	365	3547	9.70		3573	9.80	3586	9.85
15	CSb	Warm Temperate, Steppe, warm summer	Santa Barbara, California	Entire year	365	4193	11.50		4187	11.50	4218	11.55

3.5 Discussion

Despite the exponentially rising land-use change for solar parks' installations, impacts on the local climate are poorly resolved despite the profound implications for ecosystem function (Dupraz et al., 2010; Marrou et al., 2013c; Marrou et al., 2013b; Marrou et al., 2013a; Hassanpour Adeh et al., 2018; Armstrong et al., 2016; Barron-Gafford et al., 2016; Hernandez et al., 2015). Therefore, modelling approaches are strongly advised in order to build an immediate understanding with regards to solar parks local climate effects. The HIS-PV model built and evaluated in a temperate UK grassland solar park provided useful simulations under a range of diverse weather characteristics (Chapter 2 of this thesis). As a result, based on the RMSEs produced between simulated and measured datasets when tested under different whether characteristics (sections 2.5.2 and 2.5.3 of chapter 2 in this thesis) it was anticipated that across a range of climates and meteorological conditions, the model will be further in place to provide useful insight to ecosystem response to this growing land-use change.

In fact, in this study, HIS-PV model was applied to simulate soil temperature, potential evaporation, annual net shortwave radiation and based on the simulated surface temperature to estimate the effects of solar parks on the growing degree days across the equatorial, the arid and the temperate zone, where solar parks are mostly implemented. The effects of climate zone and location within a solar park showed significant differences for soil temperature at 10 cm depth among treatments (especially in the arid zone) and significant differences for potential evaporation (apart from in the temperate zone) in the summer with major differences regarding the annual incoming SW radiation among under the panels, at the gap and control areas away in all five climate zones.

However, these major differences observed at the annual incoming SW radiation, did not seem to reflect on major differences among the total amount of GDDs of under, gap and control treatments in the tested zones. Initial model parameterization limitations were assumed, especially regarding the input soil temperature component. PE seemed quite low for both arid and temperate zone, suggesting limitations and complexities with temperature simulations at the surface, which are strongly suggest thorough investigation going forward. For PE, it was also assumed that the initial parameterization of soil properties (Table 3.3) might have an effect; less critical than soil temperature parameterizations, but still worth assessing using sensitivity analyses approaches.

The results were discussed based on the two objectives and future development of HIS-PV model was addressed.

3.5.1 O1. Solar parks effect on microclimate regulators

Assessing soil temperature at 10 cm depth, PE and incoming SW simulations, the differences between control and under treatments were assumingly affected by elevation, solar zenith and weather, i.e. climate zone (Clinton, 2003). All three tested microclimate regulators in this simulations' study, declined with the increase of latitude and the differences among treatments were stronger in the Equatorial and the Arid zones (Figure 3.3, Figure 3.4, and Figure 3.5). Even though, climate zone had a stronger effect between control and under ratios of PE and soil temperature in the summer, the strongest and clearest effect was on the annual incoming SW radiation among treatments (Figure 3.5). The difference between under and control SW was of high magnitude and

consistently ~60% and between gap and control around 8%, within all zones assessed, explained by the physical presence of PV panels.

Further, the ratios of PE, which relies on the water availability for the subsequent processes (including plant productivity and decomposition), where high in the Arid and less in the equatorial and the temperate zones (Figure 3.4). In the temperate zone, PE among treatments did not deem significant because the weather and climatic conditions are not that diverse as in the equatorial and arid zones. The extremes of equatorial (for example wet or dry) and the arid (for example dry and cold at night) climatic and weather conditions, might explain the findings for PE; lower magnitude in the Arid where perhaps water in the soil available for PE is less compared to the Equatorial (Hartmann, 1994).

Also, the differences between control and under treatments, could be explained by the fact that unsheltered areas (control and gap) are more sensitive and exposed to ambient conditions (including wind and humidity), which regulate the microclimate of each area respectively (Pepin and Lundquist, 2008). Thus, solar position combined with PV panels arrays physical presence reduced the incoming SW radiation and the available water for all the subsequent ecosystem processes (see section 1.4.1.4 in chapter one of this thesis, Armstrong et al., (2014a) and Armstrong et al., (2016)) with soil temperature being substantially affected across warm zones in the summer.

In addition, the physical presence of the PV arrays in a ground-mounted design reduce significantly the sky view factor under (measured in a temperate grassland, see section 4.1 in chapter two of this thesis), and this is further expected to affect the annual net loss of the latent heat fluxes affecting soil temperature, PE and incoming SW radiation (Hassanpour Adeh et al., 2018). Evident to that, the soil under was cooler regardless of

seasonal changes at each region across the warm zones. The perturbation of the incoming SW under the PV panels especially in zones of higher latitude are expected to delay warming under the panels (Pepin and Lundquist, 2008). In addition, in previous studies, evapotranspiration fluxes, soil temperatures and solar radiation fluxes were mostly assessed associated with vegetation parameters (growth, cover, diversity, biomass) potentially affected by solar parks (Marrou et al., 2013c; Marrou et al., 2013b; Armstrong et al., 2016; Hassanpour Adeh et al., 2018). Thus, a crop model combined with HIS-PV model could provide with more concrete information regarding the causes of the impacts on these microclimate regulators.

Further, especially under the PV panels, it is assumed that plants relied mostly on the amount of the diffuse radiation for their growth (Marrou et al., 2013b). PE under the panels, is expected to affect the availability of water for photosynthesis, which will affect vegetation growth and the overall plant diversity (Marrou et al., 2013c). In addition, limited SW under the panels, and differences between gap and control, implies masking effects on vegetation at the gap. It was found that plant species diversity differed among gap and control (Armstrong et al., 2016). Based on the findings of this study and surveys from a previous study (Armstrong et al., 2016), it seemed that a multiple-use land, for example a solar park within a grassland, comprises has three different plant species communities (under, gap and control) within the same site.

3.5.2 O2. Solar parks effect on the total amount of Growing Degree Days at lower altitude zones

Growing degree days, is widely used in agronomy and crop modelling, including NDVI tools (Hassan et al., 2007; Bonhomme, 2000; McMaster and Wilhelm, 1997; Kunkel et

al., 2004; Swan et al., 1987; Taejin et al., 2016; Tucker et al., 2001), as it is strongly dependant on temperature (Hassan et al., 2007), and temperature is highly affected by climate (and this by itself, already creates changes regarding the duration of growing seasons). GDDs is a great indicator regarding the different phases of vegetation development. In this study we showed that the total amount of GDDs was not significantly affected by the physical presence of the PV arrays.

Assessing the equatorial, arid and temperate zones, which are the zones where solar PV parks are mostly implemented and where most of the global food production from lands derives from. It was clear that the area under the panels counted the lowest amount of GDDs compared with gap and control (Figure 3.6). However, the difference did not seem significant among the treatments. It was interesting how the observed differences of the annual SW radiation received among under, the gap and control treatments did not reflect to a similar manner in the total amount of growing degree days. It was assumed that GDDs and SW radiation cannot be strictly correlated, as there are other factors affecting the GDD calculation and that was mainly the surface temperature (minimum, maximum values).

In particular, the minimum of surface temperature, included in the equation of the growing degree days (section 3.3.5, Equation 2), includes mainly night-time minimum temperatures, while SW reflects only to day-time. In addition, the overall differences between under and the gap (results from Chapters 1 and 2 in this thesis) and between under and control areas (results in this study as well as from the solar parks literature available at the momentum, Table 3.1), were never reported as major. At the temperate UK grassland that mostly assessed and the model was evaluated primarily, regarding soil temperatures at 10 cm depth, the differences between the means were

approximately 2 °C different in growing season and 4 °C different out of the growing season (area under always cooler than gap versus control). The limitations in the equation of the GDDs and the overall reported differences among under, gap and control areas, do not suggest major differences in the growing degree days, especially in the temperate zone.

Further, GDDs are strongly dependant on plant species and each species grows within specific temperature (and other parameters) and temperature has a strong effect on the physiology and the morphology of the plants (Bonhomme, 2000). For example, even the growing season length differs among plant species (Great Plains; (McMaster and Wilhelm, 1997) with wheat: starting in September through July at a T_{base} = 0 °C (winter), with corn: starting in April through October and a T_{base} = 10 °C (summer) and not a T_{base} = 5 °C, (our models' initial parameterization across all zones). Therefore, calculating and quantifying the effect of solar parks on lands where vegetation is sparse or non-existed vegetation (arid zone), could also cause complexities. In the arid zone, where most the largest PV parks' installations are globally established, demonstrated a 13% decrease of GDDs under the panels compared with control treatments.

It was assumed that any differences among the treatments was related to extreme surface temperatures that occur in desert environments (arid zone) as well as the higher gain of the net sensible heat fluxes. This pointed out the difference between a shaded area (under) and an exposed to ambient conditions area (gap and control). In addition, these findings could be upscaled if a crop model was to be considered in the HIS-PV model parameterization and address potential uncertainties that derive with non-bare soil lands. Last, the factor ice and frost should be thoroughly investigated, as there are cultivated lands, crop, shrub and grasslands at the boreal zone, and continuous periods

above 0 °C (to form a growing season) allowing a more cautious investigation. Overall, there was an almost great balance among the three treatments total of GDDs at the temperate zone, which suggests that potentially those locations should be preferable when planning a new PV plant installation.

3.6 Ideas for future model development

Based on our overall findings, it is strongly suggested that HIS-PV should be combined with a crop model. Considering the existent type of cultivated vegetation (croplands, shrublands, grasslands), will help research identify and address the potential effects on GDDs at each treatment in each climate zone respectively. Solar parks are installed on agricultural lands and deserts, thus vegetation (whether sparse or dense) and its potential feedbacks on microclimate aspects (i.e. soil temperature) should be considered when investigating soil thermodynamics. At the moment, the model has the potential to predict plant temperature which if accounted for, could indicate concrete feedbacks on vegetation productivity assessments.

Further with regards to implications at the surface boundary, the foundation of HIS-PV model, is not in place to account for frost and snow cover. It is a quite sensitive and difficult area to assess even by expert modellers (Pepin and Lundquist, 2008; Albergel et al., 2015; N. Flerchinger and E. Saxton, 1989; Rempel et al., 2004), as it might take years of research and evaluations. However, we strongly believe that if crop modelling was to be added in the future, the already powerful HIS-PV model, will be reliable and essential when planning and designing solar PV parks.

Focus should be placed on investigating the effects of PV panels of different design and dimensions. We assume that different solar park design and planning such as panels

inclination, aspect and the installation of solar PV trackers instead of ground-mounted (fixed angle) would increase the amount of GDDs under the PV panels.

3.7 Conclusion

The HIS-PV model is in place to produce satisfactory simulations across different climate zones. The USA comprises great climatic variability and typical meteorological year (TMY) data broadly accessible online, when at the same time is the fourth solar PV market in the world. Undoubtably, the clear and strong effect of around 60% less SW radiation received under the panels and the fact that the amount of GDD at the Arid zone was reduced by 13%, implies long-term effects on ecosystem function. The fact that soil temperature at root zone depth and PE in the summer were also affected among the treatments across the warm zones, especially in the arid, suggests that the effect on vegetation growth will be of substantial magnitude and also the need of a crop model combination to ensure these findings. An extra model component of the temperature at the vegetation canopy, as well as the combination of HIS-PV model with a crop model, could further address the potential impacts on the vegetation growth of the hosting ecosystem. The effect of solar parks on GDD was not statistically significant regardless of some obvious decreases under. However, effects on microclimate and GDDs should be further assessed with the addition of a crop model, as it is quite crucial for ecosystem function and more specifically for food production in all five climate zones. Based on our overall implications from our findings showing the impacts of solar parks across different climate zones, we support suggestions for different designing and planning of the PV panels.

4 Chapter 4: Solar Photovoltaic Park Impacts on Local Climate and Potential Ecosystem Service Implications

4.1 Abstract

The global energy system is transitioning to low-carbon energy resources. Solar energy is predicted to be the dominant renewable in the future given improvements in efficiency and decreasing costs. This is triggering a notable and accelerating land-use change for ground-mounted systems (hereinafter referred to as solar parks). Terrestrial ecosystems represent an important carbon sink and thus land-use change has implications for climate change. Regardless of the wide global deployment of solar parks and the undoubtable importance of terrestrial ecosystems, local climatic change caused by solar parks and implications for ecosystem services provided by the hosting landscape are poorly resolved. This study provides the first synthesis of emerging understanding in this area. Fifteen studies focused on the local climate impacts were assessed, with air temperature most commonly quantified followed by solar radiation fluxes and soil temperature. There were disagreements between studies, for example with some showing a cooling effect and some a warming effect. Experimental design and the ecosystem functions that were assessed and correlated with effects on local climate aspects, were different for most of the assessed solar park studies. The

synthesised changes in local climate was used to infer potential implications for ecosystem services, supported by evidence, albeit limited, of perturbations to ecosystem processes caused by solar parks. Whilst there is some disagreement, for example, whether solar parks are a sink or a source of carbon dioxide in the atmosphere, all findings confirm that the effects on climate will have implications on ecosystem function and thus on ecosystem services. Future research is urgently needed to enhance understanding and thus explore the potential for managing solar parks to provide multiple ecosystem services. Research focus should be placed on resolving differences between climate zones and on exploring implications of different solar park designs.

Keywords: solar energy, photovoltaics, climate, ecosystem processes, ecosystem services

4.2 Introduction

A transition to low-carbon, cleaner and inexhaustible energy resources is believed to be the best solution to mitigate climate changes generated by conventional energy resources (Mendelsohn et al., 1994; Asif and Muneer, 2007; Pedraza, 2012; Chu and Majumdar, 2012). Solar energy, based on environmental, economic, and safety criteria, is the most promising resource and if supported by state policies, it could be also very profitable (Bórawski et al., 2019). Within the last five years, photovoltaics (PV) technology, has improved, decreasing costs, resulting in deployments greatly exceeding projections (IEA, 2017; 2018b; 2014; IEA/WEO, 2017; IAE/WEO, 2018; REN21, 2017; 2018). PV power generation demonstrated a historical increase of 40% in 2017, representing 2% of the total world electricity generation (IEA, 2018b). Further, the compound annual growth rate in the EU was higher for solar PV systems (48%) during 2005-2016, than any other type of renewable energy technology (EEA, 2018).

Ground-mounted PV parks (hereinafter referred to as solar parks), have been deployed across landscapes with their physical presence perturbing the surface energy balance. For example, the solar PV arrays, reduced the park's albedo; panels are darker and thus have a lower albedo (~0.1) compared with soil and/or vegetated surfaces (a typical temperate grassland ~0.25; Barron-Gafford et al. (2016)), and the intercept of solar radiation with implications for temperature, and precipitation. Terrestrial ecosystems, including deserts and grasslands, where solar parks are mostly deployed, are known to be regulated by climate and therefore, changes will have implications for ecosystem function. However, the rapid increase of solar parks deployment and associated extensive land-use change has not been supported by a concerted research to assess and quantify the range and magnitude of effects on the hosting ecosystem.

Most of the limited published research quantify the effects of solar parks on local climate, but time periods evaluated, sampling methods and analysis differed. There are contradictions between studies, for example, Taha (2013) and Millstein and Menon (2011), implied that solar parks induce a regional cooling while Barron-Gafford et al. (2016) study, implied that they induce a heat-island effect. Lack of synthesis studies stymies the useful of existing understanding of solar parks effects on ecosystem functions.

Quantification of ecosystem function effects are even more limited than for climate and highly variable between studies. For example, air temperature variability under the panels (hereinafter referred to as under) led to shorter annual growing degree days (GDDs) compared with control treatments away from the panels (Armstrong et al. (2016) and Chapter 3 of this thesis). Further, reduced accumulation of biomass was reported under driven by climate aspects including soil moisture and soil temperature

(Armstrong et al., 2016; Hassanpour Adeh et al., 2018; Dupraz et al., 2010). In addition, reduced plant cover of cucumbers under panels have been associated with evapotranspiration decreases (Marrou et al., 2013b).

Changes to ecosystem functions results in implications for ecosystem services provision (Matos et al., 2019; Montoya and Raffaelli, 2010) including, air quality, climate regulation, biomass materials and food provision, soil formation, water and nutrient cycle support and pollination regulation (UKNEA, 2014). Ecosystem services vary with ecosystem type (deserts, grasslands) as well as spatio-temporally, driven by differences on biodiversity and climatic conditions diversity (Kottek et al., 2006). Hence, different aspects of vegetation and soil conditions occur at each climate zone and thus the magnitude of change at the local climate will vary. As a result, investigating implications on ecosystem services is complex. Adding to that the impact of solar parks at the local climate creates an even more confusing understanding and establishment of solutions to promote ecosystem functions at the hosting land. However, is critical due to their constant support of human deployment (Gigliotti et al., 2019).

Developing understanding could lead to solar parks deployment and operation that promotes ecosystem services provision through multiple-land use strategies. Such schemes include agrivoltaics, firstly introduced by Goetzberger and Zastrow (1982) involving cropping under (Marrou et al., 2013c; Marrou et al., 2013b; Marrou et al., 2013a) and around PV arrays, (Ravi et al., 2014), grazing (BRE, 2014) and habitat provision, including pollinators (Walston et al., 2018). Such multiple-land use is highly appealing given the anticipated growth in solar, growing land scarcity and importance of ecosystem services for human survival and climate change adaption (Matthews et al., 2014; Mooney et al., 2009). It is important to follow a techno-ecological synergy (TES)

framework understanding and designing synergies between technological and ecological systems with ultimate target enhancing harmony between human intervention and nature (Bakshi et al., 2015; Hernandez et al., 2019).

4.2.1 Research aim

Given the accelerating rate of deployment of solar parks and critical importance of ecosystems for society, resolving the impacts of solar parks is increasingly urgent. Consequently, the aim of this study was to rapidly advance understanding of the climatic impacts of solar parks and postulate the implications for ecosystem function and consequently service provision. Moreover, to use the synthesis to identify key knowledge gaps to direct future research. To achieve this the following objectives were assessed:

O1. Synthesise current understanding of the local climate impacts of solar parks.

O2. Outline the potential implications of the altered climate on ecosystem processes and services.

O3. Identify critical research needs, optimizing solar parks hosting ecosystem sustainability.

4.3 O1. Synthesis of the current understanding of the local climate impacts of solar parks

There are fifteen published studies, and three chapters in this thesis, that have evaluated the effects of solar parks on the local climate across the five main climatic zones (classified by Köppen; Kottek et al. (2006)). The studies vary in terms of the variables measured, sampling location within the solar park and metric; daily minimum, average

and maximum ratios (Table 4.1). In this section climate aspects findings were assessed (air and soil temperature, soil moisture, humidity, wind, soil properties and solar radiation fluxes. Findings regarding the ecosystem processes including Leaf Area Index (LAI), gaseous fluxes, biomass, evapotranspiration, photosynthesis and plant diversity, were thoroughly assessed under section 4.4, associated with their subsequent ecosystems services.

Table 4.1: Aspects of climate surface properties and ecosystem processes assessed from current literature related to the effects of solar parks at the hosting ecosystem.

Publication / Variable	Makaronidou–Chapter 1	Makaronidou-Chapter 2	Makaronidou-Chapter 3	Hassanpour Adeh et al.,2018	Yang et al., 2017	Gao et al., 2016a	Gao et al., 2016b	Armstrong et al., 2016	Barron-Gafford et al., 2016	Hu et al., 2015	Taha, 2013	Fthenakis and Yu, 2013	Marrou et al., 2013a	Marrou et al., 2013b	Marrou et al., 2013c	Millstein and Menon, 2011	Dupraz et al., 2010	Total Number of publications per Variable
Air Temperature	■				■		■	■	■	■	■	■		■		■		**10**
Soil Temperature	■		■		■	■		■						■				**6**
Soil Moisture	■			■				■										**3**
Absolute and/or Relative Humidity							■	■										2
Wind (speed or direction)								■				■				■		**3**
Soil Properties	■							■										2
Solar Radiation Fluxes	■		■	■	■					■			■	■		■	■	**9**
Leaf Area Index (LAI)	■												■					2
CO_2 Fluxes	■							■								■		**3**
Biomass				■				■					■		■		■	**5**
Water Fluxes	■		■					■							■			**4**
Albedo					■						■					■		**3**
Photosynthesis								■										1
Plant Diversity and Cover								■					■					2

4.3.1 Air temperature

Air temperature was the most commonly assessed variable, quantified in ten of the 18 solar park studies (Table 4.1). However, the direction of change was contradictory with Taha (2013), Fthenakis and Yu (2013) and Millstein and Menon (2011), finding cooling and Barron-Gafford et al. (2016) study, finding heating effect. These contradictory findings could be explained by the studies' locations. For example, cooling was found on studies mostly conducted at desert (arid) environments and warming when conducted at temperate environments. Further, the studies that found cooling, were modelling studies and Taha (2013) reported air temperatures simulations at 5 m height (above solar park), when Barron-Gafford et al. (2016) study was a field study that measured air temperature at 2.5 m above PV panels. Variability of air temperature assessed from different heights above panels was supported by Gao et al. (2016b) as well. Their study showed that solar panels induce a heating effect measuring air temperatures 2 m higher from the panels, while at 10 m height, there was cooling; both compared to outside the solar park.

Among the studies, air temperature variability, was assessed using different experimental designs. For example, as mentioned some studies tested the variability of air temperature in different heights above PV panels (Millstein and Menon, 2011; Barron-Gafford et al., 2016; Fthenakis and Yu, 2013; Gao et al., 2016b; Yang et al., 2017), whilst others tested the spatio-temporal variability under, at the gap between panels' rows and away (control) from the PV panels (Marrou et al. (2013b); Armstrong et al. (2016) and in Chapter 1 of this thesis). The causal mechanisms for the observed variability were different between studies. Marrou et al. (2013b) explained the cooling

of the air temperature as a function of wind speed and incoming SW radiation, whilst Armstrong et al. (2016) and in Chapter 1 of this thesis, as a function of season, site management (vegetation) and location in a solar park. The later studies also showed that air temperature differences among treatments led to shorter annual growing degree days (GDDs) under compared with control areas (Chapter three of this thesis).

From another aspect, Gao et al. (2016b) related the variability with the power conversion of the panels, which differs between winter and summer thus causes energy budget to be different between a solar park and control areas away from it. Exceptional was the Taha (2013) study, where the cooling effect above a solar park, occurred with increases of solar PV panels' efficiency ($\varepsilon > 20\%$).

4.3.2 Soil temperature

Soil temperature was measured in six of the 18 solar park studies, three of which are Chapters of this thesis; Table 4.1). The studies assessed soil temperature at different depths, using different experimental designs and different types of vegetation were rooting in the assessed soils. All suggested that the amplitude of mean soil temperature decreased with increase in depth, under the panels soil temperature was cooler than the gap and the range of the annual mean soil temperature was greater within a solar park than in control areas away from it (Table 4.2).

Marrou et al. (2013b), investigated the soil temperature at depths of 5 cm and 25 cm at a temperate agrivoltaic site during the cropping seasons of durum wheat, cucumbers and of four varieties of lettuces. There was a daily average cooling at 25 cm depth, during growing season, for wheat (cooler) and lettuces (warmer). Armstrong et al. (2016), investigated soil temperature at 10 cm depth in a solar park at a temperate, UK

grassland, showing a 1.7 °C cooling on average in the gap in winter and a 5.2 °C cooling under the panels in summer, compared with control plot measurements. Similarly, in Chapter one of this thesis, at the same site as Armstrong et al. (2016), soil at 10 cm depth was cooler under the panels throughout the day in the growing season and the gap was 5 °C warmer than under the panels. In addition, in both studies there were major differences between the minimum and the maximum values between sampling plots under the panels and in the gaps between PV panel rows (see Appendix 2 – S.I. 2 p.207). Regardless of experimental design which was quite different and there were two years difference between the two field studies, their findings between were similar.

Gao et al. (2016a) and Yang et al. (2017) conducted their study on desert (arid) environments (i.e. sparse or no vegetation) in a quite high range of soil depths. Both studies suggested that soil temperatures at 5 cm and 10 cm depth inside a solar park, were cooler compared to control areas outside the solar park, throughout the year. Further, that the range of soil temperature in the summer was increased inside a solar park, as shown in the simulated soil temperatures at the arid climate zone in Chapter three of this thesis (section 3.4.1.1). Yang et al. (2017), implied that the solar park planning (number of PV panels' rows), was the major cause of impact on soil temperatures, because the penetration of incoming SW was majorly affected by solar park design.

4.3.3 Soil moisture

Soil moisture was measured in three of the 18 solar park studies, conducted in temperate environments; Table 4.1). The studies assessed soil moisture at different depths, using different experimental designs on lands covered by different types of vegetation.

However, two studies have concluded to similar results regardless of experimental design (as in soil temperature), stating that the soil moisture content in a solar park in growing season was higher (Table 4.2) under the PV panels and similar or with minor differences of the means under in comparison to the gap, out of the growing season (chapter one of this thesis and Hassanpour Adeh et al. (2018)). Armstrong et al. (2016) results were inconclusive.

Hassanpour Adeh et al. (2018) study showed evidence of more rapid water depletion at the gap between the panel rows, compared with control, based on soil moisture measurements at several depths. In Chapter one of this thesis (section 1.4.1.3), soil moisture at 10 cm depth along a linear transect running perpendicular between two PV panel rows (hereinafter referred to as linear transect), demonstrated an even soil moisture range between under and the gap in and out of the growing season, with maximum differences between gap and under areas observed in the evening. It was assumed that the channelling of precipitation by the PV panels (water run off at the sides of the panels) increased the spatial variability of moisture content, under the PV panels. This was further supported by Armstrong et al. (2016) who also confirmed non-significant differences between under, gap and control areas.

4.3.4 Humidity (Relative and Absolute)

Humidity was an infrequently assessed variable among the solar park studies; it was measured in just two studies (Table 4.1). Armstrong et al. (2016), assessed Relative and Absolute Humidity (RH and AH, respectively) as well as Vapor Pressure Deficit (VPD; the difference between the amount of moisture in the air and how much the air can hold when saturated; Table 4.2) at a temperate UK grassland. Armstrong et al. (2016), showed that RH was reduced under the panels throughout the daily cycle. On the other

hand, Gao et al. (2016b) showed that the RH during night-time, was increased inside the solar park (sensor at 10 m height from the PV panels) in Golmud desert (arid environment) in China.

Armstrong et al. (2016) assessed AH and significant differences between the minimum and the maximum values under the panel compare to control and gap areas were observed. For example, during the growing season, the daily minimum of absolute humidity was 1.3 $g \cdot m^{-3}$ higher and the daily maximum 5.6 $g \cdot m^{-3}$ lower compared with the gap and the control areas.

4.3.5 Wind direction and speed

Wind speed and direction in a solar park, was barely assessed regardless of the potential perturbation at the surface with assumed implications for air temperature, as reported by Armstrong et al. (2016), Millstein and Menon (2011) and Fthenakis and Yu (2013). Hassanpour Adeh et al. (2018) is the only study (to our knowledge) that has observed wind direction under (wind predominantly directed from the south) and at the gap between panels (wind distributed among many incident angles) at a temperate environment in the US; however, without providing reasoning for their observations.

Armstrong et al. (2016), found an annual 63% slowdown of wind speed at the gap between the PV panel rows compared with control areas in a temperate UK grassland. Millstein and Menon (2011) reported an increase above and a decrease in the magnitude of the afternoon south-westerly winds under the panels due to changes of the albedo and the surface roughness in desert environments. Fthenakis and Yu (2013) study, conducted in temperate environment, showed that heating and cooling of the air

temperature inside the solar park was a function of wind speed, which was south-westerly and also seemed to be affected by the physical presence of the solar park.

4.3.6 Solar radiation fluxes

The effects of solar parks on solar radiation fluxes were highly assessed by solar park studies (nine of the 18 studies; Table 4.1). Literature assessed different aspects of solar radiation fluxes. Armstrong et al. (2016) and in Chapter one of this thesis (section 1.4.1.4) PAR was assessed in the same temperate UK grassland. Dupraz et al. (2010), Marrou et al. (2013a) and (2013b), assessed the light availability under two different shade densities (50% and 70%) in the same agrivoltaic scheme. Hassanpour Adeh et al. (2018) assessed the incoming short-wave (SW) radiation whilst, Millstein and Menon (2011), Yang et al. (2017) and Marrou et al. (2013b) the incoming and the outgoing long-wave (LW) and short-wave (SW) radiation.

Averaged across the year, PAR under the PV panels was 92% lower than in the gap between the PV panel rows; PAR in the gap was similar to that at control plots (Armstrong et al., 2016). Further, in Chapter one of this thesis (section 1.4.1.4), PAR during growing season was found four times higher in the morning and afternoon and three times higher in the evening in the gap compared with under. The amount of the incoming SW radiation was reduced under the PV panels, especially diurnally during growing season in rural environments (Hassanpour Adeh et al. (2018), Marrou et al. (2013b) and in Chapter 3 of this thesis section 3.4.1.3).

Outgoing SW and LW were significantly reduced in the afternoon hours of the summer period, directly above the PV panels in a Californian desert (Millstein and Menon, 2011). However, the annual average differences between the solar park and control

areas were not significant. Yang et al. (2017), in a Chinese desert, related the increased annual LW and the decreased SW radiations, to changes at the surface temperature and found significant differences.

Radiation availability at a temperate agrivoltaic system, under two shade densities (Half Density; 50% and Full Density; 70%) was lower during the wheat cropping season, 71% and 43% at each shade treatment, respectively (Dupraz et al., 2010). At the gap between the PV panels, the light availability was less than 60%. Notably, comparisons and generalisations regarding solar radiation fluxes are impossible at the moment, as each of the studies investigates different aspects of radiation at different ecosystem types. However, all agreed that under the panels light was notably lower than the gap between panel rows and control areas.

4.4 O2. Outline the potential implications of the altered climate on ecosystem processes and services

The increased GHGs have generated significant climate change jeopardies with implications for ecosystems and humanity (Mendelsohn et al., 1994; Asif and Muneer, 2007; Pedraza, 2012; Chu and Majumdar, 2012). The capacity of ecosystems to deliver services to an already overpopulated planet is a fact and the acknowledged climate change increases the scarcity (Mooney et al., 2009). Climate changes affect ecosystem functions and results in implications for ecosystem services provision (Matos et al., 2019; Montoya and Raffaelli, 2010). As mention above, the quantified significant variability of climate aspects, including air temperature and soil moisture, which are related through the balance of incoming and outgoing energy combined with water at the surface, suggest critical implications on energy and water balance in solar parks. Therefore, based on the ecosystem services as suggested by UKNEA (UKNEA, 2014)

and the implications on energy and water balance, caused by solar parks, the followed (related to solar parks) were discussed.

4.4.1 Provisioning ecosystem services

4.4.1.1 Food provision (biomass materials)

The Leaf Area Index (LAI) is an easily measured variable and a great indicator of vegetation growth, whilst food provision for animals is critical for the accumulation of biomass, which would affect supply, and either are poorly assessed. Three of the 18 solar park studies including Chapter one of this thesis addressed the effects of solar parks on LAI (section 1.4.3). During spring 2011, Marrou et al. (2013a), found that the annual mean of LAI under the panels was significantly decreased under two different densities of shade (50% and 70% of shade). On the other hand, in Chapter one of this thesis, LAI along a linear transect, was higher under the panels compared with the gap, during growing and non-growing season months (Figure 1.8). This was explained by the higher amount of soil moisture under the panels which promoted vegetation (grasses) growth. These results could be related with Dupraz et al. (2010), who found minor effects on the annual mean above ground biomass at 50% shade but significant effects at 70% of shade, for wheat during growing season. Further, showed evidence of a decreased yield production of wheat under the panels associated with the decreased solar radiation fluxes.

Biomass accumulation and food provision are also associated with the vegetation management of a land hosting a solar park which was proven to affect plants' diversity (Armstrong et al. (2016) and Chapter one in this thesis see Table 5 in SI.1, p.207). In a UK temperate grassland hosting a solar park, Armstrong et al. (2016) conducted a

vegetation survey which showed that under the panels there were fewer species than at the gap and control treatments. Further, that mostly forbs and legumes thrive at the gap and in control compared to under the panels' diversity. For Chapter one of this thesis, a vegetation survey was run in the same site, to assess the plants' diversity four years post-construction of the solar park. Both *Achillea millefolium* and P*hleum pratense*, which were the most prevalent in 2013's survey by Armstrong et al. (2016) were not present under the panels in 2015's survey (see SI.1 Table 5, p.207).

Apart from the effect on plant diversity, the morphological and phenotypical characteristics of the vegetation were shown to be affected by the physical presence of the PV panels (Marrou et al., 2013b). These changes affect the ratios of biomass as well as of the LAI but remain unaddressed. It is expected that due to higher amounts of moisture, the leaves will be bigger, greener and thicker (storing more water), for most of the year. However, this is highly dependent on the species and the climate zone, because wheat for example did not vary significantly under shade and at control areas, compared with lettuce and cucumbers (Marrou et al., 2013b).

The plant cover was also affected by the physical presence of the PV panels for both lettuces and cucumbers during growing season (Marrou et al., 2013b). Lettuces cover was higher under the panels than at the control areas (almost by 150%) due to the morphological adaptation of the lettuce leaf size arrangement under shade. The cucumbers thrived in the control treatments compared with under the panels (less than 33% cover), which corresponded with the time period during which significant differences were found on the actual evapotranspiration between under and control areas (detailed in Marrou et al. (2013c)). As mentioned above, each type of vegetation responds differently under shade and under diverse climatic conditions, therefore future

assessments would be complicated to understand but is urgently needed, especially with agrivoltaics on the rise.

Adapting to the local climate changes is hard and spatio-temporal dislocations of plant species are expected; associated to climate change (Montoya and Raffaelli, 2010). This will affect the amount of biomass materials produced from a terrestrial ecosystem and will be further affected within a solar park. In the literature assessed for this study (Table 4.1), biomass and food provision were correlated with the light and water availability, with microclimate and the gaseous fluxes perturbation from solar parks. Lettuce varieties demonstrated a strong ability to produce biomass more efficiently with limited light resources (Marrou et al., 2013a). Further, Dupraz et al. (2010), found minor effects on the annual mean above ground biomass at 50% shade but significant effects at 70% of shade, for wheat during growing season.

On the other hand, in a temperate grassland, areas away and at the gap between panel rows biomass was four times higher than under the panels, associated with microclimate and vegetation management (Armstrong et al., 2016). Hassanpour Adeh et al. (2018), also found greater amount of biomass at the gap than under in an unirrigated pastureland which often experiences water stress. Further investigations on vegetation in different climatic zones and lands are critical in order to increase the probability of the assumed causes.

A framework with shade tolerant species and their potential to adapt under panels is urgently required, as most findings regarding biomass provision are from three types of crops (e.g. lettuces, cucumber, wheat, agave; Dupraz et al. (2010); Marrou et al. (2013c); Marrou et al. (2013b); Marrou et al. (2013a); Ravi et al. (2014)). Dinesh and Pearce (2016), suggested a short list of crops which might adapt in agrivoltaic systems

but have not been evaluated yet, including broccoli, hog peanut, yam, sweet potato, spinach, parsley, arugula and chard.

The assessments on the impacts of solar parks on vegetation, are the poorest, with above ground biomass and the leaf area index receiving most of the research focus. However, the experimental designs of the current studies differed significantly, the crop types which have been investigated were too specific (lettuces, cucumbers, durum wheat and mixed grassland species) and the correlation to establish the causes differed as well. Therefore, it is obvious that the need for further research is urgent, especially with vegetation being the protagonist in multiple-use lands, with remote-sensing approaches deeming the most sensible.

4.4.1.2 Fibre provision

There have been studies investigating agrivoltaic systems with cultivations rich in fibre such us durum wheat (Marrou et al., 2013b; Dupraz et al., 2010). Experiments conducted on the Paulownia variety wheat grown under shade in an agroforestry scheme, showed a reduction in wheat yield by 51% (Li et al., 2008), while Dupraz et al. (2010) reported that in a 60% light availability reduction, there was only a 19% reduction in wheat yield. There is limited research assessing crop yields in solar parks, and most of the comparisons to grasp some understanding regarding reductions caused by shade, are using agroforestry literature. However, as seen in this example for durum wheat, comparisons between agroforestry and agrivoltaic schemes might run into great differences and thus inaccuracies with regards to the result (Dinesh and Pearce, 2016).

4.4.1.3 Fresh water

The provisioning of fresh water does not directly apply within the ground-mounted solar parks scope reviewed in this PhD study, in comparison with floating solar schemes. Thus, implications on fresh-water provision could not be directly speculated with this form of design (Qi and Zhang, 2017).

4.4.1.4 Genetic resources

Physiology and morphology of plants with long-term effects on phenotypes and genotypes of potentially rare species have been reportedly affected by climatic changes (Kumar, 2015), especially changes on net precipitation, net solar radiation and evaporation (FAO, 2015; 2011; Dupraz et al., 2010; Marrou et al., 2013b; Marrou et al., 2013a). There have been evidence by two solar park studies, which conducted plant surveys across the same solar park (Chapter 1 of this thesis, Tables in S.I.1 p. 207 and Armstrong et al. (2016)), that grassland species diversity changed in a period of two years. It was related to site's management (sheep grazing in the winter and machinery cuts throughout the year) but should be thoroughly investigated to avoid any implications on plant genetic resources provision from multi-land use solar parks as this particular one in Westmill (Westmill Solar Farm, 2011).

4.4.2 Regulating ecosystem services

4.4.2.1 Climate regulation

Climate is regulated among others, by air temperature, gaseous fluxes, precipitation and the overall weather patterns at a global and local scale (Zari, 2017). Solar parks can influence climate in two ways, directly, by changing local climate with potential

implications for regional climate, and through altering the lands' carbon source-sink status and therefore atmospheric CO_2 concentrations. However, there is uncertainty on whether solar parks induce cooling, or heating (Table 4.2). In addition, wind and humidity (closely related to gaseous fluxes and weather patterns), findings are extremely limited and carbon dioxide fluxes, including net ecosystem exchange, soil respiration and photosynthesis, were addressed only from two studies including chapter one of this thesis.

Specifically, Armstrong et al. (2016) showed that regardless of season, the soil under the panels demonstrated the lowest soil CO_2 respiration (cooler air under) and photosynthesis ratios (low ratios of solar radiation) compared with the areas at the gap between panel rows and control areas. The variability was further supported by the existent vegetation and by the reduced wind speed under the panels.

Further, Net Ecosystem Exchange (NEE) demonstrated contradictions with regards to whether under and gap were a sink or a source of CO_2 in the atmosphere (Armstrong et al. (2016) and in Chapter one of this thesis; Figure 1.9). Armstrong et al. (2016) found that during the summer the gap between the panel rows was a greater sink of CO_2 compared to under the panels while out of growing season the control was the greatest sink among the three treatments. Annually, under was a sink while gap and control were a source of CO_2 to the atmosphere. On the other hand, in Chapter one of this thesis (section 1.3.2.4), there were evidence that both gap and under were a sink of CO_2 during most of the fieldwork visits. Further, the area under was shown to be a source out of the growing season.

Contradictions may occur because each year the gaseous fluxes vary depending on the weather conditions (Luo and Zhou, 2006). Further, uncertainties may occur due the fact

that CO_2 fluxes are the most poorly assessed factors by solar park studies, despite of the strong implications on soil moisture and temperature which influence plant growth (Phillips and Nickerson, 2015). It needs further assessment especially when considering wider deployment of multiple-use lands, including agrivoltaic systems.

4.4.2.2 Pollination Regulation

The effects of solar parks on climate aspects and their associated ecosystem functions, have had a strong impact on biodiversity. Evidence showed decreased plant diversity under the panels and reports for prevalence of specific shade-tolerant species were addressed from two surveys run with two years difference at the same solar park (Armstrong et al. (2016) and in Chapter one of this thesis). Changes on plant diversity in a solar park, suggested implications on pollinators, which are already in danger due to the extensive land fragmentation from climate change. Watson et al. (2002), investigated the potential of multiple-use lands introducing pollinator habitats in a solar park. In their study, they have identified over 3,500 km^2 of agricultural land near existing and planned solar energy facilities where pollinators habitats creation could deliver profit on ecosystem services.

4.4.2.3 Hazard Regulation

Solar parks provide clean and renewable energy; however, the solar panels are made of chemical materials which are currently under investigation with regards to their safest ways of disposal after solar park decommissioning. There are recycling projects assessing new ways of dealing with solar parks waste, as well as manufacturing new eco-friendly materials, to replace the hazardous which were primarily used in industry (Fthenakis, 2018; Xu et al., 2018; Babayigit et al., 2016). Apart from this aspect, solar parks waste is not assumed as hazardous compared with the waste deriving by other

types of energy resources (i.e. nuclear energy waste), especially when there are evidence that some of these hazardous solar panels' waste materials could be recycled to produce mesoporous silica material for soils (Ma and Ruan, 2013).

4.4.2.4 Noise Regulation

In Westmill Solar Park; UK temperate grassland hosting a solar park (Westmill Solar Farm, 2011), there are wind turbines installed close to the solar park. This is quite normal as many large-scale projects involve both types of renewable infrastructure within the same land unit. It is anticipated that industrial wind turbines are a new source of noise, in a previously quite rural area. Animal Conservation papers found that wind turbines noise decreased bird nesting in a grassland and thus were suggested to be implemented in crop lands, which support lower passerines compared to grasslands (Krecia et al., 1999). Further, wind turbines affected squirrels community emitting vocalizations that alert others to the presence of a predator (Rabin et al., 2006).

In addition, Environmental Health studies investigating sleeping patterns and disturbances, showed that the noise deriving by the propellers of the wind turbines had moderate to strong effects on the sleep of residents close to wind parks (Nissenbaum et al., 2012; van den Berg, 2004; Knopper and Ollson, 2011; Schmidt and Klokker, 2014; Bolin et al., 2011). Regarding solar parks and their potential impact on noise regulation, would be noise produced by inverters. They produce a fair amount of noise but are still significantly quieter than a vacuum cleaner and only during daytime.

4.4.2.5 Disease and Pest Regulation

There are implications for increased pest and diseases on lettuces cultivations, under the PV panels, due to the increased air humidity and limited air circulation compared with

the gap or control areas away from the panels (Marrou et al., 2013b). One of the main negative effects of shading on crops is usually the increase of fungal diseases (Roberts and Paul, 2006). These evidences suggest the need for future research, especially with the wide deployment of solar parks on multiple-use lands.

4.4.2.6 Regulation of water, air and soil quality

The regulation of water, air and soil quality are highly interdependent to all the climate aspects and ecosystem processes that are expected to be affect by a solar park (thoroughly mentioned and assessed under section 4.4). Here, there were some additions with regards to the water use efficiency from precipitation and PV panels surface cleaning water runoff and their implications to the water and soil quality.

For example, there have been suggestions implying that the amount of water used to clean the PV panels and dust suppression are similar to the amounts required for annual agave growth, suggesting the possibility of integrating the two systems to maximize the efficiency of land and water use to produce both electricity and liquid fuel in a semi-arid located solar park (Ravi et al., 2014). Also, that water used for cleaning and water from precipitation collected in containers in the solar park, could be widely used in agrivoltaic systems as well, as being the main method or irrigation any type of solar park (Dinesh and Pearce, 2016; Hernandez et al., 2019).

However, there are severe implications for soil and water quality during panels cleaning procedures (Qi and Zhang, 2017). Cleaning panels involves the use of chemical products, mostly non-bioproducts, to remove dust and any dirt (bird droppings) that would affect the energy production. Cleaning products contain chromium which mainly consists of hexavalent and trivalent chromium compounds. Their toxicity is undoubtable and inhibits the growth of crops and using wastewater that contains

chromium to irrigate will reduce crop yield and harden the soil. Even though other cleaning technologies (e.g., electrostatic) exist, most are not yet commercially available, and the impacts of conventional technologies (e.g., cleaning using chemical sprays) on the environment are partially resolved (Hernandez et al., 2014). Wastewater runoff leaches into the soil, might also have a long-term effect at the water table in the solar park.

4.4.3 Supporting ecosystem services

4.4.3.1 Water Cycling

Solar parks physical presence may affect the water cycle, redistributing precipitation, altering rates of evaporation and transpiration as discussed in some of the published solar park studies (Table 4.1). Overall, effects of precipitation in solar parks, were poorly addressed, with current findings showing that the PV panels' design, allowed the penetration of some water under the panels (sides of the panels' frame and water runoff at the front of the southern panel edge). Only two studies measured the amount of precipitation and both were conducted in the same UK temperate grassland (Armstrong et al. (2016) and in Chapter one of this thesis section 1.4.1.5). In Chapter one of this thesis there were evidence of water intake under the PV panels explained by the diagonal flow of rain and by the panels design (water run off at the sides of the panels). Perturbations at the amount of water intake by the surface, implied effects on evapotranspiration.

Impacts on water cycle can be affected by ecosystem type and co-land use (multiple-use lands such as agrivoltaics). For example, Marrou et al. (2013c) assessed cucumbers and lettuces actual evapotranspiration (AET), soil water potential (water storage) and

transpiration during cropping season. Their findings showed that AET under the PV panels, was more affected by shading in spring than in summer and that plant transpiration was reduced by 31% for lettuces under shade. On the other hand, the function Evaporation/Transpiration was found to increase significantly under shade. Further, at 25 cm depth, under shade lettuces maintained their water potential to 50 kPa compared with the 65 kPa in control areas and the cucumbers demonstrated a water potential of 80 kPa going deeper (30 cm depth).

In addition, Hassanpour Adeh et al. (2018) showed that the area under the panels was 328% more efficient, decreasing the ratios of potential evaporation (PE) at the gap between panels rows. The further low PET lead to increased grasses water use efficiency. At the control areas there were evidence of depletion through ET and scarcity reported during the growing season. In Chapter three of this thesis, PE in different climate zones was assessed (section 3.4.1.2). The area under, was constantly evaporating less compared with gap and control (three times lower in the equatorial, double in the arid).

Marrou et al. (2013c) associated the water use efficiency with biomass accumulation which for lettuces under shade reached daily a 67% to 87%. Water potential which is highly related to water use efficiency by the soil affecting the ratios of plant biomass (Marrou et al., 2013a). On the other hand, cucumbers accumulation of the total dry matter was reduced by ~40 % compared to control areas under full sun. Thus, investigating those variables at each species can be complicated as for example, cucumber appears more sensitive under shade than lettuces. Thus, the water available for evaporation under panels stays in the soil, this leads to increased soil moisture content and as a result to changes at the phenological characteristics of the vegetation

such as plant growth and biomass production, which obviously will vary with plant species, spatially and temporally.

4.4.3.2 Soil formation

Soil physical properties, including bulk density and organic matter, affect soil formation, thus soil health and plant growth (Saini, 1966). Soil health and plant growth are essential for maintaining habitats and biodiversity. Therefore, quantifying the effects of solar parks on soil is crucial. However, only two studies (Armstrong et al. (2016) and Chapter one of this thesis; section 1.4.2) assessed solar parks effects on soil physical and biochemical properties. Armstrong et al. (2016) and in Chapter one of this thesis, were conducted in the same UK temperate grassland with two years difference between the two field studies.

The effects of solar parks on climate aspects and their associated ecosystem functions, have had a strong impact on biodiversity. Evidence showed decreased plant diversity under the panels and reports for prevalence of specific shade-tolerant species were addressed from two surveys run with two years difference at the same solar park (Armstrong et al., 2016; Makaronidou, 2019). Changes on plant diversity in a solar park, suggests implications on pollinators, which are already in danger due to the extensive land fragmentation from climate change. Watson et al. (2002), investigated the potential of multiple-use lands introducing pollinator habitats in a solar park. In their study, they have identified over 3,500 km^2 of agricultural land near existing and planned solar energy facilities where pollinators habitats creation could deliver profit on ecosystem services.

4.4.3.3 Soil formation through the nutrient cycle

Armstrong et al. (2016) showed no spatial nor seasonal variability in total carbon (C) and nitrogen (N), bulk density, particle size distribution and microbial C and N. However, in Chapter one of this thesis, there were evidence of spatial variability of bulk density and organic matter, related to high amounts of soil moisture under the PV panels (section 1.4.2). The magnitude deemed low, and the correlation between bulk density and organic matter was negative (Keller and Håkansson, 2010; Gao et al., 2012; DelVecchia et al., 2014). This implied that the soil conditions within a solar park recovered four years after the extensive perturbation during construction and post-construction (compaction from machinery and vegetation re-seeding, respectively).

4.4.3.4 Primary production

Induced microclimate caused by solar parks was shown to affect the energy flow across a land hosting a solar park (studies assessing part of the issue as seen in Table 4.1 as well as in Chapter one of this thesis) strongly affected primary production; vegetation in a solar park (thoroughly assessed in above). Climate factors influence primary productivity differently and depends on the type of vegetation and the climate zone, for example, desert vegetation is closely related to both precipitation and temperature (Han et al., 2016). Thus, for once again, the assessment on solar parks local climate effects across different climate zones, combined with physical based models associated with crop models, would provide critical information and help building strategies to promote the supply of ecosystem services.

4.5 Limited and non-inclusive findings is solar parks with great implications for the Water-Energy Balance

Given the variability and spatio-temporal differences among the location which were assessed by current literature (Table 4.1), and acknowledging that the observed climate aspects investigated across the four chapters of this thesis, (including air temperature, precipitation, soil moisture, evaporation), are related through the balance of incoming and outgoing energy combined with water at the surface, allowed us to further highlight, the critical need to assess their interactive effects on energy and water balance in solar parks. It is assumed that in an already changed climate, time of day, seasonal and spatial differences in a solar park, should be monitored regardless of solar parks' size, especially given their widespread deployment, as the effects on the local climate, are proportional to the potential effects on the global climate regulation.

Below follows a summary that describes the illustration of the impacts of solar parks in aspects of climate and on ecosystem processes (Table 4.2) as reported from the fifteen solar park studies and the first three Chapters of this thesis. Daytime, night-time and annual averages increase and/or decrease variability were reported only when assessed by more than three studies (Table 4.1). Apart from the fact that results were at times contradictory, which prohibits accurate assumptions going forward, the summary highlighted even bigger gaps assessing specific times of day in the subsequent seasons (growing and non-growing) as well as across different climate zones. There were limited to non-reported metrics during night-time, which would provide information including transpiration rates. Also, the day-time reported metrics, reported in three and more studies, mostly end up to contradictions (air temperature for example), or to not enough data to report statements with certainty, for example regarding the effects on

evaporation under the panels in a temperate ecosystem, or an arid desert ecosystem (where solar parks are mostly widely deployed).

Similar observations regarding knowledge gaps out of the growing season. Most researchers investigating a new topic as the one investigated in this PhD study, primarily focused their assessments on growing season impacts, as it is the season when most of the ecosystem functions occur and thus growing season is the main regulator of the ecosystem services supply. Despite that, research is still in juvenile stage, as solar parks where implemented almost two decades ago and any assumption or long-term impact is expected to appear within the next decade (before and right after the decommission stage).

Regardless, the wide global deployment of solar parks across different ecosystem types, different climate zones, under different management strategies, different PV panels planning, placement and design, along with the speed of this deployment to achieve the ultimate transition to clean energy resources, implies massive global land-use change. The implications of this massive land-use change on microclimate and the subsequent processes are unresolved, run into contradictions (due to limited research available), each follows a different experimental design disabling any establishment of causes. There is strong evidence of potential impacts at the energy and water balance, as well as evidence of ecosystem recovery four years post-construction, increased crop and pollination yields under the panels (Table 4.1). In an already changed climate, assessing all the above, increases the already high complexity of the topic, however we urge the scientific community to focus on this field of research.

Table 4.2:Literature review findings related to solar parks' effects on aspects of climate and ecosystem processes. Arrows showing whether the average of the studies showed an increase, a decrease, a contradiction, a simultaneous increase and a decrease reflected to experimental design, of each of the mostly tested variables. Red colour for Under the panels, blue colour for the Gap between PV panel rows, green for the Control areas and yellow colour for above and in the area with PV panels compared to Control. Equality symbol, grey colour, demonstrated the findings with same response among investigated areas inside a solar park and Control.

Variable	Growing Season			Non-Growing Season			Annual		
	Day	Daily	Night	Day	Daily	Night	Day	Daily	Night
Air Temperature	↑ ↑ ↕ ↓	↑	↑ ↑	↓ =	↓ ↓ ↑			↓ ↕	↑
Soil Temperature	↓	↑ ↑ ↓		↓	↓ ↕ ↕			↓ ↓ =	
Soil Moisture	↑ ↓								
Biomass		↑ ↓						↑ ↑ ↓	
Longwave-LW								↓ ↕	↕
Shortwave-SW	↑	↑ ↓ ↓						↑ ↕ ↓	↓
Evaporation and ET		↑ ↓			↑			↑	
Albedo		↓			↑		↑	↑	↑

4.6 O3. Critical research needs optimizing solar parks hosting ecosystem sustainability

This synthesis study reviewed fifteen publications and the three results chapters of this thesis, all associated with impacts of solar parks at the local climate, highlighting the urgent need for future research. The existing studies are limited, aim to answer varying questions while applying different methodologies. This prevents reliable generalisations across different climatic zones, ecosystem types and solar park designs, whilst solar energy generation is exponentially increasing across the globe.

Interest in sustainability is increasing at the engineering sector, and lately several approaches account for environmental impacts of infrastructure at the hosting environment. It is anticipated that future research on solar parks should be approached by a combination of strategic engineering of solar technologies and ecology principals to promote sustainability of solar energy across diverse hosting environments. The ultimate target is to create a win-win situation, promoting parallelly clean energy provision by solar parks and ecosystem services provision, from the same land unit.

Techno-ecological synergies are the outcomes deriving by technology and nature processes for the benefit of ecosystem's sustainability (Bakshi et al., 2015; Hernandez et al., 2019). For example, in an agrivoltaic scheme using PV panels design to harvest water for the irrigation of the hosting land, could result to several techno-ecological synergies outcomes (seven in number; Hernandez et al. (2019)). These positive outcomes could ultimately promote ecosystem services and supply, reducing air pollution, regulate the climate, secure food and energy, while increasing water use efficiency and pollination (Hernandez et al., 2019; Bakshi et al., 2015).

At this stage, modelling approaches verified with field data, including remote sensing approaches, are strongly suggested as they provide rapid and cost-effective information (Chapters two and three of this thesis). The majority of the related solar studies focused their investigations on daily averages reports and mostly during the growing season. However, nocturnal metrics are also crucial to identify effects on ecosystem function including for example transpiration. Potential increase of transpiration was caused by vegetation removal and gravel underlayment which had as a result cooling of the PV panels (Hernandez et al., 2019). Thus, land management should be always considered when trying to address potential and size of impacts from solar parks at the local climate and the overall water and energy balance.

In addition, all future studies apart from accounting for daily averages should further account for minimum and maximum values of climate variables (air temperature, soil moisture, soil temperature, humidity, wind speed and solar radiation fluxes). All types of metrics are essential as they could be used to assess variability of ecosystem functions including vegetation growth; for example, air temperature minimum and maximum are essential calculating the amount of growing degree days.

Moreover, experimental designs are also crucial addressing variability which might differ from one design to another. Comparisons between inside and outside a solar park are critical, but differences among randomly selected locations inside a solar park including under panels, gap between panel rows, panels' sides, control areas away from panels, linear transects grasping under and gap areas should be also considered. There was high variability reported among different areas inside a solar park and all suggest further investigation.

Below, there are suggestions for future research categorised as Ecological and Techno-Ecological approaches, terms borrowed from a recent study by Hernandez et al. (2019), which would be also interesting if expanded in the southern hemisphere as well. All ideas reported here, are strongly associated with crucial ecosystem services. The most relevant to our study and approach, (i.e. ground-mounted solar parks microclimate variability), were mainly those mentioned under section 4.4. In particular, related to air pollution reduction, climate regulation, animal welfare, food system resilience, habitat of species, land sparing, maintenance of genetic diversity, pollination, water-use efficiency and quality, supplied by solar park ecosystem functions.

4.6.1 Ideas for Future Research

- Identify whether solar parks induce cooling or heating and if this is related to climate zone and/or height (surface to above PV panels) that air temperature was measured. Assessing the wind, solar radiation and air temperature vertical profiles could establish weather solar parks induce cooling or heating (Fthenakis and Yu, 2013).
- Investigate plants diversity variability throughout the years post-construction of solar parks, associated with microclimate variability. This should include species growth, accounting for yield production and biomass accumulation.
- Investigate the abundance of small mammals (i.e. brown hare, owls) as well as live-stock solar parks forage quality associated with biomass materials and food provision. Examine whether a solar park would be used by raptor species (shelter areas from PV arrays).

- Identify whether solar parks sink or source carbon dioxide in the atmosphere across climate zones; is it associated with vegetation (dense, sparse or non) and/or varies depending on the weather conditions (Luo and Zhou, 2006).
- Investigate the effect of low solar radiation fluxes under the panels on plants diversity and biomass, across different climate zones.
- Expand the evaluation of shade-tolerant species for agrivoltaic applications to other species apart from lettuces and cucumbers, including broccoli, hog peanut, yam, sweet potato, spinach, parsley, arugula and chard (Dinesh and Pearce, 2016). Investigate the species growth, for example accounting for yield production and biomass accumulation under the panels compared to control areas.
- Simulate soil temperatures by testing different solar panels' dimensions deriving by real-life solar parks and quantify implications of design on energy and water balance
- Quantify the effect of redistributing precipitation under the panels and in front of the southern panel edge (water pools created from runoff) on the surface energy and water balance across different climate zones; implications for soil physical and biochemical properties including soil bulk density and organic matter which affect soil health and plant growth (Saini, 1966).
- Support water cycle by consider practices and technics to increase the water availability under the panels. For example, establish collectors (drainpipes) to store water from the panels' runoff at the southern panel edges which could then be used for irrigation.

- A carbon calculator life cycle analysis of solar parks, would be beneficial and promote the outcome of several techno-ecological synergies including air pollution reduction and climate regulation (Hernandez et al., 2019).
- Investigate how cleaning of the PV panels with chemicals to prohibit dust deposition, would affect plant-soil traits including Evapotranspiration and thus provision of services including food provision, biodiversity maintenance, habitats and pollination.

4.7 Conclusion

There is a global effort for an energy transition to low-carbon resources and solar energy is the most promising. Impacts of the solar parks deployment on the hosting land are poorly assessed. Terrestrial ecosystems are sensitive demonstrating low availabilities in water and fluctuations in temperatures. These sensitivities vary with climate zone and thus different types of vegetation. Maintaining grasslands, shrublands and any types of ecosystems where solar parks are installed was the target when new strategies as multiple-use lands where initially introduced. However, assessing the UK framework of solar parks establishment there was a clear distinction regarding the grades of a land which would host a solar park. The areas proposed for a solar park establishment would have to be low grade and not ideal for agriculture use (BRE, 2014). If the proposed area could be used for agriculture, then the proposal should thoroughly explain and provide information explaining why the proposed land-use change. It is strongly suggested, that policy makers create firmer frameworks as well as guide the stake holders with cautious delivering environmental and financial benefits for all sides involved. With solar parks changing the land-use, the effect is larger, and thus ecosystems services are expected to be altered. Relating the impacts of solar parks at the local climate to the provision of ecosystem services shows the urgency of establishing the causes and find solutions to

tackle the effects and promote ecosystem services supply. Chances to optimise the effects through multiple-use lands sound appealing. Apart from research purposes, this synthesis is an easily accessible framework to communicate the complexity of understanding the implications of solar parks on ecosystem services to stake holders, policy makers and the public. The existing studies are limited, aim to answer varying questions and use different methodologies. This prevents reliable generalisations across different climatic zones, ecosystem types and solar park designs. At this stage modelling approaches verified with field data are strongly suggested as they allow predictions to expand on larger areas and for long-term metrics which is extremely practical and costless. Research findings are urgently needed to enhance understanding and thus explore the potential for managing solar parks to promote several techno-ecological outcomes.

5 References

Abu-Hamdeh, N. H. 2003. Thermal Properties of Soils as Affected by Density and Water Content. *Biosystems Engineering,* 86(1)**,** 97–102.

Acevedo, E. 2002. Wheat Growth and Physiology.

Adams, A. S. & Keith, D. W. 2013. Are Global Wind Power Resource Estimates Overstated? *Environmental Research Letters,* 8(1)**,** 10.

Agodzo, S. K., Nishio, T. & Yamamoto, T. 1997. Trickle Irrigation of Okra Based on Small Pan Evaporation Schedule under Glasshouse Condition. *Rural and Environment Engineering,* 1997(33)**,** 19-36.

Alam, M. & P. Trooien, T. 2001. Estimating Reference Evapotranspiration with an Atmometer. *Applied Engineering in Agriculture,* 17(2)**,** 153.

Albergel, C., Dutra, E., Muñoz-Sabater, J., Haiden, T., Balsamo, G., Beljaars, A., Isaksen, L., De Rosnay, P., Sandu, I. & Wedi, N. 2015. Soil Temperature at Ecmwf: An Assessment Using Ground-Based Observations. *Journal of Geophysical Research: Atmospheres,* 120(4)**,** 1361-1373.

Allen, R. G., Pereire, L. S., Raes, D. & Smith, M. 1998. Crop Evapotranspiration - Guidlines for Computing Crop Water Requirements. *FAO Irrigation and drainage paper 56.* 56 ed. Rome: FAO - Food and Agriculture Organization of the United Nations.

Alvenäs, G. & Jansson, P.-E. 1997. Model for Evaporation, Moisture and Temperature of Bare Soil: Calibration and Sensitivity Analysis. *Agricultural and Forest Meteorology,* 88(1-4)**,** 47-56.

Armstrong, A., Ostle, N. J. & Whitaker, J. 2016. Solar Park Microclimate and Vegetation Management Effects on Grassland Carbon Cycling. *Environmental Research Letters,* 11(7)**,** 12.

Armstrong, A., Waldron, S., Ostle, N. J., Richardson, H. & Whitaker, J. 2015. Biotic and Abiotic Factors Interact to Regulate Northern Peatland Carb. *Ecosystems,* 18(8)**,** 1395-1409.

Armstrong, A., Waldron, S., Whitaker, J. & Ostle, N. J. 2014a. Wind Farm and Solar Park Effects on Plant-Soil Carbon Cycling: Uncertain Impacts of Changes in Ground-Level Microclimate. *Global Change Biology,* 20(6)**,** 1699-706.

Armstrong, A., Waldron, S., Whitaker, J. & Ostle, N. J. 2014b. Wind Farm and Solar Park Effects on Plant-Soil Carbon Cycling: Uncertain Impacts of Changes in Ground-Level Microclimate. *Glob Chang Biol,* 20(6)**,** 1699-706.

Arnold, N. S., Willis, I. C., Sharp, M. J., Richards, K. S. & Lawson, W. J. 1996. A Distributed Surface Energy-Balance Model for a Small Valley Glacier. I. Development and Testing for Haut Glacier D' Arolla, Valais, Switzerland. *Journal of Glaciology,* 42(140)**,** 77-89.

Arora, V. K. & Boer, G. J. 2005. A Parameterization of Leaf Phenology for the Terrestrial Ecosystem Component of Climate Models. *Global Change Biology,* 11(1)**,** 39-59.

Asif, M. & Muneer, T. 2007. Energy Supply, Its Demand and Security Issues for Developed and Emerging Economies. *Renewable and Sustainable Energy Reviews,* 11(7)**,** 1388-1413.

Babayigit, A., Ethirajan, A., Muller, M. & Conings, B. 2016. Toxicity of Organometal Halide Perovskite Solar Cells. *Nature Materials,* 15(3)**,** 247-251.

Bakshi, B. R., Ziv, G. & Lepech, M. D. 2015. Techno-Ecological Synergy: A Framework for Sustainable Engineering. *Environmental Science & Technology,* 49(3)**,** 1752-1760.

Bardgett, R. D., Mawdsley, J. L., Edwards, S., Hobbs, P. J., Rodwell, J. S. & Davies, W. J. 1999. Plant Species and Nitrogen Effects on Soil Biological Properties of Temperate Upland Grasslands. *Functional Ecology,* 13(5)**,** 650-660.

Barnett, K. L. & Facey, S. L. 2016. Grasslands, Invertebrates, and Precipitation: A Review of the Effects of Climate Change. *Frontiers in Plant Science,* 7**,** 1196.

Barron-Gafford, G. A., Minor, R. L., Allen, N. A., Cronin, A. D., Brooks, A. E. & Pavao-Zuckerman, M. A. 2016. The Photovoltaic Heat Island Effect: Larger Solar Power Plants Increase Local Temperatures. *Scientific Reports,* 6**,** 35070.

Barron, E. J., Sloan, J. L. & Harrison, C. G. A. 1980. Potential Significance of Land—Sea Distribution and Surface Albedo Variations as a Climatic Forcing Factor; 180 M.Y. To the Present. *Palaeogeography, Palaeoclimatology, Palaeoecology,* 30**,** 17-40.

Best, M. J. 1998. A Model to Predict Surface Temperatures. *Boundary-Layer Meteorology,* 88(2)**,** 279-306.

Best, M. J., Pryor, M., Clark, D. B., Rooney, G. G., Essery, R. L. H., Ménard, C. B., Edwards, J. M., Hendry, M. A., Porson, A., Gedney, N., Mercado, L. M., Sitch, S., Blyth, E., Boucher, O., Cox, P. M., Grimmond, C. S. B. & Harding, R. J. 2011. The Joint Uk Land Environment Simulator (Jules), Model Description – Part 1: Energy and Water Fluxes. *Geosci. Model Dev.,* 4(3)**,** 677-699.

Blennow, K. 1995. Sky View Factors from High-Resolution Scanned Fish-Eye Lens Photographic Negatives. *Journal of Atmospheric and Oceanic Technology,* 12(6)**,** 1357-1362.

Bogardi, J. J., Dudgeon, D., Lawford, R., Flinkerbusch, E., Meyn, A., Pahl-Wostl, C., Vielhauer, K. & Vörösmarty, C. 2012. Water Security for a Planet under Pressure: Interconnected Challenges of a Changing World Call for Sustainable Solutions. *Current Opinion in Environmental Sustainability,* 4(1)**,** 35-43.

Bolin, K., Bluhm, G., Eriksson, G. & Nilsson, M. E. 2011. Infrasound and Low Frequency Noise from Wind Turbines: Exposure and Health Effects. *Environmental Research Letters,* 6(3)**,** 035103.

Bonan, G. 2008. Ecological Climatology. 2 ed. CGD's Terrestrial Sciences Section: Cambridge University Press.

Bonhomme, R. 2000. Bases and Limits to Using 'Degree.Day' Units. *European Journal of Agronomy,* 13(1)**,** 1-10.

Bórawski, P., Yashchenko, T., Sviderskyi, A. & Dunn, J. W. 2019. Development of Renewable Energy Market in the Eu with Particular Regard to Solar Energy. *VII International Scientific Conference Determinants of Regional Development*.

Braithwaite, R. J. & Olesen, O. B. 1990. A Simple Energy-Balance Model to Calculate Ice Ablation at the Margin of the Greenland Ice Sheet. *Journal of Glaciology,* 36(123)**,** 222-228.

Bre 2013. Planning Guidance for the Development of Large Scale Ground Mounted Solar Pv Systems. *In:* CENTER, N. S. (ed.). BRE National Solar Center.

Bre 2014. Agricultural Good Practice Guidance for Solar Farms. *In:* SCURLOCK, J. (ed.). BRE National Solar Centre.

Brock, B. W. & Arnold, N. S. 2000. A Spreadsheet-Based (Microsoft Excel) Point Surface Energy Balance Model for Glacier and Snow Melt Studies. *Earth Surface Processes and Landforms,* 25(6)**,** 649-658.

Businger, J. A., Wyngaard, J. C., Izumi, Y. & Bradley, E. F. 1971. Flux-Profile Relationships in the Atmospheric Surface Layer. *Journal of the Atmospheric Sciences,* 28(2)**,** 181-189.

Calvert, K. & Mabee, W. 2015. More Solar Farms or More Bioenergy Crops? Mapping and Assessing Potential Land-Use Conflicts among Renewable Energy Technologies in Eastern Ontario, Canada. *Applied Geography,* 56**,** 209-221.

Camillo, P. J. & Gurney, R. J. 1986. A Resistance Parameter for Bare-Soil Evaporation Models. *Soil Science,* 141(2).

Cao, H.-X., Hanan, J. S., Liu, Y., Liu, Y.-X., Yue, Y.-B., Zhu, D.-W., Lu, J.-F., Sun, J.-Y., Shi, C.-L., Ge, D.-K., Wei, X.-F., Yao, A.-Q., Tian, P.-P. & Bao, T.-L. 2012. Comparison of Crop Model Validation Methods. *Journal of Integrative Agriculture,* 11(8)**,** 1274-1285.

Capell, A. 2016. *Solar Power in Britain* [Online]. UK: Adam Smith Research Trust. Available: https://www.adamsmith.org/research/research [Accessed October 14, 2016 2016].

Carder, A. C. 1960. Atmometer Assemblies, a Comparison. *Canadian Journal of Plant Science,* 40(4)**,** 700-706.

Cardoso, E. J. B. N., Vasconcellos, R. L. F., Bini, D., Miyauchi, M. Y. H., Santos, C. a. D., Alves, P. R. L., Paula, A. M. D., Nakatani, A. S., Pereira, J. D. M. & Nogueira, M. A. 2013. Soil Health: Looking for Suitable Indicators. What Should Be Considered to Assess the Effects of Use and Management on Soil Health? *Scientia Agricola,* 70**,** 274-289.

Carrosio, G. & Scotti, I. 2019. The 'Patchy' Spread of Renewables: A Socio-Territorial Perspective on the Energy Transition Process. *Energy Policy,* 129**,** 684-692.

Cebecauer, T. & Suri, M. 2015. Typical Meteorological Year Data: Solargis Approach. *Energy Procedia,* 69**,** 1958-1969.

Champeaux, J. L., Masson, V. & Chauvin, F. 2006. Ecoclimap: A Global Database of Land Surface Parameters at 1 Km Resolution. *Meteorological Applications,* 12(1)**,** 29-32.

Chen, Y., Yang, K., Tang, W., Qin, J. & Zhao, L. 2012. Parameterizing Soil Organic Carbon's Impacts on Soil Porosity and Thermal Parameters for Eastern Tibet Grasslands. *Science China Earth Sciences,* 55(6)**,** 1001-1011.

Chu, S. & Majumdar, A. 2012. Opportunities and Challenges for a Sustainable Energy Future. *Nature,* 488(7411)**,** 294-303.

Claassen, H. C. & Riggs, A. C. 1993. An Estimate of the Roughness Length and Displacement Height of Sonoran Desert Vegetation, South-Central Arizona. *Water-Resources Investigations Report.* - ed.

Clinton, B. D. 2003. Light, Temperature, and Soil Moisture Responses to Elevation, Evergreen Understory, and Small Canopy Gaps in the Southern Appalachians. *Forest Ecology and Management,* 186(1)**,** 243-255.

Conant Richard, T., Cerri Carlos, E. P., Osborne Brooke, B. & Paustian, K. 2017. Grassland Management Impacts on Soil Carbon Stocks: A New Synthesis. *Ecological Applications,* 27(2)**,** 662-668.

Dagar, J. C. & Tewari, V. P. 2017. *Agroforestry: Anecdotal to Modern Science*: Springer Verlag, Singapore.

Davidoff, B. & Selim, H. M. 1988. Correlation between Spatially Variable Soil Moisture Content and Soil Temperature. *Soil Science,* 145(1)**,** 1-10.

Davidson, E. A., The Woods Hole Research Centre, P. B., Woods Hole, Ma 02543 USA,, Belk, E., The Woods Hole Research Centre, P. B., Woods Hole, Ma 02543 USA,, Boone, R. D. & Institute of Arctic Biology, U. O. A., Fairbanks, Ak 99775 USA 1998. Soil Water Content and Temperature as Independent or Confounded Factors Controlling Soil Respiration in a Temperate Mixed Hardwood Forest. *Global Change Biology,* 4(2)**,** 217-227.

Day, R. W. & Quinn, G. P. 1989. Comparisons of Treatments after an Analysis of Variance in Ecology. *Ecological Monographs,* 59(4)**,** 433-463.

De Vries, D. A. 1963. *Physics of Plant Environment,* Amsterdam: North - Holland Publishing Company.

Deardorff, J. W. 1974. Three-Dimensional Numerical Study of the Height and Mean Structure of a Heated Planetary Boundary Layer. *Boundary-Layer Meteorology,* 7(1)**,** 81-106.

Degroot, R. S., Wilson, M. A. & Boumans, R. M. J. 2002. A Typology for the Classification, Description and Valuation of Ecosystem Functions, Goods and Services. *Ecological Economics,* 41(3)**,** 393-408.

Delta-T Devices, L. UK-a. *Bf3 Sunshine Sensor* [Online]. UK: Delta-T Devices Ltd. Available: https://www.delta-t.co.uk/wp-content/uploads/2016/11/BF3-User-Manual.pdf.

Delta-T Devices, L. UK-b. *Ml3 Thetaprobe Soil Moisture Sensor* [Online]. UK: Delta-T Devices Ltd. Available: https://www.delta-t.co.uk/product/ml3/.

Delvecchia, A. G., Bruno, J. F., Benninger, L., Alperin, M., Banerjee, O. & De Dios Morales, J. 2014. Organic Carbon Inventories in Natural and Restored Ecuadorian Mangrove Forests. *PeerJ,* 2**,** e388.

Dincer, I. 1999. Environmental Impacts of Energy. *Energy Policy,* 27(14)**,** 845-854.

Dincer, I. 2000. Renewable Energy and Sustainable Development: A Crucial Review. *Renewable and Sustainable Energy Reviews,* 4(2)**,** 157-175.

Dinesh, H. & Pearce, J. M. 2016. The Potential of Agrivoltaic Systems. *Renewable and Sustainable Energy Reviews,* 54**,** 299-308.

Dupraz, C., Marrou, H., Talbot, G., Dufour, L., Nogier, A. & Ferard, Y. 2010. Combining Solar Photovoltaic Panels and Food Crops for Optimising Land Use: Towards New Agrivoltaic Schemes. *Renewable Energy,* 36(10)**,** 2725-2732.

Ecoexperts, T. 2018. *Solar Panel Comparison Website* [Online]. Available: https://www.theecoexperts.co.uk/solar-panels/infographic.

Eea 2018. Renewable Energy in Europe - 2018. *Recent growth and knock-on effects.* Luxembourg: European Environment Agency.

Eia. 2016. *Solar, Natural Gas, Wind Make up Most 2016 Generation Additions - Today in Energy - U.S. Energy Information Administration (Eia)* [Online]. U.S. Energy Information Administration. Available: http://www.eia.gov/todayinenergy/detail.cfm?id=25172 [Accessed March 1, 2016 2016].

Eia 2018. Annual Energy Outlook 2018 with Projections to 2050. Washington, DC: U.S. Department of Energy.

Emmett, B., Frogbrook, Z., Chamberlain, P., Giffiths, R., Pickup, R., Poskitt, J., Reynolds, B., Rowe, E., Spurgeon, D., Rowland, P., Wilson, J. & Wood, C. 2008. Soils Manual. *In:* 03/07 (ed.) *CS Technical Report No.3/07.* Centre of Ecology and Hydrology (Natural Environment Research Council).

Esri 2011. Arcgis Desktop: Release 10. Redlands, CA: Environmental Systems Research Institute.

Essery, R., Bunting, P., Rowlands, A., Rutter, N., Hardy, J., Melloh, R., Link, T., Marks, D. & Pomeroy, J. 2008. Radiative Transfer Modeling of a Coniferous Canopy Characterized by Airborne Remote Sensing. *Journal of Hydrometeorology,* 9(2)**,** 228-241.

Evans, A., Strezov, V. & Evans, T. J. 2009. Assessment of Sustainability Indicators for Renewable Energy Technologies. *Renewable and Sustainable Energy Reviews,* 13(5)**,** 1082-1088.

Fao 1996. The State of Food and Agriculture. *In:* ZEGARRA, F. L., ROSSMILLER, G. E., J.SKOET, TEODOSIJEVIC, S., ARENA, G., IACOACCI, P. L. & ONORASCENZO, O. (eds.). Rome: FAO.

Fao 2011. Coping with Climate Change: The Importance of Genetic Resources for Food Security. Rome.

Fao 2015. Coping with Climate Change - the Roles of Genetic Resources for Food and Agriculture. Rome.

Farley, K. A., Kelly, E. F. & Hofstede, R. G. M. 2004. Soil Organic Carbon and Water Retention after Conversion of Grasslands to Pine Plantations in the Ecuadorian Andes. *Ecosystems,* 7(7)**,** 729-739.

Farouki, R. T. 1986. The Characterization of Parametric Surface Sections. *Computer Vision, Graphics, and Image Processing,* 33(2)**,** 209-236.

Federer, C. A. 1968. Spatial Variation of Net Radiation, Albedo and Surface Temperature of Forests. *AMS Meteorological society***,** 789 - 795.

Florides, G. & Kalogirou, S. 2007. Ground Heat Exchangers—a Review of Systems, Models and Applications. *Renewable Energy,* 32(15)**,** 2461-2478.

Forster, P. & Ramaswamy, V. 2007. Changes in Atmospheric Constituents and in Radiative Forcing. IPCC.

Fowler, A. & Brown, V. 1994. Site Management and Climate Change. Natural England Research Reports.

Frank, T. 2005. Climate Change Impacts on Building Heating and Cooling Energy Demand in Switzerland. *Energy and Buildings,* 37(11)**,** 1175-1185.

Frazer, G. W., Canham, C. D. & Lertzman, K. P. 1999. Gap Light Analyzer (Gla): Imaging Software to Extract Canopy Structure and Gap Light Transmission Indices from True-Colour Fisheye Photographs, Users Manual and Program Documentation, Version 2.0. Cary Institute of Ecosystem Studies: Simon Frazer University, Bournaby, British Columbia, and the Institute of Ecosystem Studies, Millbrook, New York.

Frontini, F., Marzoli, M. & Doust, N. 2013. Investigation of Different Simulation Tools for Solar Photovoltaic Modules. *IBPSA.*

Fthenakis, V. & Yu, Y. 2013. Analysis of the Potential for a Heat Island Effect in Large Solar Farms. *IEEE Conference.* IEEE.

Fthenakis, V. M. 2018. Chapter Iv-1-a - Overview of Potential Hazards. *In:* KALOGIROU, S. A. (ed.) *Mcevoy's Handbook of Photovoltaics (Third Edition).* Academic Press.

Gales, B. E. N., Kander, A., Malanima, P. & Rubio, M. a. R. 2007. North Versus South: Energy Transition and Energy Intensity in Europe over 200 Years. *European Review of Economic History,* 11(2)**,** 219-253.

Gallagher, M. W., Nemitz, E., Dorsey, J. R., Fowler, D., Sutton, M. A., Flynn, M. & Duyzer, J. 2002. Measurements and Parameterizations of Small Aerosol Deposition Velocities to Grassland, Arable Crops, and Forest: Influence of Surface Roughness Length on Deposition. *Journal of Geophysical Research: Atmospheres,* 107(D12)**,** AAC 8-1-AAC 8-10.

Gao, W., Ren, T., Bengough, A. G., Auneau, L., Watts, C. W. & Whalley, W. R. 2012. Predicting Penetrometer Resistance from the Compression Characteristic of Soil. *Soil Science Society of America Journal,* 76(2)**,** 361.

Gao, X., Yang, L., Lyu, F., Ma, L., Hui, X., Hou, X. & Li, H. 2016a. *Effect of Pv Farm on Soil Temperature in Golmud Deser Tarea*.

Gao, X., Yang, L., Lyu, F., Ma, L., Hui, X., Hou, X. & Li, H. 2016b. *Observational Study on the Impact of the Large Solar Farm on Air Temperature and Humidity in Desert Areas of Golmud*.

Gavin, H. & Agnew, C. T. 2000. Estimating Evaporation and Surface Resistance from a Wet Grassland. *Physics and Chemistry of the Earth, Part B: Hydrology, Oceans and Atmosphere,* 25(7-8)**,** 599-603.

Gigliotti, M., Schmidt-Traub, G. & Bastianoni, S. 2019. The Sustainable Development Goals. *In:* FATH, B. (ed.) *Encyclopedia of Ecology (Second Edition).* Oxford: Elsevier.

Ginley, D. S. & Parilla, P. A. 2013. Solar Energy: A Common-Sense Vision. *Frontiers in Energy Research,* 1.

Global Fse, L. UK. *Superfast Thermapen* [Online]. UK. Available: https://www.globalfse.co.uk/superfast-thermapen-blue-49-9-to-299-9-c?utm_source=google_shopping&gclid=Cj0KCQiAzMDTBRDDARIsABX4AWy3_FL9ZgqQIh81nn0DGLmZHpDdr85dc8LOUcOp2j8Cph-pJSqgrf4aAqIYEALw_wcB.

Goetzberger, A. & Zastrow, A. 1982. On the Coexistence of Solar-Energy Conversion and Plant Cultivation. *International Journal of Solar Energy,* 1(1)**,** 55-69.

Gong, Y., Cao, Q. & Sun, Z. 2003. The Effects of Soil Bulk Density, Clay Content and Temperature on Soil Water Content Measurement Using Time-Domain Reflectometry. *Hydrological Processes,* 17(18)**,** 3601-3614.

Granberg, G., Grip, H., Löfvenius, M. O., Sundh, I., Svensson, B. H. & Nilsson, M. 1999. A Simple Model for Simulation of Water Content, Soil Frost, and Soil Temperatures in Boreal Mixed Mires. *Water Resources Research,* 35(12)**,** 3771-3782.

Gupta, B., Shah, D. O., Mishra, B., Joshi, P. A., Gandhi, V. G. & Fougat, R. S. 2015. Effect of Top Soil Wettability on Water Evaporation and Plant Growth. *Journal of Colloid and Interface Science,* 449**,** 506-513.

Gupta, S. C., Radke, J. K. & Larson, W. E. 1981. Predicting Temperatures of Bare and Residue Covered Soils with and without a Corn Crop1. *Soil Science Society of America Journal,* 45(2)**,** 405-412.

Hales, K., Neelin, J. D. & Zeng, N. 2004. Sensitivity of Tropical Land Climate to Leaf Area Index: Role of Surface Conductance Versus Albedo. *Journal of Climate,* 17(7)**,** 1459-1473.

Hall, I. J., Prairie, R. R., Anderson, H. E. & Boes, E. C. 1978. *Generation of a Typical Meteorological Year*: ; Sandia Labs., Albuquerque, NM (USA).

Han, F., Kang, S., Buyantuev, A., Zhang, Q., Niu, J., Yu, D., Ding, Y., Liu, P. & Ma, W. 2016. Effects of Climate Change on Primary Production in the Inner Mongolia Plateau, China. *International Journal of Remote Sensing,* 37(23)**,** 5551-5564.

Hardy, J. P., Melloh, R., Koenig, G., Marks, D., Winstral, A., Pomeroy, J. W. & Link, T. 2004. Solar Radiation Transmission through Conifer Canopies. *Agricultural and Forest Meteorology,* 126(3)**,** 257-270.

Hartmann, D. L. 1994. Chapter 5 the Hydrologic Cycle. *International Geophysics.* Academic Press.

Hassan, Q. K., Bourque, C. P. A., Meng, F.-R. & Richards, W. Spatial Mapping of Growing Degree Days: An Application of Modis-Based Surface Temperatures and Enhanced Vegetation Index. 2007. SPIE, 12.

Hassanpour Adeh, E., Selker, J. S. & Higgins, C. W. 2018. Remarkable Agrivoltaic Influence on Soil Moisture, Micrometeorology and Water-Use Efficiency. *PLOS ONE,* 13(11)**,** e0203256.

Hastie, T. & Tibshirani, R. 1986. *Generalised Additive Models,* Statistical Science.

Hatfield, J. L. & Prueger, J. H. 2015. Temperature Extremes: Effect on Plant Growth and Development. *Weather and Climate Extremes,* 10**,** 4-10.

He, Y., D'odorico, P., De Wekker, S. F. J., Fuentes, J. D. & Litvak, M. 2010. On the Impact of Shrub Encroachment on Microclimate Conditions in the Northern Chihuahuan Desert. *Journal of Geophysical Research: Atmospheres,* 115(D21).

Hernandez, R. R., Armstrong, A., Burney, J., Ryan, G., Moore-O'leary, K., Diédhiou, I., Grodsky, S. M., Saul-Gershenz, L., Davis, R., Macknick, J., Mulvaney, D., Heath, G. A., Easter, S. B., Hoffacker, M. K., Allen, M. F. & Kammen, D. M. 2019. Techno–Ecological Synergies of Solar Energy for Global Sustainability. *Nature Sustainability,* 2(7)**,** 560-568.

Hernandez, R. R., Easter, S. B., Murphy-Mariscal, M. L., Maestre, F. T., Tavassoli, M., Allen, E. B., Barrows, C. W., Belnap, J., Ochoa-Hueso, R., Ravi, S. & Allen, M. F. 2014. Environmental Impacts of Utility-Scale Solar Energy. *Renewable and Sustainable Energy Reviews,* 29**,** 766-779.

Hernandez, R. R., Hoffacker, M. K., Murphy-Mariscal, M. L., Wu, G. C. & Allen, M. F. 2015. Solar Energy Development Impacts on Land Cover Change and Protected Areas. *Proceedings of the National Academy of Sciences,* 112(44)**,** 13579.

Hewins, D. B., Lyseng, M. P., Schoderbek, D. F., Alexander, M., Willms, W. D., Carlyle, C. N., Chang, S. X. & Bork, E. W. 2018. Grazing and Climate Effects on Soil Organic Carbon Concentration and Particle-Size Association in Northern Grasslands. *Scientific Reports,* 8(1)**,** 1336.

Hoffmann, W. A. & Jackson, R. B. 2000. Vegetation–Climate Feedbacks in the Conversion of Tropical Savanna to Grassland. *Journal of Climate,* 13(9)**,** 1593-1602.

Hu, A., Levis, S., Han, W., He, M., Washington, W. M., Oleson, K. W., Van Ruijven, B. J. & Strand, W. G. 2015. Impact of Solar Panels on Global Climate. *Nature Climate Change,* 6**,** 5.

Hu, Z., Yu, G., Fu, Y., Sun, X., Li, Y., Shi, P., Wang, Y. & Zheng, Z. 2008. Effects of Vegetation Control on Ecosystem Water Use Efficiency within and among Four Grassland Ecosystems in China. *Global Change Biology,* 14(7)**,** 1609-1619.

Iae/Weo 2018. World Energy Outlook 2018. International Energy Agency.

Iea 2014. Technology Roadmap: Solar Photovoltaic Energy. *In:* PHILIBERT, C. & JOHNSTON, A. (eds.) *Solar Photovoltaic Energy.* International Energy Agency: IEA.

Iea 2017. Renewables 2017. *Renewables 2017|Analysis and forecast to 2022.* www.iea.org: International Energy Agency.

Iea 2018a. Key World Energy Statistics. International Energy Agency.

Iea. 2018b. *Solar Pv - Tracking Clean Energy Progress* [Online]. International Energy Agency. Available: https://www.iea.org/renewables2018/ 2018].

Iea/Weo 2017. World Energy Outlook 2017. *WEO-2017.* www.iea.org: IEA.

Ieefa 2018. Solar Is Driving a Global Shift in Electricity Markets. *In:* BUCKLEY, T. & SHAH, K. (eds.) *Rapid cost deflation and broad gais in scale.* Institute for Energy Economics and Financial Analysis.

Ipcc 2018. Global Warming of 1.5 °C. *In:* MASSON-DELMOTTE, V., PORTNER, H.-O., SKEA, J., ZHAI, P., ROBERTS, D., SHUKLA, P. R., PIRANI, A., MOUFOUMA-OKIA, W., PEAN, C., PIDCOCK, R., CONNORS, S., MATTHEWS, J. B. R., CHEN, Y., ZHOU, X., COMIS, M. I., LONNOY, E., MAYOCK, T., TIGNOR, M. & WATERFIELD, T. (eds.) *Summary for Policymakers.* Switzerland: Intergovernmental Panel on Climate Change.

Jackson, R. D. 1973. Diurnal Changes in Soil Water Content During Drying1

Sssa Special Publication 5. *Field Soil Water Regime*. Madison, WI: Soil Science Society of America.

Jacome, A., Bernier, M., Chokmani, K., Gauthier, Y., Poulin, J. & De Sève, D. 2013. Monitoring Volumetric Surface Soil Moisture Content at the La Grande Basin Boreal Wetland by Radar Multi Polarization Data. *Remote Sensing,* 5(10)**,** 4919.

James, S. E., Pärtel, M., Wilson, S. D. & Peltzer, D. A. 2003. Temporal Heterogeneity of Soil Moisture in Grassland and Forest. *Journal of Ecology,* 91(2)**,** 234-239.

Jenny, H., Bingham, F. & Padilla-Saravia, B. 1948. Nitrogen and Organic Matter Contents of Equatorial Soils of Colombia, South America. *Soil Science,* 66(3).

Jin, M. & Liang, S. 2006. An Improved Land Surface Emissivity Parameter for Land Surface Models Using Global Remote Sensing Observations. *Journal of Climate,* 19(12)**,** 2867-2881.

Jones, M. J. 1973. The Organic Matter Content of the Savanna Soils of West Africa. *Journal of Soil Science,* 24(1)**,** 42-53.

Kala, J., Evans, J. P., Pitman, A. J., Schaaf, C. B., Decker, M., Carouge, C., Mocko, D. & Sun, Q. 2014. Implementation of a Soil Albedo Scheme in the Cablev1.4b Land Surface Model and Evaluation against Modis Estimates over Australia. *Geosci. Model Dev.,* 7(5)**,** 2121-2140.

Kamat, P. V. 2007. Meeting the Clean Energy Demand: Nanostructure Architectures for Solar Energy Conversion. *The Journal of Physical Chemistry C,* 111(7)**,** 2834-2860.

Kang, S., Kim, S., Oh, S. & Lee, D. 2000. Predicting Spatial and Temporal Patterns of Soil Temperature Based on Topography, Surface Cover and Air Temperature. *Forest Ecology and Management,* 136(1)**,** 173-184.

Keller, T. & Håkansson, I. 2010. Estimation of Reference Bulk Density from Soil Particle Size Distribution and Soil Organic Matter Content. *Geoderma,* 154(3)**,** 398-406.

Kemp, P. R., Reynolds, J. F., Pachepsky, Y. & Chen, J.-L. 1997. A Comparative Modeling Study of Soil Water Dynamics in a Desert Ecosystem. *Water Resources Research,* 33(1)**,** 73-90.

Kettridge, N. & Baird, A. 2006. A New Approach to Measuring the Aerodynamic Resistance to Evaporation within a Northern Peatland Using a Modified Bellani Plate Atmometer. *Hydrological Processes,* 20(19)**,** 4249-4258.

Kettridge, N. & Baird, A. 2008. Modelling Soil Temperatures in Northern Peatlands. *European Journal of Soil Science,* 59(2)**,** 327-338.

Kettridge, N., Thompson, D. K., Bombonato, L., Turetsky, M. R., Benscoter, B. W. & Waddington, J. M. 2013. The Ecohydrology of Forested Peatlands: Simulating the Effects of Tree Shading on Moss Evaporation and Species Composition. *Journal of Geophysical Research: Biogeosciences,* 118(2)**,** 422-435.

Klein, J. A., Harte, J. & Zhao, X.-Q. 2005. Dynamic and Complex Microclimate Responses to Warming and Grazing Manipulations. *Global Change Biology,* 11(9)**,** 1440-1451.

Knopper, L. D. & Ollson, C. A. 2011. Health Effects and Wind Turbines: A Review of the Literature. *Environmental Health,* 10(1)**,** 78.

Kottek, M., Grieser, J., Beck, C., Rudolf, B. & Rubel, F. 2006. World Map of the Koppen-Geiger Climate Classification Updated. *Meteorologische Zeitschrift,* 15(3)**,** 259-263.

Krecia, L. L., Higgins, K. F. & Naugle, D. E. 1999. Effects of Wind Turbines on Upland Nesting Birds in Conservation Reserve Program Grasslands. *The Wilson Bulletin,* 111(1)**,** 100-104.

Kumar, S. 2015. Impact of Climate Change on Plant Genetic Resources.

Kunkel, K. E., Easterling, D. R., Hubbard, K. & Redmond, K. 2004. Temporal Variations in Frost-Free Season in the United States: 1895–2000. *Geophysical Research Letters,* 31(3).

Lang, A. & Thorpe, M. R. 1989. Xylem, Phloem and Transpiration Flows in a Grape: Application of a Technique for Measuring the Volume of Attached Fruits to High Resolution Using Archimedes' Principle. *Journal of Experimental Botany,* 40(10)**,** 1069-1078.

Lee, S.-H. & Park, S.-U. 2007. A Vegetated Urban Canopy Model for Meteorological and Environmental Modelling. *Boundary-Layer Meterorology,* 126(1)**,** 29.

Lenderink, G., Van Ulden, A., Van Den Hurk, B. & Van Meijgaard, E. 2007. Summertime Inter-Annual Temperature Variability in an Ensemble of Regional Model Simulations: Analysis of the Surface Energy Budget. *Climatic Change,* 81(1)**,** 233-247.

Li-Cor, B. 2017. *Li-3100c Area Mater* [Online].

Li, F., Meng, P., Fu, D. & Wang, B. 2008. Light Distribution, Photosynthetic Rate and Yield in a Paulownia-Wheat Intercropping System in China. *Agrofor. Syst.,* 74**,** 163-172.

Li, J. 2017. Assessing the Accuracy of Predictive Models for Numerical Data: Not R nor R2, Why Not? Then What? *PloS one,* 12(8)**,** e0183250-e0183250.

Li, J. & Heap, A. D. 2011. A Review of Comparative Studies of Spatial Interpolation Methods in Environmental Sciences: Performance and Impact Factors. *Ecological Informatics,* 6(3)**,** 228-241.

Li, T., Heuvelink, E., Dueck, T. A., Janse, J., Gort, G. & Marcelis, L. F. M. 2014. Enhancement of Crop Photosynthesis by Diffuse Light: Quantifying the Contributing Factors. *Annals of Botany,* 114(1)**,** 145-156.

Li, Z., Chen, Y., Shen, Y., Liu, Y. & Zhang, S. 2013. Analysis of Changing Pan Evaporation in the Arid Region of Northwest China. *Water Resources Research,* 49(4)**,** 2205-2212.

Li, Z., Wang, J., Tang, H., Huang, C., Yang, F., Chen, B., Wang, X., Xin, X. & Ge, Y. 2016. Predicting Grassland Leaf Area Index in the Meadow Steppes of Northern China: A Comparative Study of Regression Approaches and Hybrid Geostatistical Methods. *Remote Sensing,* 8(8).

Liu, H., Feng, J., Sun, J., Wang, L. & Xu, A. 2015. Eddy Covariance Measurements of Water Vapor and Co 2 Fluxes above the Erhai Lake. *Science China Earth Sciences,* 58(3)**,** 317-328.

Liu, X. & Luo, T. 2011. Spatiotemporal Variability of Soil Temperature and Moisture across Two Contrasting Timberline Ecotones in the Sergyemla Mountains, Southeast Tibet. *Arctic, Antarctic, and Alpine Research,* 43(2)**,** 229-238.

Luo, Y. & Zhou, X. 2006. Chapter 5 - Controlling Factors. *In:* LUO, Y. & ZHOU, X. (eds.) *Soil Respiration and the Environment.* Burlington: Academic Press.

Ma, C.-M. & Ruan, R.-T. 2013. Adsorption of Toluene on Mesoporous Materials from Waste Solar Panel as Silica Source. *Applied Clay Science,* 80-81**,** 196-201.

Mahfouf, J. F., Manzi, A. O., Noilhan, J., Giordani, H. & Déqué, M. 1995. The Land Surface Scheme Isba within the Météo-France Climate Model Arpege. Part I. Implementation and Preliminary Results. *Journal of Climate,* 8(8)**,** 2039-2057.

Mahfouf, J. F. & Noilhan, J. 1991. Comparative Study of Various Formulations of Evaporations from Bare Soil Using in Situ Data. *Journal of Applied Meteorology,* 30(9)**,** 1354-1365.

Makaronidou, M. 2019. *Assessment on the Local Climate Effects of Solar Photovoltaic Parks.* PhD Alternative thesis by papers, Lancaster University.

Marrou, H., Dufour, L. & Wery, J. 2013c. How Does a Shelter of Solar Panels Influence Water Flows in a Soil–Crop System? *European Journal of Agronomy,* 50**,** 38-51.

Marrou, H., Guilioni, L., Dufour, L., Dupraz, C. & Wery, J. 2013b. Microclimate under Agrivoltaic Systems: Is Crop Growth Rate Affected in the Partial Shade of Solar Panels? *Agricultural and Forest Meteorology,* 177**,** 117-132.

Marrou, H., Wery, J., Dufour, L. & Dupraz, C. 2013a. Productivity and Radiation Use Efficiency of Lettuces Grown in the Partial Shade of Photovoltaic Panels. *European Journal of Agronomy,* 44**,** 54-66.

Masson, V., Champeaux, J.-L., Chauvin, F., Meriguet, C. & Lacaze, R. 2003. A Global Database of Land Surface Parameters at 1-Km Resolution in Meteorological and Climate Models. *Journal of Climate,* 16(9)**,** 1261-1282.

Matos, P., Vieira, J., Rocha, B., Branquinho, C. & Pinho, P. 2019. Modeling the Provision of Air-Quality Regulation Ecosystem Service Provided by Urban Green Spaces Using Lichens as Ecological Indicators. *Science of The Total Environment,* 665**,** 521-530.

Matthews, S. N., Iverson, L. R., Peters, M. P., Prasad, A. M. & Subburayalu, S. 2014. Assessing and Comparing Risk to Climate Changes among Forested Locations: Implications for Ecosystem Services. *Landscape Ecology,* 29(2)**,** 213-228.

Mcewing, K. R., Fisher, J. P. & Zona, D. 2015. Environmental and Vegetation Controls on the Spatial Variability of Ch4 Emission from Wet-Sedge and Tussock Tundra Ecosystems in the Arctic. *Plant and Soil,* 388(1)**,** 37-52.

Mcilroy, I. C. & Angus, D. E. 1964. Grass, Water and Soil Evaporation at Aspendale. *Agricultural Meteorology,* 1(3)**,** 201-224.

Mcmaster, G. S. & Wilhelm, W. W. 1997. Growing Degree-Days: One Equation, Two Interpretations. *Agricultural and Forest Meteorology,* 87(4)**,** 291-300.

Mendelsohn, R., Nordhaus, W. D. & Shaw, D. 1994. The Impact of Global Warming on Agriculture: A Ricardian Analysis. *The American Economic Review,* 84(4)**,** 19.

Metoffice. 2018. *How We Measure Temperature* [Online]. MetOffice. Available: https://www.metoffice.gov.uk/guide/weather/observations-guide/how-we-measure-temperature.

Millstein, D. & Menon, S. 2011. Regional Climate Consequences of Large-Scale Cool Roof and Photovoltaic Array Deployment. *Environmental Research Letters,* 6(3)**,** 10.

Montoya, J. & Raffaelli, D. 2010. *Climate Change, Biotic Interactions and Ecosystem Services*.

Mooney, H., Larigauderie, A., Cesario, M., Elmquist, T., Hoegh-Guldberg, O., Lavorel, S., Mace, G. M., Palmer, M., Scholes, R. & Yahara, T. 2009. Biodiversity, Climate Change, and Ecosystem Services. *Current Opinion in Environmental Sustainability,* 1(1)**,** 46-54.

Moot, D. J., Scott, W. R., Roy, A. M. & Nicholls, A. C. 2000. Base Temperature and Thermal Time Requirements for Germination and Emergence of Temperate Pasture Species. *New Zealand Journal of Agricultural Research,* 43(1)**,** 15-25.

Morecroft, M. D., Taylor, M. E. & Oliver, H. R. 1998. Air and Soil Microclimates of Deciduous Woodland Compared to an Open Site. *Agricultural and Forest Meteorology,* 90(1)**,** 141-156.

N. Flerchinger, G. & E. Saxton, K. 1989. Simultaneous Heat and Water Model of a Freezing Snow-Residue-Soil System I. Theory and Development. *Transactions of the ASAE,* 32(2)**,** 565-0571.

Nag, C. 2018. Nag Fortran Builder.

Nemitz, E., Loubet, B., Lehmann, B. E., Cellier, P., Neftel, A., Jones, S. K., Hensen, A., Ihly, B., Tarakanov, S. V. & Sutton, M. A. 2009. Turbulence Characteristics in Grassland Canopies and Implications for Tracer Transport. *Biogeosciences,* 6(8)**,** 1519-1537.

Nissenbaum, M., Aramini, J. & Hanning, C. 2012. Effects of Industrial Wind Turbine Noise on Sleep and Health. *Noise and Health,* 14(60)**,** 237-243.

Noaa 2016. National Centers for Environmental Information. National Oceanic and Atmospheric Administratin.

Noaa. 2019. *Global Carbon Dioxide Growth in 2018 Reached 4th Highest on Record* [Online]. U.S. Department of Commerce: National Oceanic and Atmospheric Administration. Available: https://www.noaa.gov/news/global-carbon-dioxide-growth-in-2018-reached-4th-highest-on-record [Accessed March 22, 2019 2019].

Novick, K., Stoy, P., Katul, G., Ellsworth, D., Siqueira, M., Juang, J. & Oren, R. 2004. Carbon Dioxide and Water Vapor Exchange in a Warm Temperate Grassland. *Oecologia,* 138(2)**,** 259-274.

Nrel 2005. 1991-2005 Update: Typical Meteorological Year 3. *National Solar Radiation Data Base.* National Renewable Energy Laboratory: NREL.

Ogle, D., Stannard, M., P., S. & St John, L. 2010. Plant Guide for Sheep Fescue (Festuca Ovina L.). USDA-Natural Resources Conservation Service, Idaho and Washington Plant Materials Program. .

Oke, T. R. 1987. *Boundary Layer Climates,* London: Taylor & Francis Group.

Ostle, N. J., Levy, P. E., Evans, C. D. & Smith, P. 2009a. Uk Land Use and Soil Carbon Sequestration. *Land Use Policy,* 26, Supplement 1(0)**,** S274-S283.

Ostle, N. J., Smith, P., Fisher, R., Ian Woodward, F., Fisher, J. B., Smith, J. U., Galbraith, D., Levy, P., Meir, P., Mcnamara, N. P. & Bardgett, R. D. 2009b. Integrating Plant–Soil Interactions into Global Carbon Cycle Models. *Journal of Ecology,* 97(5)**,** 851-863.

Paruelo, J. M., Aguiar, M. R. & Golluscio, R. A. 1988. Soil Water Availability in the Patagonian Arid Steppe: Gravel Content Effect. *Arid Soil Research and Rehabilitation,* 2(1)**,** 67-74.

Pedraza, J. M. 2012. <the Current and Future Role of Renewable and Nuclear Energy in Latin America and the Caribbean. *IJEEE.* 2012 ed.: Nova Science Publishers Inc.

Pepin, N. C. & Lundquist, J. D. 2008. Temperature Trends at High Elevations: Patterns across the Globe. *Geophysical Research Letters,* 35(14).

Pérez, F. L. 1996. Cryptogamic Soil Buds in the Equatorial Andes of Venezuela. *Permafrost and Periglacial Processes,* 7(3)**,** 229-255.

Phillips, C. L. & Nickerson, N. 2015. Soil Respiration. *Reference Module in Earth Systems and Environmental Sciences.* Elsevier.

Phogat, V., Skewes, M., Cox, J. & Simunek, J. 2016. Statistical Assessment of a Numerical Model Simulating Agro Hydrochemical Processes in Soil under Drip Fertigated Mandarin Tree. *Irrigation & Drainage Systems Engineering,* 5(1).

Pogson, M., Hastings, A. & Smith, P. 2013. How Does Bioenergy Compare with Other Land-Based Renewable Energy Sources Globally? *GCB Bioenergy,* 5(5)**,** 513-524.

Pp Systems, L. USA. Egm-4 Environmental Gas Monitor. USA.

Preston, C. M., Simard, M., Bergeron, Y., Bernard, G. M. & Wasylishen, R. E. 2017. Charcoal in Organic Horizon and Surface Mineral Soil in a Boreal Forest Fire Chronosequence of Western Quebec: Stocks, Depth Distribution, Chemical Properties and a Synthesis of Related Studies. *Frontiers in Earth Science,* 5(98).

Qi, A., Holland, R. A., Taylor, G. & Richter, G. M. 2018. Grassland Futures in Great Britain – Productivity Assessment and Scenarios for Land Use Change Opportunities. *Science of The Total Environment,* 634**,** 1108-1118.

Qi, L. & Zhang, Y. 2017. Effects of Solar Photovoltaic Technology on the Environment in China. *Environmental Science and Pollution Research,* 24(28)**,** 22133-22142.

Qian, Y. L., Fry, J. D., Wiest, S. C. & Upham, W. S. 1996. Estimating Turfgrass Evapotranspiration Using Atmometers and the Penman-Monteith Model. *Crop Science,* 36(3)**,** cropsci1996.0011183X003600030030x.

R Core Team 2017. R: A Language and Environment for Statistical Computing. *R Foundation for Statistical Computing* Vienna, Austria.

Rabin, L. A., Coss, R. G. & Owings, D. H. 2006. The Effects of Wind Turbines on Antipredator Behavior in California Ground Squirrels (Spermophilus Beecheyi). *Biological Conservation,* 131(3)**,** 410-420.

Ravi, S., Lobell, D. B. & Field, C. B. 2014. Tradeoffs and Synergies between Biofuel Production and Large Solar Infrastructure in Deserts. *Environmental Science & Technology,* 48(5)**,** 3021-3030.

Recp 2017. Global Market Outlook, for Solar Power 2017-2021. Africa-EU REnewable Energy Cooporation Programme.

Recp 2018. Global Market Outlook, for Solar Power 2018-2022. Africa-EU REnewable Energy Cooporation Programme.

Reichstein, M., Rey, A., Freibauer, A., Tenhunen, J., Valentini, R., Banza, J., Casals, P., Cheng, Y., Grünzweig, J. M., Irvine, J., Joffre, R., Law, B. E., Loustau, D., Miglietta, F., Oechel, W., Ourcival, J.-M., Pereira, J. S., Peressotti, A., Ponti, F., Qi, Y., Rambal, S., Rayment, M., Romanya, J., Rossi, F., Tedeschi, V., Tirone, G., Xu, M. & Yakir, D. 2003. Modeling Temporal and Large-Scale Spatial Variability of Soil Respiration from Soil Water Availability, Temperature and Vegetation Productivity Indices. *Global Biogeochemical Cycles,* 17(4).

Rempel, A. W., Wettlaufer, J. S. & Worster, M. G. 2004. Premelting Dynamics in a Continuum Model of Frost Heave. *Journal of Fluid Mechanics,* 498**,** 227-244.

Ren21 2017. Renewables 2017 Global Status Report. Paris: REN21 Secretariat.

Ren21 2018. Renewables 2018 Global Status Report. *Renewable Energy Policy Network for the 21st Century.* Paris: REN21 Secretariat.

Roberts, M. R. & Paul, N. D. 2006. Seduced by the Dark Side: Integrating Molecular and Ecological Perspectives on the Influence of Light on Plant Defence against Pests and Pathogens. *New Phytologist,* 170(4)**,** 677-699.

Rochette, P., Desjardins, R. L. & Pattey, E. 1991. Spatial and Temporal Variability of Soil Respiration in Agricultural Fields. *Canadian Journal of Soil Science,* 71(2)**,** 189-196.

Rockström, J., Steffen, W., Noone, K., Persson, Å., Chapin Iii, F. S., Lambin, E. F., Lenton, T. M., Scheffer, M., Folke, C., Schellnhuber, H. J., Nykvist, B., De Wit, C. A., Hughes, T., Van Der Leeuw, S., Rodhe, H., Sörlin, S., Snyder, P. K., Costanza, R., Svedin, U., Falkenmark, M., Karlberg, L., Corell, R. W., Fabry, V. J., Hansen, J., Walker, B., Liverman, D., Richardson, K., Crutzen, P. & Foley, J. A. 2009. A Safe Operating Space for Humanity. *Nature,* 461**,** 472.

Rounsevell, M. D. A. & Reay, D. S. 2009. Land Use and Climate Change in the Uk. *Land Use Policy,* 26, Supplement 1(0)**,** S160-S169.

Rstudio, T. 2015. Rstudio: Integrated Development for Rstudio Inc. Boston, MA.

Saini, G. R. 1966. Organic Matter as a Measure of Bulk Density of Soil. *Nature,* 210**,** 1295.

Sánchez-Lozano, J. M., Henggeler Antunes, C., García-Cascales, M. S. & Dias, L. C. 2014. Gis-Based Photovoltaic Solar Farms Site Selection Using Electre-Tri: Evaluating the Case for Torre Pacheco, Murcia, Southeast of Spain. *Renewable Energy,* 66**,** 478-494.

Sánchez-Lozano, J. M., Teruel-Solano, J., Soto-Elvira, P. L. & Socorro García-Cascales, M. 2013. Geographical Information Systems (Gis) and Multi-Criteria Decision Making (Mcdm) Methods for the Evaluation of Solar Farms Locations: Case Study in South-Eastern Spain. *Renewable and Sustainable Energy Reviews,* 24**,** 544-556.

Sándor, R., Barcza, Z., Acutis, M., Doro, L., Hidy, D., Köchy, M., Minet, J., Lellei-Kovács, E., Ma, S., Perego, A., Rolinski, S., Ruget, F., Sanna, M., Seddaiu, G., Wu, L. & Bellocchi, G. 2017. Multi-Model Simulation of Soil Temperature, Soil Water Content and Biomass in Euro-Mediterranean Grasslands: Uncertainties and Ensemble Performance. *European Journal of Agronomy,* 88**,** 22-40.

Schlesinger, W. H. 1984. *The Role of Terrestrial Vegetation in the Global Carbon Cycle : Measurement by Remote Sensing,* Chichester [West Sussex] ; New York: Published on behalf of the Scientific Committee on Problems of the Environment (SCOPE) of the International Council of Scientific Unions (ICSU) by Wiley.

Schmidt, J. H. & Klokker, M. 2014. Health Effects Related to Wind Turbine Noise Exposure: A Systematic Review. *PloS one,* 9(12)**,** e114183-e114183.

Schneider, C. A., Rasband, W. S. & Eliceiri, K. W. 2012. Nih Image to Imagej: 25 Years of Image Analysis. *Nature Methods,* 9**,** 671.

Shuttleworth, W. J. & Wallace, J. S. 1985. Evaporation from Sparse Crops-an Energy Combination Theory. *Quarterly Journal of the Royal Meteorological Society,* 111(469)**,** 839-855.

Sinclair, T. R. & Seligman, N. A. 2000. Criteria for Publishing Papers on Crop Modeling. *Field Crops Research,* 68(3)**,** 165-172.

Skye Instruments, L. UK. *Skr 110 Red/Far-Red Pyranometer Sensor with the Skr100 Display Meter* [Online]. UK. Available: http://www.skyeinstruments.com/news-events/red-far-red-sensor/.

Snyder, W. C., Wan, Z., Zhang, Y. & Feng, Y. Z. 1998. Classification-Based Emissivity for Land Surface Temperature Measurement from Space. *International Journal of Remote Sensing,* 19(14)**,** 2753-2774.

Sobota, T. 2014. Fourier's Law of Heat Conduction. *In:* HETNARSKI, R. B. (ed.) *Encyclopedia of Thermal Stresses.* Dordrecht: Springer Netherlands.

Song, Y., Zhou, D., Zhang, H., Li, G., Jiin, Y. & Li, Q. 2013. Effects of Vegetation Height and Density on Soil Temperature variations. *Chinese Science Bulletin,* 58(8)**,** 907.

Stenseth, N. C., Mysterud, A., Ottersen, G., Hurrell, J. W., Chan, K.-S. & Lima, M. 2002. Ecological Effects of Climate Fluctuations. *Science,* 297(5585)**,** 1292.

Stursova, M. & Sinsabaugh, R. L. 2008. Stabilization of Oxidative Enzymes in Desert Soil May Limit Organic Matter Accumulation. *Soil Biology and Biochemistry,* 40(2)**,** 550-553.

Swan, J. B., Schneider, E. C., Moncrief, J. F., Paulson, W. H. & Peterson, A. E. 1987. Estimating Corn Growth, Yield, and Grain Moisture from Air Growing Degree Days and Residue Cover1. *Agronomy Journal,* 79(1)**,** 53-60.

Taejin, P., Sangram, G., Hans, T., Eugénie, S. E., Kjell-Arild, H., Stein Rune, K., Victor, B., Ramakrishna, R. N. & Ranga, B. M. 2016. Changes in Growing Season Duration and Productivity of Northern Vegetation Inferred from Long-Term Remote Sensing Data. *Environmental Research Letters,* 11(8)**,** 084001.

Taha, H. 2013. The Potential for Air-Temperature Impact from Large-Scale Deployment of Solar Photovoltaic Arrays in Urban Areas. *Solar Energy,* 91**,** 358-367.

Teasdale, J. R. & Mohler, C. L. 1993. Light Transmittance, Soil Temperature, and Soil Moisture under Residue of Hairy Vetch and Rye. *Agron. J.,* 85(3)**,** 673-680.

Thom, A. S., Thony, J. L. & Vauclin, M. 1981. On the Proper Employment of Evaporation Pans and Atmometers in Estimating Potential Transpiration. *Quarterly Journal of the Royal Meteorological Society,* 107(453)**,** 711-736.

Thomas, R., Graven, H., Sir Hoskins, B. & Prentice, I. C. 2016. What Is Meant by 'Balancing Sources and Sinks of Greenhouse Gases' to Limit Global Temperature Rise? London: Imperial College.

Thornley, J. H. M., Fowler, D. & Cannell, M. G. R. 2006. Terrestrial Carbon Storage Resulting from Co2 and Nitrogen Fertilization in Temperate Grasslands. *Plant, Cell & Environment,* 14(9)**,** 1007-1011.

Tian, Y., Peters-Lidard, C. D., Harrison, K. W., Prigent, C., Norouzi, H., Aires, F., Boukabara, S., Furuzawa, F. A. & Masunaga, H. 2014. Quantifying Uncertainties in Land-Surface Microwave Emissivity Retrievals. *IEEE Transactions on Geoscience and Remote Sensing,* 52(2)**,** 829-840.

Trucco, C., Schuur, E. a. G., Natali, S. M., Belshe, E. F., Bracho, R. & Vogel, J. 2012. Seven-Year Trends of Co2exchange in a Tundra Ecosystem Affected by Long-Term Permafrost Thaw. *Journal of Geophysical Research: Biogeosciences,* 117(G2).

Tucker, C. J., Slayback, D. A., Pinzon, J. E., Los, S. O., Myneni, R. B. & Taylor, M. G. 2001. Higher Northern Latitude Normalized Difference Vegetation Index and Growing Season Trends from 1982 to 1999. *International Journal of Biometeorology,* 45(4)**,** 184-190.

Tukey, J. W. 1977. *Exploratory Data Analysis,* Reading, Mass.: Reading, Mass. : Addison-Wesley Pub. Co.

Tulus, V., Abokersh, M. H., Cabeza, L. F., Vallès, M., Jiménez, L. & Boer, D. 2019. Economic and Environmental Potential for Solar Assisted Central Heating Plants in the Eu Residential Sector: Contribution to the 2030 Climate and Energy Eu Agenda. *Applied Energy,* 236**,** 318-339.

Uk Government, N. S. 2018. Digest of Uk Energy Statistics (Dukes): Renewable Sources of Energy. *In:* STATISTICS, N. (ed.). UK Government webpage.

Uk National Statistics 2017. Solar Photovoltaics Development. *In:* DEPARTMENT FOR BUSINESS, E. I. S. (ed.).

Uknea 2014. Uk National Ecosystem Assessment Follow-On. *In:* ALBON, S., TURNER, K. & WATSON, R. (eds.) *Synthesis of the Key Findings.* http://uknea.unep-wcmc.org/: UKNEA.

Un 2015. Adoption of the Paris Agreement, 21st Conference of the Parties;. *Framework Convention on Climate Change* United Nations : Paris.

Unruh, J. B. 2015. *Daily Light Requirements for Grass Species* [Online]. West Florida Research and Education Center: University of Florida. 2015].

Uyan, M. 2013. Gis-Based Solar Farms Site Selection Using Analytic Hierarchy Process (Ahp) in Karapinar Region, Konya/Turkey. *Renewable and Sustainable Energy Reviews,* 28**,** 11-17.

Van De Griend, A. A. & Owe, M. 1994. Bare Soil Surface Resistance to Evaporation by Vapor Diffusion under Semiarid Conditions. *Water Resources Research,* 30(2)**,** 181-188.

Van Den Berg, G. P. 2004. Effects of the Wind Profile at Night on Wind Turbine Sound. *Journal of Sound and Vibration,* 277(4)**,** 955-970.

Vargas, J. M. & Turgeon, A. J. 2003. *Poa Annua: Physiology, Culture and Control of Annual Bluegrass*.

Verma, S. B., Kim, J. & Clement, R. J. 1989. Carbon Dioxide, Water Vapor and Sensible Heat Fluxes over a Tallgrass Prairie. *Boundary-Layer Meteorology,* 46(1)**,** 53-67.

Villegas, J. C., Breshears, D. D., Zou, C. B. & Royer, P. D. 2010. Seasonally Pulsed Heterogeneity in Microclimate: Phenology and Cover Effects Along Deciduous Grassland–Forest Continuum. *Vadose Zone Journal,* 9(3)**,** 537-547.

Voudouris, V. 2013. Energy Policy and Security through the Lenses of Stochastic Portfolio Theory and the Aceges Model. *In:* VOUDOURIS, V. (ed.) *Global Energy Policy and Security.* Springer.

Walston, L. J., Mishra, S. K., Hartmann, H. M., Hlohowskyj, I., Mccall, J. & Macknick, J. 2018. Examining the Potential for Agricultural Benefits from Pollinator Habitat at Solar Facilities in the United States. *Environmental Science & Technology,* 52(13)**,** 7566-7576.

Wang, Y. P. & Jarvis, P. G. 1990. Influence of Crown Structural Properties on Par Absorption, Photosynthesis, and Transpiration in Sitka Spruce: Application of a Model (Maestro). *Tree Physiology,* 7(1-2-3-4).

Waring, R. H. & Running, S. W. 2007. Water Cycle. *Forest Ecosystems (Third Edition).* San Diego: Academic Press.

Watson, R., Wright, C. J., Mcburney, T., Taylor, A. J. & Linforth, R. S. T. 2002. Influence of Harvest Date and Light Integral on the Development of Strawberry Flavour Compounds. *Journal of experimental Botany***,** 8.

Wec 2016. World Energy Sources | Solar 2016. https://www.worldenergy.org.

Westmill Solar Farm, C.-O. 2011. *Westmill Solar* [Online]. UK. Available: http://www.westmillsolar.coop/home.asp 2011].

Who 2014. Quantitative Risk Assessment of the Effects of Climate Change on Selected Causes of Death, 2030s and 2050s. *In:* HALES, S., KOVATS, S., LLOYD, S. & CAMPBELL-LENDRUM, D. (eds.) *Climate change and human health.* Geneva, Switzerland: World Health Organization.

Wilcox, J. C. & Sly, W. K. 1976. Use of Negative Values of Potential Evapotranspiration in Estimation of Annual Irrigation Requirements. *Canadian Journal of Soil Science,* 56(4)**,** 507-509.

Wood, S. N. 2006. *Generalized Additive Models: An Introduction with R,* Texts in Statistical Science: Boca Raton: Chapman & Hall/CRC.

Xu, Y., Li, J., Tan, Q., Peters, A. L. & Yang, C. 2018. Global Status of Recycling Waste Solar Panels: A Review. *Waste Management,* 75**,** 450-458.

Xuan, L., Xian-Xiang, L., Suraj, H., Matthias, R. & Erik, V. 2017. Evaluation of an Urban Canopy Model in a Tropical City: The Role of Tree Evapotranspiration. *Environmental Research Letters,* 12(9)**,** 094008.

Yan, H., Wang, X., Hao, P. & Dong, L. 2012. Study on the Microclimatic Characteristics and Human Comfort of Park Plant Communities in Summer. *Procedia Environmental Sciences,* 13**,** 755-765.

Yang, L., Gao, X., Lv, F., Hui, X., Ma, L. & Hou, X. 2017. *Study on the Local Climatic Effects of Large Photovoltaic Solar Farms in Desert Areas*.

Zari, M. P. 2017. 1 - Utilizing Relationships between Ecosystem Services, Built Environments, and Building Materials. *In:* PETROVIĆ, E. K., VALE, B. & ZARI, M. P. (eds.) *Materials for a Healthy, Ecological and Sustainable Built Environment.* Woodhead Publishing.

Zeng, X. & Dickinson, R. E. 1998. Effect of Surface Sublayer on Surface Skin Temperature and Fluxes. *Journal of Climate,* 11(4)**,** 537-550.

Zeng, X. & Wang, A. 2007. Consistent Parameterization of Roughness Length and Displacement Height for Sparse and Dense Canopies in Land Models. *Journal of Hydrometeorology,* 8(4)**,** 730-737.

Appendices

Appendices

Appendix 1 – S.I. 1

Microclimatic observations – graphs

Air temperature

Table 1. Daily minimum, maximum and mean air temperature during growing and non-growing season in degrees Celsius (°C).

Growing Season	**Morning (min/max/mean)**			**Afternoon (min/max/mean)**			**Evening (min/max/mean)**		
Under	8	22.3	15.7	12.3	26.6	18.8	14.1	27.5	19.2
Gap	7.8	26	16.9	11.5	36.3	21	14.6	30.8	20.8
Transect	7.8	26	16.4	11.5	36.3	20.1	14.1	30.8	20.2
Non-Growing Season									

Under	2.7	14.4	10.1	5.1	19.8	13.4	11.5	20	16.1
Gap	2.6	15.2	10.1	4.8	20	13.4	11	19.2	16
Transect	2.6	15.2	10.1	4.8	20	13.4	11	20	16

Soil Temperature

Table 2. Daily minimum, maximum and mean air temperature during growing and non-growing season in degrees Celsius (°C).

Growing Season	**Morning (min/max/mean)**			**Afternoon (min/max/mean)**			**Evening (min/max/mean)**		
Under	9.9	18.3	14.1	10.6	23.7	14.7	11.2	19.6	14.4
Gap	11.2	21.5	15.9	12.6	24	17.5	13.6	28.4	19.2

Transect	9.9	21.5	15.2	10.6	24	16.4	11.2	28.4	17.3
Non-Growing Season									
Under	2.6	12.7	9.2	3.9	13.8	9.2	9.6	14.5	11.1
Gap	2.2	12.6	9	2.8	13.7	9.5	9.6	14.8	11.6
Transect	2.2	12.7	9.1	2.8	13.8	9.4	9.6	14.8	11.4

Soil Moisture

Table 3. Daily minimum, maximum and mean soil moisture during growing and non-growing season in (m3/m3).

Growing Season	**Morning (min/max/mean)**			**Afternoon (min/max/mean)**			**Evening (min/max/mean)**		
Under	0.037	0.478	0.295	0.076	0.482	0.292	0.034	0.540	0.286
Gap	0.03	0.477	0.267	0.012	0.441	0.250	0.048	0.387	0.220
Transect	0.030	0.478	0.278	0.012	0.482	0.260	0.034	0.540	0.245
Non-Growing Season									
Under	0.186	0.522	0.400	0.107	0.472	0.383	0.173	0.510	0.400
Gap	0.200	0.521	0.390	0.165	0.499	0.391	0.161	0.520	0.390
Transect	0.186	0.522	0.390	0.107	0.500	0.388	0.161	0.520	0.400

Photosynthetic Active Radiation

Table 4. Daily minimum, maximum and mean air temperature during growing and non-growing season in μmol m^{-2} s^{-1}

Growing Season	**Morning (min/max/mean)**			**Afternoon (min/max/mean)**			**Evening (min/max/mean)**		
Under	9	1530	207	28	2110	218	15	1298	327
Gap	68	2490	641	135	2900	975	93	1565	343
Transect	9	2490	417	28	2900	672	15	1565	622
Non-Growing Season									
Under	3	303	80	7	1450	103	3	280	64
Gap	30	1600	378	45	1822	681	30	910	345

Transect	3	1600	259	7	1822	450	3	910	233

Jars Experiment for Precipitation and Evaporation

Precipitation **Growing Season**	**Min**	**Max**	**Mean**		**Non-Growing** **Season**	**Min**	**Max**	**Mean**
Under	0	61	21.44		Under	0	78	17.3
Gap	26	80	60.25		Gap	30	163	86.02

Evaporation **Growing Season**	**Min**	**Max**	**Mean**		**Non-Growing** **Season**	**Min**	**Max**	**Mean**

Under	0.3	37.3	22.47		Under	-55.6	53.3	0.77
Gap	12.3	53.3	33.64		Gap	-85.7	133.4	21.24

Table 5. Plant species survey (period May-September 2015)

Transect 1	**Distance (m)**	**Plant Species**
	1.25	Festuca ovina, Poa annua
	7.50	Festuca ovina, Poa annua

Transect 2	Distance (m)	Plant Species
	1.25	Festuca rubra, Poa annua, Festuca ovina, Poa pratensis
	7.50	Plantago lanceolata, Trifolium repens, Poa annua

Transect 3	Distance (m)	Plant Species
	1.25	Poa annua
	7.50	Festuca ovina, Brachypodium sylvaticum, Trifolium repens

Transect 4	Distance (m)	Plant Species
	1.25	Poa annua, Rumex obtusifolius
	7.50	Leucanthemum vulgare, Festuca ovina, Poa annua, Plantago lanceolata, Brachypodium sylvaticum

Transect 5	Distance (m)	Plant Species
	1.25	Poa annua, Rumex obtusifolius
	7.50	Leucanthemum vulgare, Festuca ovina, Poa annua, Trifolium repens, Lotus corniculatus, Trifolium pratense, Festuca rubra

H2. Soil properties (some extra GAMs including testing the variability of GWC)

Soil bulk density was affected by distance, organic matter and GWC ($p < 0.001$ and R^2 =60%). The amount of soil bulk density under was higher, compared with the gap (Figure 1(a)). Bulk density fell between a range of 0.75 g/cm^3 to 1.15 g/cm^3 for the area under and 0.60 g/cm^3 to 1.05 g/cm^3 for the gap area, representing a slight decrease from under to the gap. There was an obvious positive correlation between bulk density and the gravimetric water content (Figure 1(b)) as well as a similar trend along the transect.

The available organic matter demonstrated a slight increase from the northern panel edge onwards, with fluctuations along the gap (Figure 1(a)). Organic matter under, was lower compared with the gap ($p < 0.001$), and negatively correlated to the bulk density. The spatial factor had a strong effect on the organic matter and the GWC explained the rest of the variation in the GAM ($p < 0.001$ and R^2 = 25%; Figure 1(a)).

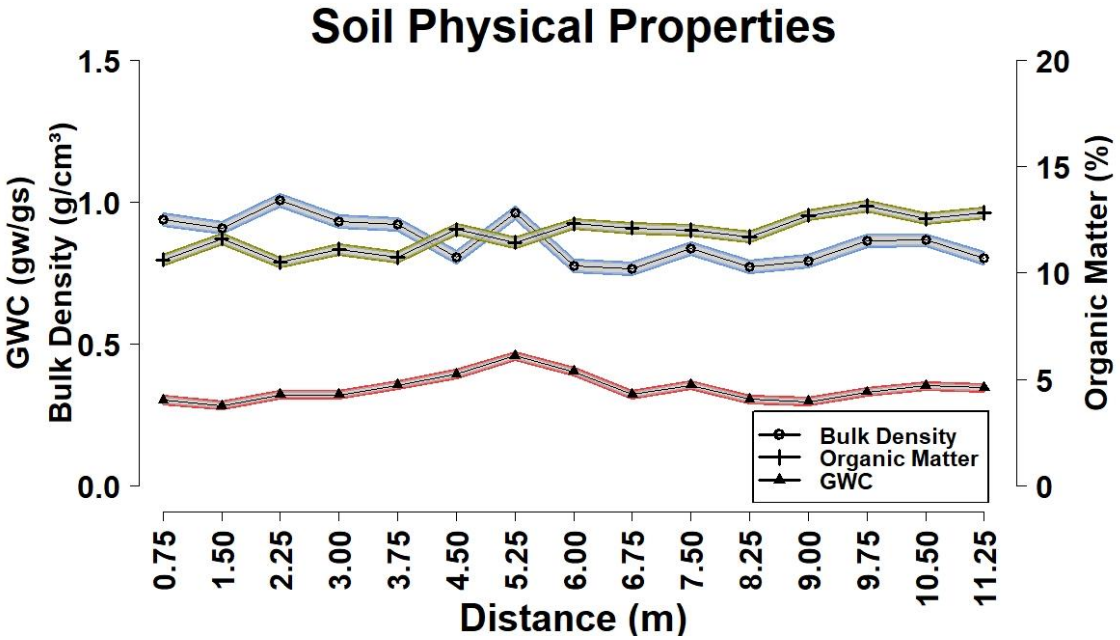

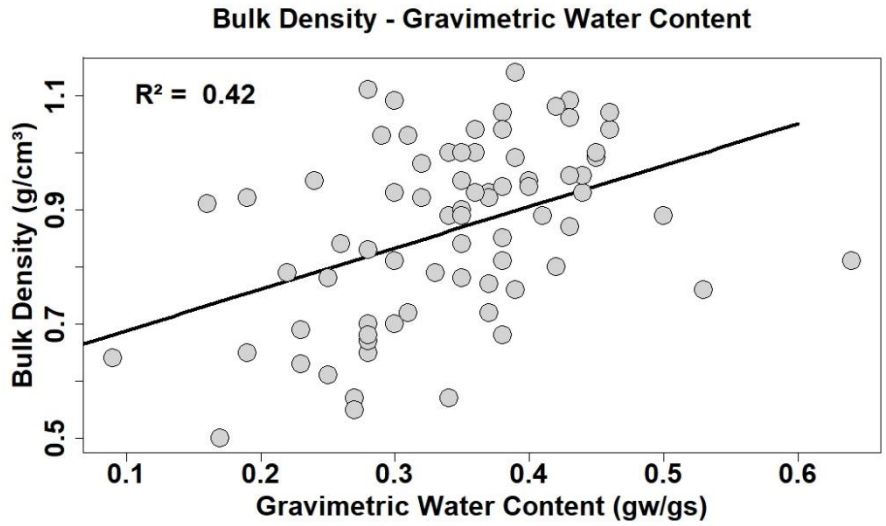

Figure 1 (a) All tested physical properties and (b) the correlation between bulk density and gravimetric water content.

Appendix 2 – S.I. 2

HIS-PV control and HIS-PV u&g models' comparison with logged measurements

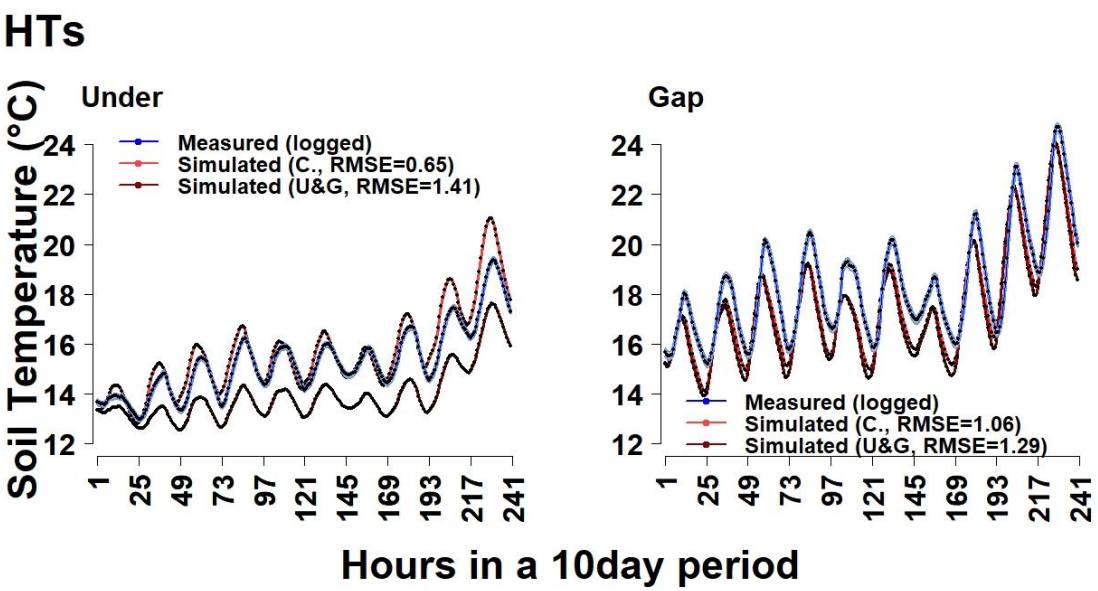

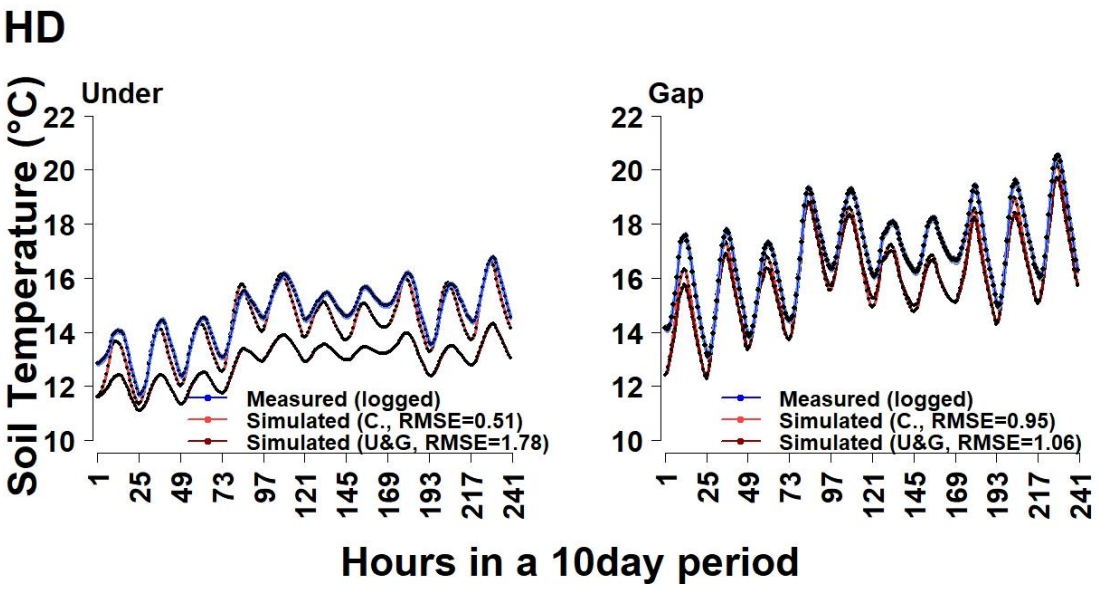

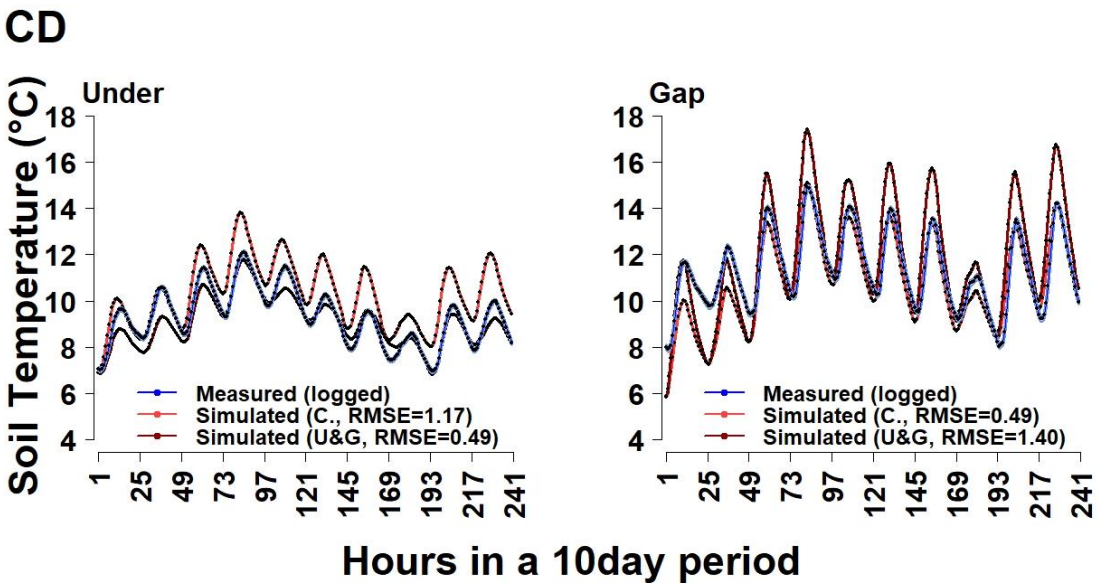

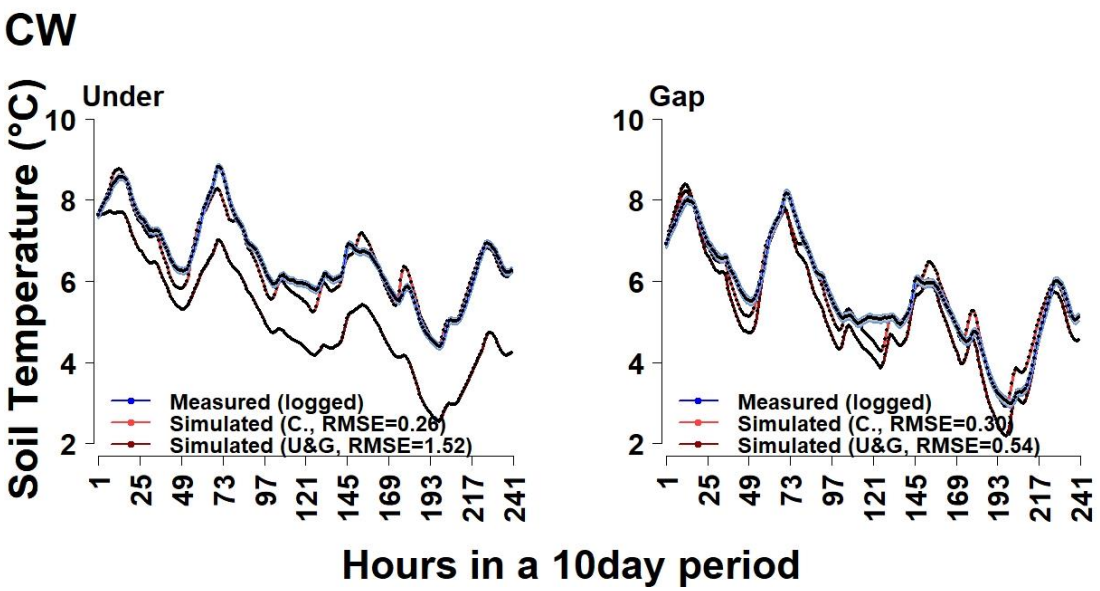

Table 1. A comparison between the control and the u&g HIS-PV models at a 10cm depth with the logged measurements

Period	Location	Logged Min and Max soil temperature (°C)	Control HIS-PV RMSE (°C)	U&G HIS-PV RMSE (°C)	Difference RMSE (°C)
HTs	Under	13 / 19.4	0.65	1.41	0.76

HTs	Gap	15.2 / 24.7	1.06	1.29	0.23
HD	Under	11.7 / 16.8	0.52	1.78	1.26
HD	Gap	13.1 / 20.5	0.95	1.06	0.11
CD	Under	7 / 12.1	1.18	0.49	0.69
CD	Gap	7.9 / 14.9	0.99	1.40	0.41
CW	Under	4.4 / 8.8	0.26	1.52	1.26
CW	Gap	2.3 / 8.2	0.30	0.54	0.24
MCs	Under	9.8 / 10.7	1.23	0.45	0.78
MCs	Gap	9.4 / 13.1	0.98	0.66	0.32

HIS-PV control and HIS-PV u&g models' comparison with instantaneous measurements

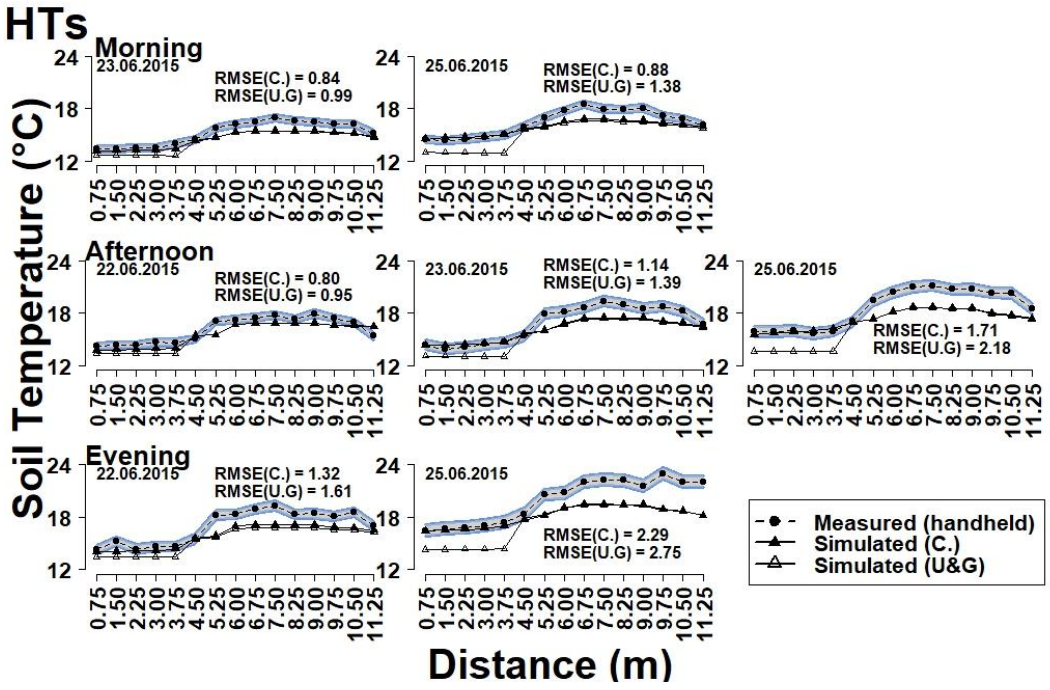

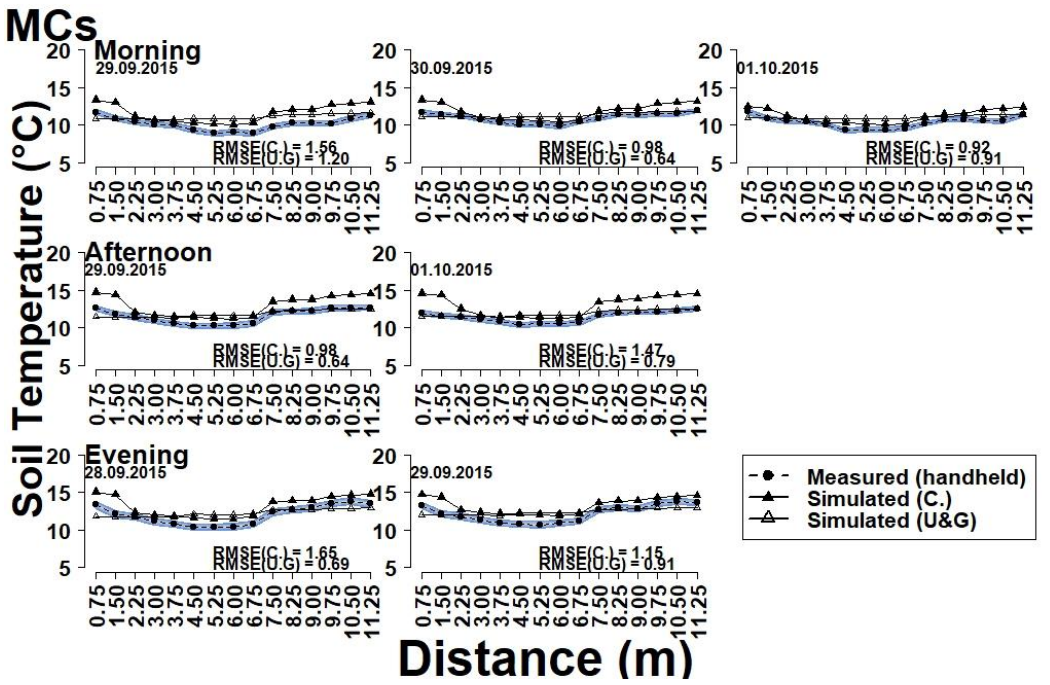

Table 2. A comparison between the control and the u&g HIS-PV models at a 10cm depth with the instantaneous measurements

Period	Date	TOD	Control HIS-PV RMSE (°C)	Under & Gap HIS-PV RMSE (°C)	RMSE Difference
HTs	23.06.2015	M	0.84	0.99	0.15
HTs	25.06.2015	M	0.88	1.38	0.5
HTs	22.06.2015	A	0.8	0.95	0.15
HTs	23.06.2015	A	1.17	1.39	0.22
HTs	25.06.2015	A	1.71	2.18	0.47
HTs	22.06.2015	E	1.32	1.62	0.6
HTs	25.06.2015	E	2.29	2.75	0.46
MCs	29.09.2015	M	1.56	1.2	0.36
MCs	30.09.2015	M	0.98	0.64	0.34
MCs	01.10.2015	M	0.92	0.91	0.01
MCs	29.09.2015	A	1.47	0.79	0.68
MCs	01.10.2015	A	1.65	0.69	0.96
MCs	28.09.2015	E	1.26	1.02	0.24
MCs	29.09.2015	E	1.5	0.91	0.59

HIS-PV control model evaluation with logged data during periods HD, CD and CW

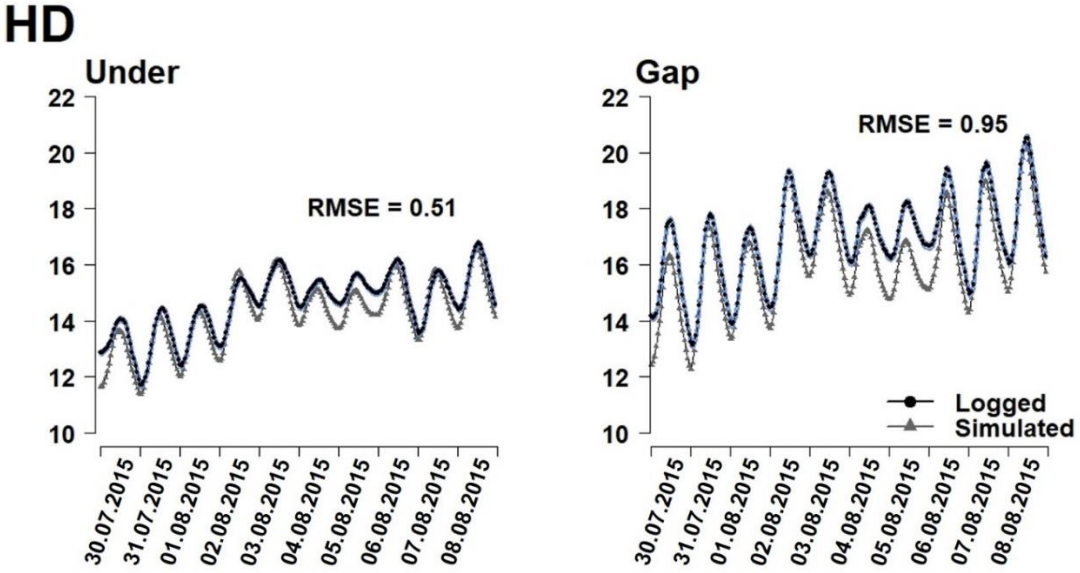

Figure 1. Hot and Dry (HD) period

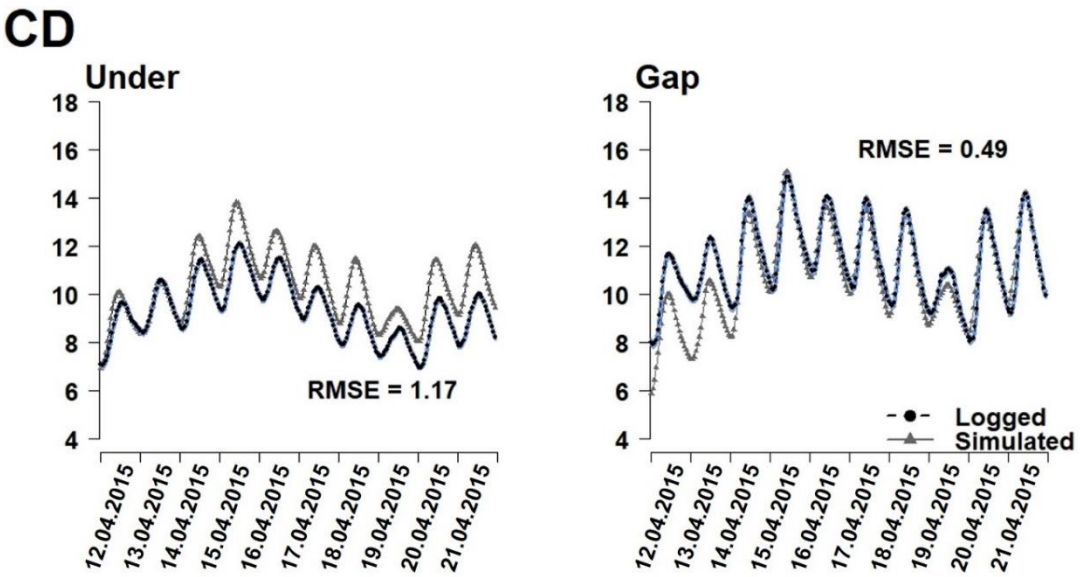

Figure 2. Cold and Dry (CD) period

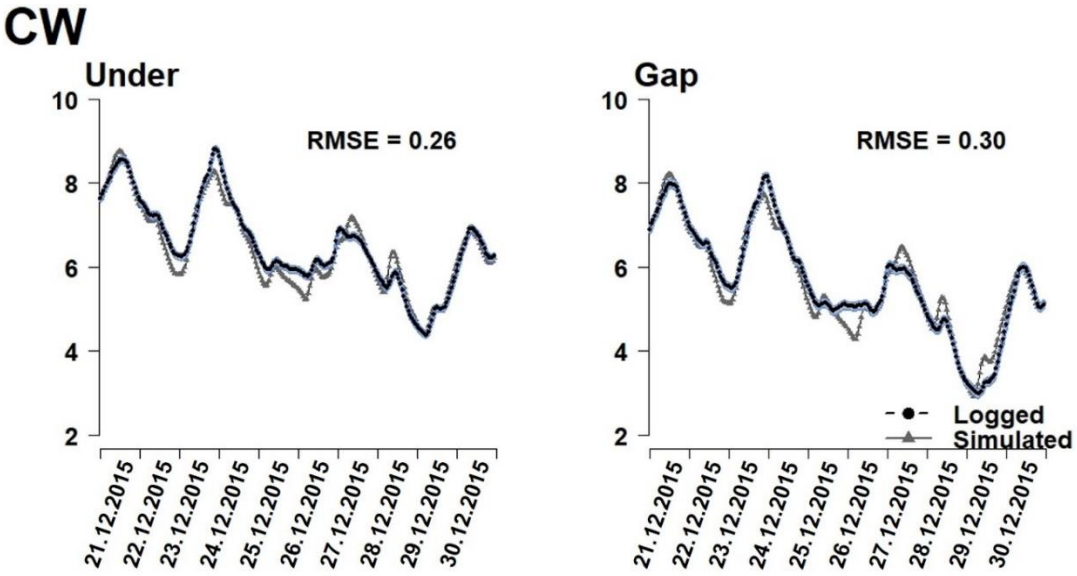

Figure 3. Cold and Wet (CW) period

Appendix 3 – S.I. 3

Table 1. Sites geospatial and climatological information

No	KCC	Climatic description	Location	Latitude (degrees °)	Longitude (degrees °)	Altitude (m)	Met-Station (NREL source)
1	Af	Equatorial, fully humid	Hilo, Hawaii	19.717	-155.05	9	918250
2	Af	Equatorial, fully humid	West Palm Beach Int Arpt, Florida	26.683	-80.1	6	722030
3	Am	Equatorial, monsoonal	Miami, Florida	25.817	-80.3	11	722020
4	Aw	Equatorial, winter dry	Key West, Florida	24.55	-81.75	1	722010
5	Aw	Equatorial, winter dry	Naples, Florida	26.15	-81.767	3	722038

6	BSh	Arid, Steppe, hot arid	Laredo, Texas	27.57	-99.49	142	752520
7	BSk	Arid, Steppe, cold arid	Reno, Nevada	39.483	-119.767	1342	724840
8	BSk	Arid, Steppe, cold arid	Denver Int Arpt, Colorado	39.833	-104.65	1650	725650
9	BWh	Arid, Desert, hot arid	Las Vegas McCarran Int Arpt, Nevada	36.083	-115.15	648	723860
10	BWk	Arid, Desert, cold arid	Coldfield, Nevada (Tonopah Airport Met Station)	38.067	-117.083	1655	724855
11	Cfb	Warm Temperate, fully humid, warm summer	Wytheville, Virginia	36.9	-81.35	780	724056
12	CSa	Warm Temperate, Steppe, hot summer	Sacramento, California	38.5	-121.5	5	724830
13	CSb	Warm Temperate, Steppe, warm summer	Portland, Oregon	45.6	-122.617	6	726980

14	CSb	Warm Temperate, Steppe, warm summer	Santa Barbara Municipal Arpt, California	34.433	-119.85	3	723925
15	CSb	Warm Temperate, Steppe, warm summer	San Francisco, California	37.617	-122.4	2	724940
16	Dfa	Snow, fully humid, hot summer	Lincoln, Nebraska	40.833	-96.767	357	725510
17	Dfc	Snow, fully humid, cool summer	Fairbanks, Alaska	64.817	-147.85	133	702610
18	DSc	Snow, Steppe, cool summer	Homer, Alaska	59.65	-151.483	27	703410
19	DWa	Snow, Dessert, hot summer	Valentine, Nebraska	42.867	-100.55	789	725670
20	DWb	Snow, Desert, warm summer	Dickinson, North Dakota	46.8	-102.8	788	727645
21	ET	Alpine	Barrow W post-W Rogers Airport, Alaska	71.32	-156.62	10	700260

22	ET	Alpine	Mekoryuk, Alaska	60.367	-166.267	15	702185
23	ET	Alpine	Savoonga, Alaska	63.683	-170.5	17	702035
24	ET	Alpine	Gambell, Alaska	63.783	-171.75	8	702040
25	ET	Alpine	Dutch Harbor, Alaska	53.9	-166.55	4	704890

Soil Temperature in 10 cm depth

Table 2. Daily mean soil temperature in 10 cm depth across five climate zones.

Climate Zone	Daily Mean Soil temperature °C (min/max/mean) - Under	Daily Mean Soil temperature °C (min/max/mean) - Gap	Daily Mean Soil temperature °C (min/max/mean) - Control
A, Equatorial	17.4 / 26.6 / 23.1	16.5 / 27.9 / 23.7	17.2 / 27.9 / 23.8
B. Arid	4.4 / 27.4 / 16.3	1.4 / 31.1 / 16.7	1.8 / 31 / 16.9
C. Temperate	9.3 / 21.8 / 16.4	8.1 / 23.1 /16.5	8.1 / 23.2 / 16.6
D. Boreal	-7 / 19.30 / 6.65	-7.7 / 19.4 / 6.3	-7.8 / 19.4 / 6.3
E. Polar	-15.7 / 7.9 / 1.5	-16.3 / 7.7 / -2.1	-16.4 / 7.6 / -2.2

Table 3. Percentage and absolute values differences of the simulated daily mean soil temperature in 10 cm depth between under-control and gap-control treatments. Subtracted with base the control simulations.

	Control vs Under (°C)			Control vs Gap (°C)		
	min	max	mean	min	max	mean
Equatorial	-0.2	1.3	0.7	0.7	0	0.1
Arid	-2.5	3.6	0.6	0.4	-0.1	0.2
Temperate	-1.2	1.4	0.2	0	0.1	0.1
Boreal	-0.8	0.1	-0.3	-0.1	0	0
Polar	-0.7	-0.3	-3.7	-0.1	-0.1	-0.1

Potential Evaporation

Table 4. Daily mean, min and max of PE of the soil across five climate zones

Climate Zone	Daily (min/max/mean)– Under	Daily (min/max/mean) - Gap	Daily (min/max/mean) - Control
Equatorial	0.65 / 2.35 / 1.40	0.35 / 3.50 / 2	0.60 / 3.50 / 2.10
Arid	0.90 / 8.25 / 3.80	0.35 / 13 / 5.10	0.50 / 12.85 / 5.20
Temperate	0.60 / 3.20 / 1.70	0.40 / 4.20 / 1.90	0.40 / 4.25 / 1.90
Boreal	0.20 / 2.10 / 1.05	0.10 / 2.30 / 1.05	0.10 / 2.35 / 1.10
Polar	-0.08 / 1.05 / 0.35	0.04 / 1.10 / 0.40	-0.10 / 1.05 / 0.40

Table 5. Percentage and absolute values differences of the simulated daily mean potential evaporation (PE) between under-control and gap-control treatments. Subtracted with base the control simulations.

	Control vs Under (°C)			Control vs Gap (°C)		
	min	max	mean	min	max	mean
Equatorial	-0.05	0.65	0.70	0.25	0	0.10
Arid	-0.40	4.6	1.40	0.15	-0.15	0.10
Temperate	-0.20	1.05	0.20	0	0.05	0
Boreal	-0.10	0.25	0.05	0	0.05	0.05
Polar	0.02	0	0.05	0	-0.05	0

Incoming Short-wave (SW) radiation at the surface

Table 6. Daily mean, min and max of SW of the soil across five climate zones

Climate Zone	Daily (min/max/mean)– Under	Daily (min/max/mean) - Gap	Daily (min/max/mean) - Control
Equatorial	54.20 / 120 / 74.60	160.70 / 178 / 174	188 / 189 / 188.60
Arid	57.20 / 102.30 / 68.30	141.50 / 153.50 / 149.70	161.80 / 162.90 / 162.40
Temperate	49 / 95.20 / 62.50	134.70 / 142.70 / 139.30	152 / 152.50 / 152.25
Boreal	45.70 / 86.40 / 58.80	112.60 / 120 / 118	129 / 130 / 129.80
Polar	30.90 / 50.90 / 38	72.15 / 75.60 / 74.50	80.40 / 81.20 / 80.70

Table 7. Annual percental differences of the simulated incoming SW (W/m^2) at the surface between Under-Control and Gap-Control treatments.

Under vs Control	Gap vs Control

	min		max		mean		min		max		mean	
Equatorial	36.40%	133.80	71.25%	69	60.50%	114	5.70%	27.30	14.80%	11.00	7.70%	14.60
Arid	37.20%	104.60	64.80%	60.60	58%	94.10	5.40%	20.30	13.10%	9.40	7.80%	12.70
Temperate	37.50%	103	67.90%	57.30	58.90%	89.75	6.30%	17.30	11.40%	9.80	8.50%	12.95
Boreal	33.60%	83.30	64.85%	43.60	54.70%	71	7.60%	16.40	13.45%	10	9.10%	11.80
Polar	36.65%	49.50	61.80%	30.30	52.75%	42.70	6.30%	8.25	10.25%	5.60	7.75%	6.20

Table 8. The mean and the standard deviation of the total of GDDs (ºC) during growing season at each climate zone

ID	Climate Zone	Treatment	Mean of the Summed GDDs (ºC)	St. Dev. of the summed GDDs	Mean of the daily GDDs	St. Dev. of the daily GDDs
1	Equatorial	Under	6319	385	17.43	0.94
2	Equatorial	Gap	6542	512	17.93	1.40
3	Equatorial	Control	6595	538	18.07	1.47
4	Arid	Under	3410	1618	15.12	2.69
5	Arid	Gap	3909	1723	17.48	2.61
6	Arid	Control	3905	1747	17.43	2.73
7	Temperate	Under	3469	629	11.91	1.60

8	Temperate	Gap	3563	550	12.34	2.06
9	Temperate	Control	3578	558	12.38	2.08